

**Report No. CDOT-DTD-R-2001-16  
Final Report**

# **REVISING THE AASHTO GUIDELINES FOR DESIGN AND CONSTRUCTION OF GRS WALLS**

**Jonathan T. H. Wu  
University of Colorado at Denver**



**November 2001**

**COLORADO DEPARTMENT OF TRANSPORTATION  
RESEARCH BRANCH**

The contents of this report reflect the views of the authors, who are responsible for the facts and accuracy of the data presented herein. The contents do not necessarily reflect the official views of the Colorado Department of Transportation or the Federal Highway Administration. This report does not constitute a standard, specification, or regulation.

# REVISING THE AASHTO GUIDELINES FOR DESIGN AND CONSTRUCTION OF GRS WALLS

by

Jonathan T. H. Wu

Report No. CDOT-DTD-R-2001-16

Prepared by  
University of Colorado at Denver

Sponsored by the  
Colorado Department of Transportation  
In cooperation with the  
U.S. Department of Transportation  
Federal Highway Administration

November 2001

Colorado Department of Transportation  
Research Branch  
4201 E. Arkansas Ave.  
Denver, CO 80222  
(303)757-9506

1. Report No. CDOT-DTD-R-2001-16	2. Government Accession No.	3. Recipient's Catalog No.	
4. Title and Subtitle REVISING THE AASHTO GUIDELINES FOR DESIGN AND CONSTRUCTION OF GRS WALLS		5. Report Date November 2001	
7. Author(s) Jonathan T. H. Wu		6. Performing Organization Code	
9. Performing Organization Name and Address University of Colorado at Denver 1200 Larimer Street Denver, CO 80217		8. Performing Organization Report No. 2001-16	
12. Sponsoring Agency Name and Address Colorado Department of Transportation 4201 E. Arkansas Ave. Denver, CO 80222		10. Work Unit No. (TRAIS)	
15. Supplementary Notes Prepared in Cooperation with the U.S. Department of Transportation, Federal Highway Administration		11. Contract or Grant No.	
16. Abstract This report addresses four proposed revisions to the AASHTO guidelines concerning design and construction of GRS walls (AASHTO, 1996). The proposed revisions are regarding: <ul style="list-style-type: none"> <li>• lateral earth pressure on wall facing</li> <li>• long-term deformation</li> <li>• truncated reinforcement at wall base and the CTI tails</li> <li>• embedment and leveling pad</li> </ul> For each of the proposed revisions, the deficiencies in the current AASHTO guidelines are addressed in detail; the literature on the research findings and measured performance is presented; and the specific revision is proposed. The limitations and practical implications of each proposed revision are also discussed.  <b>Implementation</b> The proposed revisions on design and construction of GRS walls can readily be implemented in Section 504 Concrete Block Facing MSE Walls of the Standard Specifications, the Colorado Department of Transportation.		13. Type of Report and Period Covered	
17. Key Words retaining walls, mechanically stabilized earth (MSE), AASHTO guidelines, geosynthetic-reinforced soil (GRS)		14. Sponsoring Agency Code	
19. Security Classif. (of this report) Unclassified		20. Security Classif. (of this page) Unclassified	21. No. of Pages
18. Distribution Statement		22. Price	

## Executive Summary

This report addresses four proposed revisions to the AASHTO guidelines concerning design and construction of GRS walls (AASHTO, 1996). The proposed revisions are regarding:

- lateral earth pressure on wall facing
- long-term deformation
- truncated reinforcement at wall base and the CTI tails
- embedment and leveling pad

For each of the proposed revisions, the deficiencies in the current AASHTO guidelines are addressed in detail; the literature on the research findings and measured performance is presented; and the specific revision is proposed. The limitations and practical implications of each proposed revision are also discussed. The following is a brief summary of each proposed revision:

- Lateral Earth Pressure: The Rankine active pressure employed by the current AASHTO guidelines is shown to be much too large for evaluating the facing stability. A “bin pressure” diagram on the wall facing is proposed for segmental GRS walls. It is also proposed that the use of heavy facing blocks or mechanical connections (such as pins, lips and keys) should be discouraged. A reinforced soil, when properly designed and constructed, is sufficiently stable by itself without any external support. The facing should only serve as a construction aid, a façade of the wall, and a barrier to prevent surface sloughing of the reinforced fill. The facing need not be a load-carrying element of the wall system. It should be noted that Rankine active earth pressure should continue to be used for evaluating external stability of a reinforced soil mass and for evaluating internal stability concerning reinforcement rupture failure.
- Long-Term Deformation: The deficiencies of the current AASHTO guidelines on long-term deformation are: (1) imposing fairly large safety factors on short-term reinforcement strength to obtain long-term design strength without any regard to soil-reinforcement interaction, and (2) multiplying the safety factors for creep, construction damage, chemical/biological degradation, and durability to obtain a

cumulative safety factor implies that all these factors are interrelated, which is clearly untrue. Laboratory soil-reinforcement interactive tests, finite element analysis, and measured behavior of in-service walls have conclusively indicated that creep deformation will be negligible when a well-compacted granular backfill is employed. Full-scale tests have also indicated that long-term degradation is not a design issue since a degraded reinforcement will restrain lateral deformation of the soil in a manner similar to an intact reinforcement. Based on the research findings, observed long-term behavior and the author's judgment, recommended values of the cumulated long-term reduction factor,  $k$ , are presented. The recommended  $k$ -values are a function of backfill type and placement condition, reinforcement spacing, and polymer type and weight of the reinforcement. A rational method for predicting creep deformation of a GRS wall, based on the Soil-Geosynthetic Interactive Performance (SGIP) tests, is also presented.

- Truncated Base Wall and CTI Tails: It is proposed that truncated length of reinforcement near the wall base be allowed in situations where excavation of an existing slope is needed yet it is impractical for placement of full design length of reinforcement. Finite element studies have indicated that a truncated base wall is a viable alternative when a well-compacted granular backfill is employed in the construction of a GRS wall on a competent foundation. The truncation angle can be as high as 45 degrees from the horizontal plane. Note that the external stability of the GRS wall needs to be checked thoroughly when a truncated base wall is used. Many truncated base walls have been constructed with satisfactory performance. The CTI tails of 3 ft in length measured from the back of the facing blocks have been found to increase facing stability. This measure should only be used with well-compacted granular backfill.
- Embedment and Leveling Pad: It is proposed that embedment is not necessary for GRS walls. Non-propped GRS walls can be safely constructed with zero embedment or with a small embedment (say  $\leq 8$  in., one typical block height). It is also proposed that, in lieu of the concrete leveling pad under the first course of facing blocks, a leveling pad of compacted gravel or compacted road base material be used. The use of a road base pad has been shown to ease the leveling process

and facilitate construction. A large number of GRS walls have been constructed with zero to 8 in. embedment and have demonstrated satisfactory performance characteristics.

## **Table of Contents**

<u>Chapter</u>	<u>Page</u>
1. INTRODUCTION.....	1
1.1 Geosynthetic-Reinforced Soil (GRS) Wall.....	1
1.2 Internally Stabilized Wall Versus Externally Stabilized Wall....	9
1.3 Fundamental Deficiencies of the AASHTO Guidelines for Design and Construction of GRS Walls.....	12
1.3.1 Failure Mechanism.....	12
1.3.2 Relationship between Spacing and Strength of Reinforcement.....	14
1.3.3 Lateral Earth Pressure.....	16
1.3.4 Safety Factors.....	18
1.4 Proposed Revisions of the AASHTO Guidelines.....	22
2. LATERAL EARTH PRESSURE ON WALL FACING.....	24
2.1 Lateral Earth Pressure on the Facing of a GRS Wall.....	24
2.2 Literature on Lateral Earth Pressure of GRS Walls.....	27
2.2.1 Reinforced Soil Mass Loading Experiments, Turner-Fairbank Highway Research Center, McLean, Virginia.....	27
2.2.2 Bed Sheet Reinforcement Loading Test, Rifle, Colorado.....	30
2.2.3 Commerce City Walls, Commerce City, Colorado.....	30
2.2.4 AMOCO Test Wall and U. K. Test Wall.....	33
2.2.5 Full-Scale Loading Test of an IFF Reinforced Soil Retaining Wall.....	38
2.2.6 Fox Wall, Denver, Colorado.....	42
2.2.7 Grand County Wall, Grand County, Colorado.....	48
2.2.8 Large-Scale Tests, University of Strathclyde, Glasgow.....	49

2.2.9	Finite Element Analysis.....	51
2.3	Proposed Lateral Earth Pressure Diagram.....	53
2.4	Limitations and Practical Implications.....	56
3.	LONG-TERM DEFORMATION.....	62
3.1	Long-Term Creep Behavior of Geosynthetics.....	62
3.2	Long-Term Pullout Behavior of Geosynthetics.....	69
3.3	Soil-Geosynthetic Interactive Creep Tests.....	69
3.3.1	Soil-Geosynthetic Interactive Performance Test.....	69
3.3.2	A Modified Long-Term Performance Test.....	70
3.3.3	Unit Cell Test and ASPR Test.....	79
3.4	Finite Element Analysis of Long-Term Creep Performance.....	84
3.5	In-Service GRS Walls and Field Measurement.....	84
3.5.1	Glenwood Canyon Wall.....	89
3.5.2	Tucson Wall.....	91
3.5.3	NGI Wall.....	96
3.5.4	JR Wall.....	99
3.5.5	Highbury Wall.....	103
3.5.6	Algonquin Wall.....	103
3.5.7	Seattle Wall.....	106
3.5.8	Summary and Conclusions on Long-Term Performance of the In-Service GRS Walls.....	109
3.6	Rate of Creep Deformation: Field Performance and the SGIP Tests.....	114
3.6.1	Creep Rate of In-Service GRS Walls.....	114
3.6.2	Creep Rate of the SGIP Tests.....	116
3.6.3	Creep Rate Equation.....	118
3.7	Proposed Methods to Account for Long-Term Deformation in Design.....	120
3.7.1	Cumulative Long-Term Reduction Factor, $k$ .....	120
3.7.2	A Rational Method for Predicting Creep	

	Deformation.....	123
3.7.3	Measures for Alleviating Excessive Long-Term Deformation.....	124
4.	TRUNCATED-BASE WALLS AND CTI TAILS.....	126
4.1	Studies on Truncated-Base Walls and the CTI Tails.....	126
4.1.1	Finite Element Analysis by Chou and Wu.....	126
4.1.2	DeBeque Canyon Wall.....	130
4.1.3	Finite Element Analysis by Thomas and Wu.....	135
4.2	Proposed Guidelines for Truncated Base and Tails.....	137
5.	EMBEDMENT AND LEVELING PAD.....	139
5.1	Field Performance.....	139
5.2	Proposed Embedment and Leveling Pad.....	140
6.	CONCLUDING REMARKS.....	141
	REFERENCES.....	142

## Chapter 1

### INTRODUCTION

This Chapter begins with an introduction of Geosynthetic-Reinforced Soil (GRS) walls and a review of the differences between an internally stabilized retaining wall and an externally stabilized retaining wall, follows with brief discussions of the fundamental deficiencies of the AASHTO guidelines for design and construction of GRS walls, and concludes with an overview of the proposed revisions of the AASHTO guidelines, including limitations of the proposed revisions.

#### 1.1 Geosynthetic-Reinforced Soil (GRS) Wall

A Geosynthetic-Reinforced Soil (GRS) wall comprises two major components: a facing element and a geosynthetic-reinforced soil mass. Figure 1.1 shows the schematic diagram of a typical GRS wall with segmental concrete block facing.

The facing of a GRS wall may take various shapes and forms. It may be made of various materials, including concrete, timber, metal, automobile tires, shotcrete, gabion, and different processed materials (such as compressed tire chips). Figure 1.2 shows various facing elements that have been used in the construction of GRS walls.

A geosynthetic reinforced soil mass is a soil mass reinforced with layers of geosynthetic reinforcement. It is a well-known fact that soil is weak in tension and strong in compression and shear. The concept of reinforcing a soil mass by incorporating a material that is strong in tensile resistance is similar to that of reinforced concrete. The reinforcing mechanisms of a reinforced soil and reinforced concrete, however, are somewhat different. In a reinforced soil, the bonding between the soil and the reinforcement is derived primarily from soil-geosynthetic interface friction, and in some cases from adhesion and passive

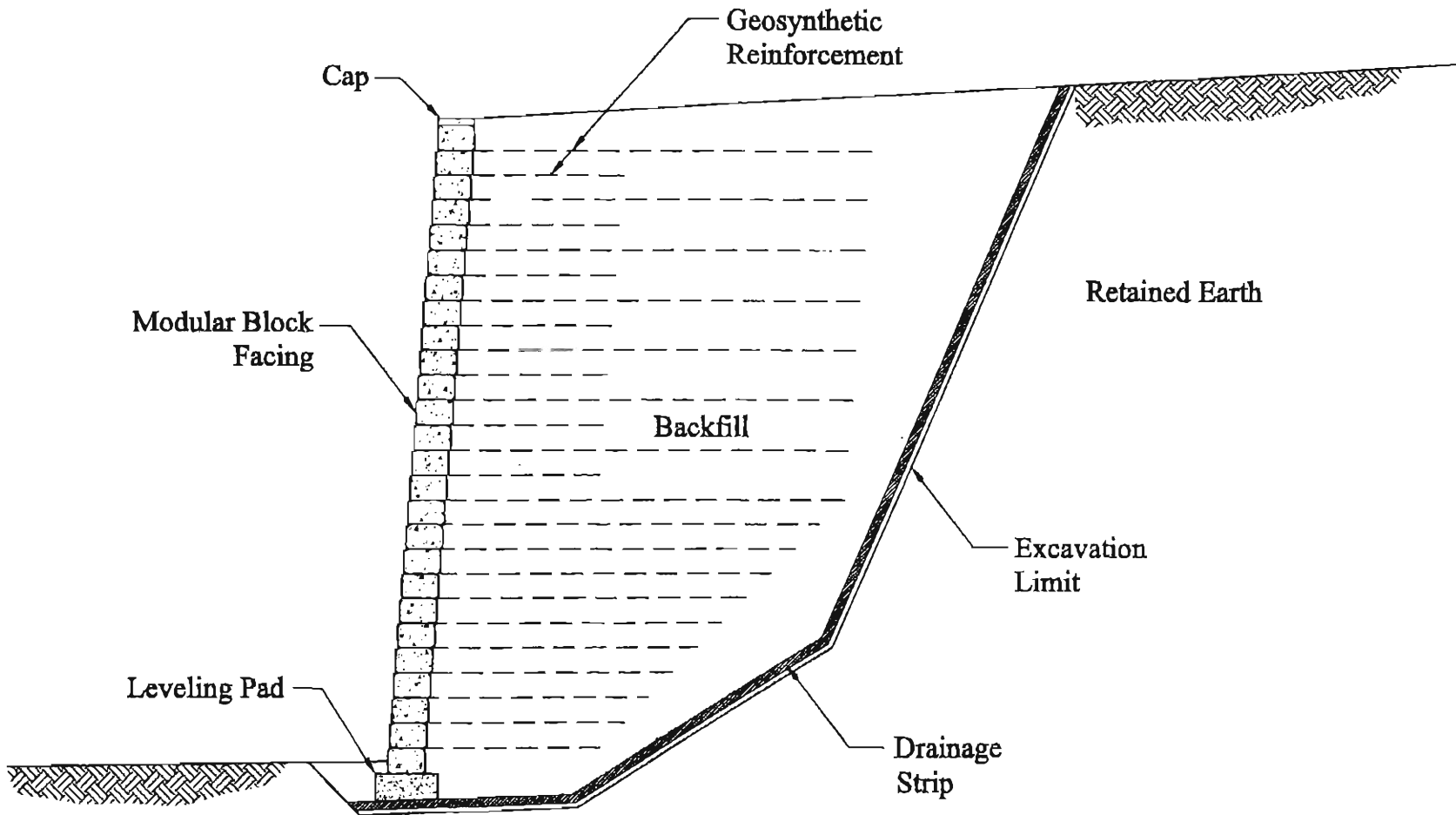
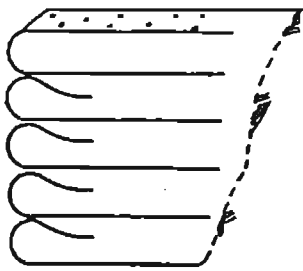
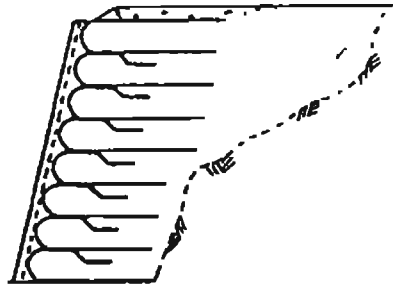


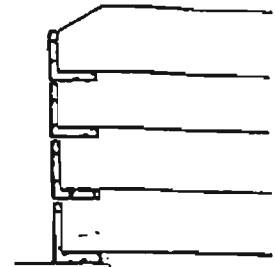
Figure 1.1 Typical cross-section of a segmental GRS Wall



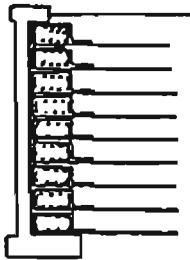
*wrapped-faced wall*



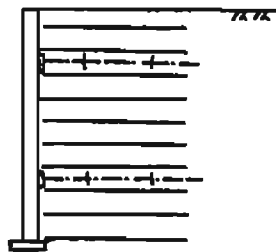
*wrapped-faced wall  
with shotcrete cover*



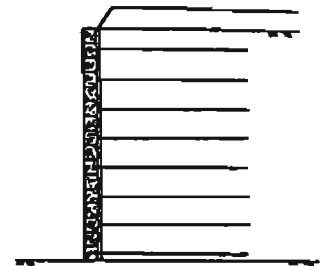
*GRS wall with  
articulated concrete  
facing*



*GRS wall with  
full-height concrete  
facing  
(two-phase construction)*



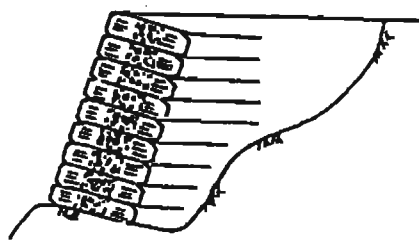
*full-height concrete  
MSB wall  
(CTI MSB Wall)*



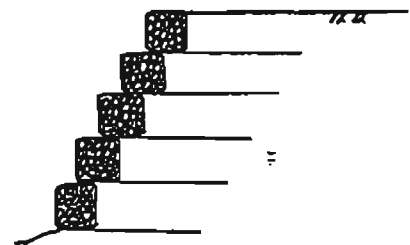
*timber-faced wall*



*modular block wall*



*tire-faced wall*



*gabion-faced wall*

Figure 1.2 GRS walls with different facings (after Wu, 1994)

resistance. Through the interface friction, the reinforcement *restrains lateral deformation of the soil* adjacent to the reinforcement, and consequently increases the stiffness and strength of the soil mass.

The improvement in the stiffness and strength can be evaluated in a number of ways. The triaxial tests conducted by Broms (1977) illustrate clearly the beneficial effects of geosynthetic reinforcements when they are strategically placed inside a soil mass. Figure 1.3 shows the results of two sets of triaxial tests performed on an unreinforced sand specimen (Curve 1 in Figure 1.3) and three reinforced sand specimens (Curves 2, 3 and 4 in Figure 1.3). The tests show that the reinforcements, when placed at locations that can effectively restrain lateral deformation of the soil, will increase the stiffness and strength of the soil. It is to be noted that the reinforcing effect is negligible at small strains. To mobilize the reinforcing effect, there needs to be a certain amount of lateral deformation, although the deformation needed is generally fairly small.

The effect of geosynthetic inclusion can also be evaluated by examining the results of finite element analysis of a soil-geosynthetic composite. Figure 1.4 shows the lateral stress distributions of an unreinforced soil mass and a reinforced soil mass. The latter has three layers of geosynthetic reinforcements placed at the top, middle and bottom of the soil mass. It is seen that the lateral stress in the reinforced soil mass is much higher than in the unreinforced soil mass. Moreover, the lateral stress in the reinforced soil mass is pronouncedly higher surrounding the reinforcements than away from the reinforcements. Figure 1.5 shows the vertical stress distributions of the two soil masses. It is seen that there is little difference between the reinforced and unreinforced soil masses.

Figure 1.6 shows a simple demonstration of the effect of geosynthetic inclusion. It shows a clean sand at its steepest stable angle (the angle of repose) and the same sand reinforced with strips of paper placed horizontally inside the sand. The inclusion of the paper allows the sand to assume a vertical slope in a stable state. Note that the paper at the face of the slope is needed to

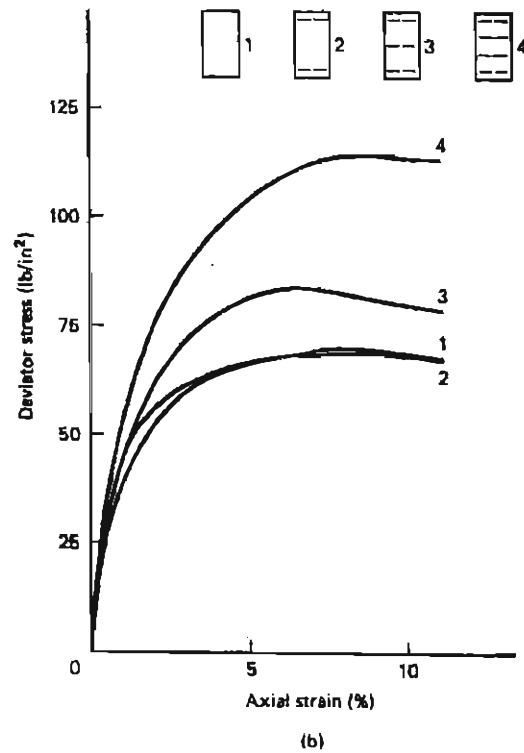
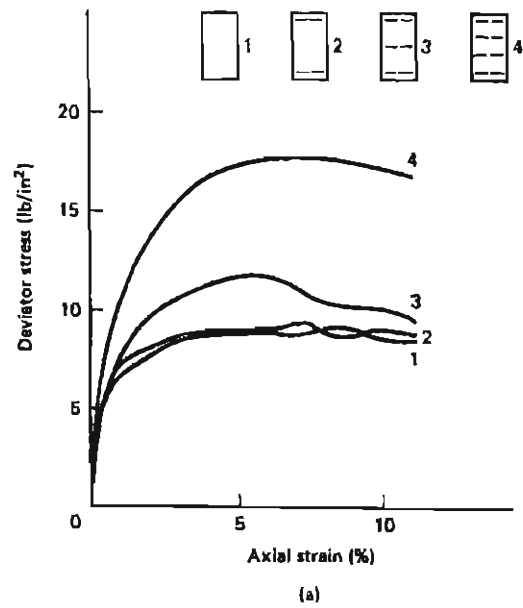


Figure 1.3 Triaxial Test Results of reinforced and unreinforced dense sand (a) at 3 psi confining pressure and (b) at 30 psi confining pressure (after Broms, 1977)

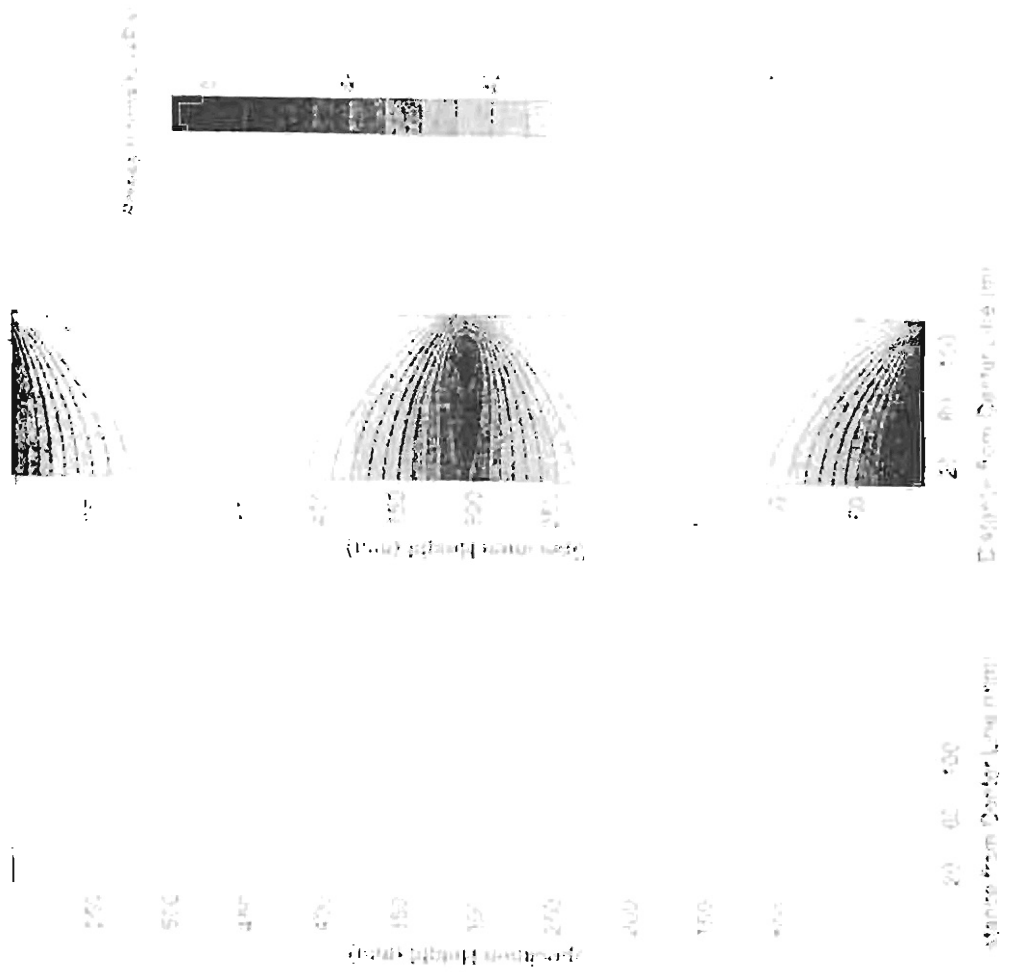


Figure 1.4 Lateral stress distributions of an unreinforced soil mass and a reinforced soil mass (after Ketchum and Wu, 2000)

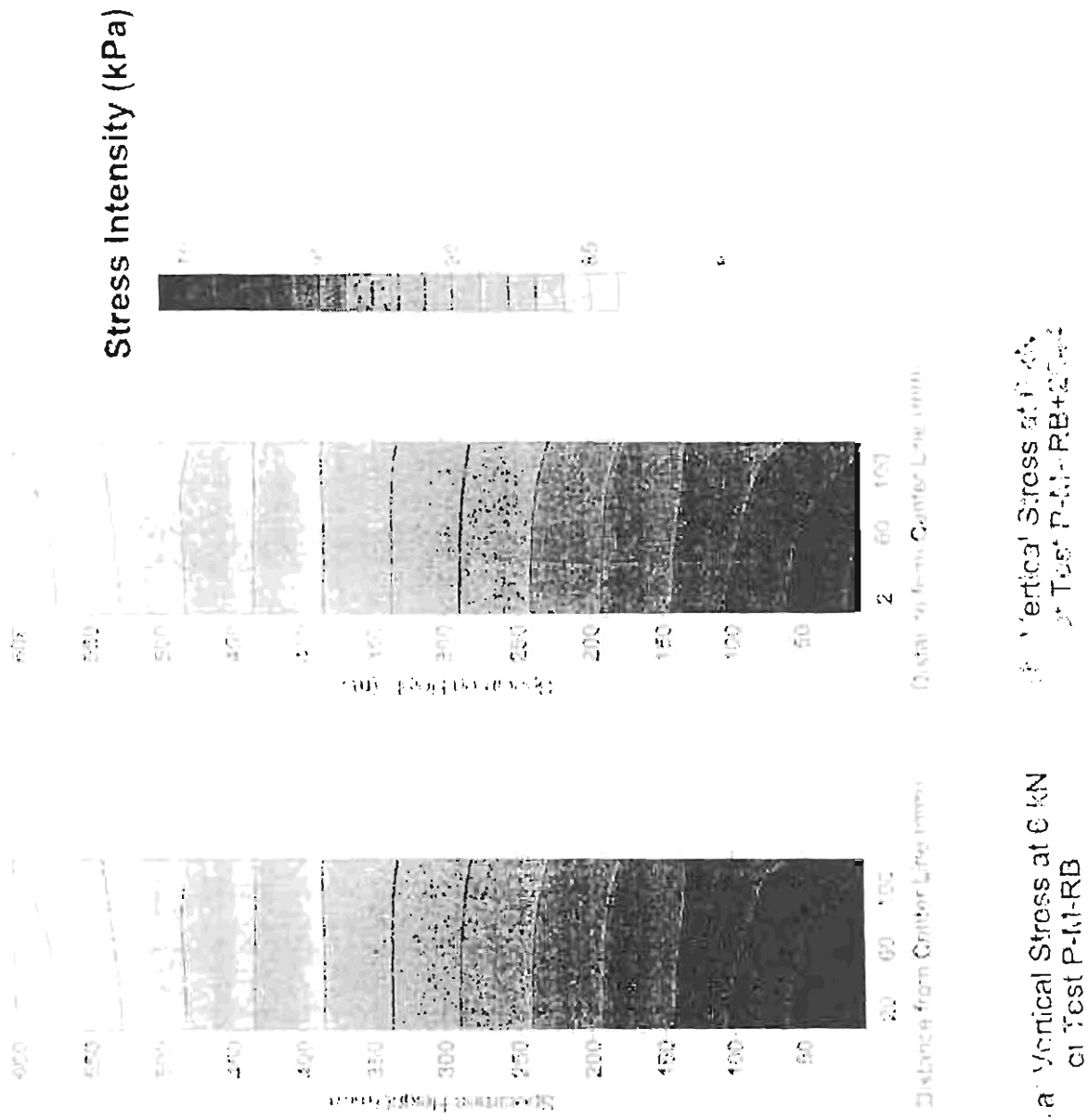
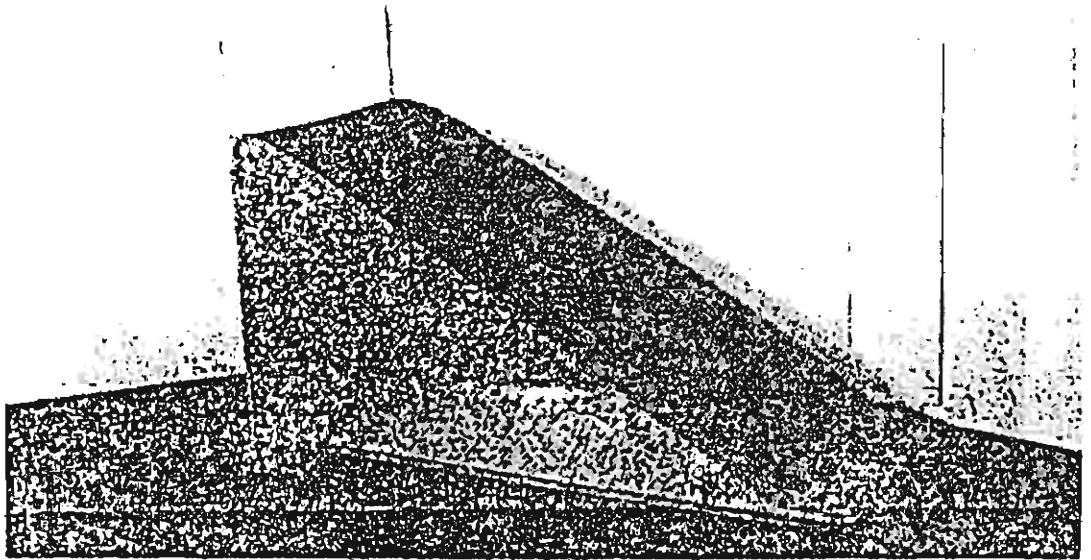


Figure 1.5 Vertical stress distribution of an unreinforced soil mass and a reinforced soil mass (after Ketchart and Wu, 2004)

(a) Unreinforced Sand (with maximum stable slope)



(b) Reinforced sand

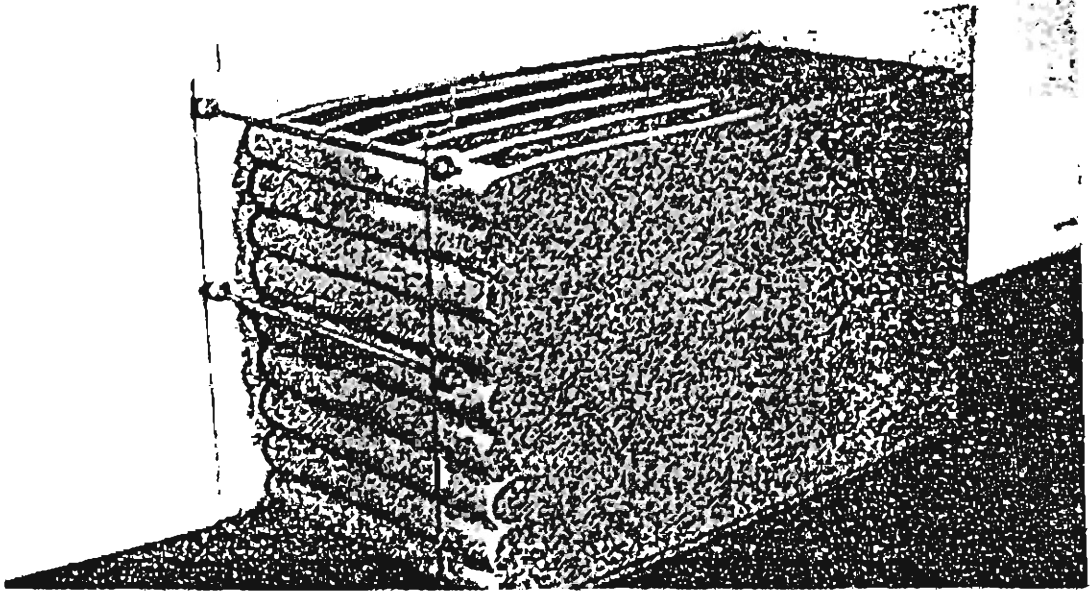


Figure 1.6 A clean sand (a) at its steepest stable slope when unreinforced, (b) reinforced with strips of paper (after Mitchell and Villet, 1987)

prevent running of sand although it does not provide any major load-carrying functions.

## **1.2 Internally Stabilized Wall versus Externally Stabilized Wall**

In the design of a "conventional" retaining wall (i.e., gravity, semi-gravity and cantilever walls), the objective is to design a retaining structure that is sufficiently stiff to withstand the earth pressure due to the weight of the soil mass behind the wall and the loads applied on the wall. These retaining walls stabilize a soil mass externally by "brutal" forces and are referred to as "externally stabilized retaining walls."

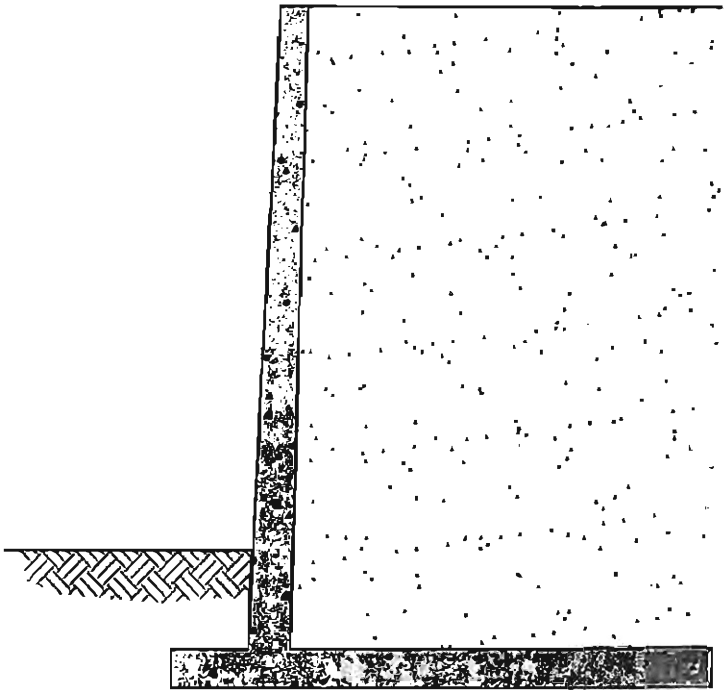
On the other hand, in the design of a GRS retaining structure (or, more precisely, a "pure" GRS retaining structure), the objective is to design a reinforced soil mass that will be sufficiently stable by itself without the need of any means of external support. As the soil mass in a "pure" GRS wall is stabilized internally by the inclusion of reinforcement sheets, the wall is referred to as an "internally stabilized retaining wall."

Note that the facing in an internally stabilized retaining wall is generally required to prevent sloughing of the vertical (or near vertical) surface of the reinforced soil mass. The facing also serves as a construction aid and as façade of a GRS wall. It is, however, not a major load-carrying element.

Figure 1.7 illustrates an internally stabilized retaining wall versus an externally stabilized retaining wall. It is important to point out that embedment of wall base beneath the ground surface is often needed to obtain sufficient resistance in an externally stabilized retaining wall. This is not the case with an internally stabilized retaining wall.

For an internally reinforced GRS wall, the effect of reinforcement spacing has been found to have a very strong effect on the wall performance. Michael Adams of the Federal Highway Administration has recently conducted a series of large-scale model tests of a GRS mass to investigate the effect of reinforcement spacing (see Figure 1.8). It was found that reinforcement spacing

- Externally Stabilized -



- Internally Stabilized -

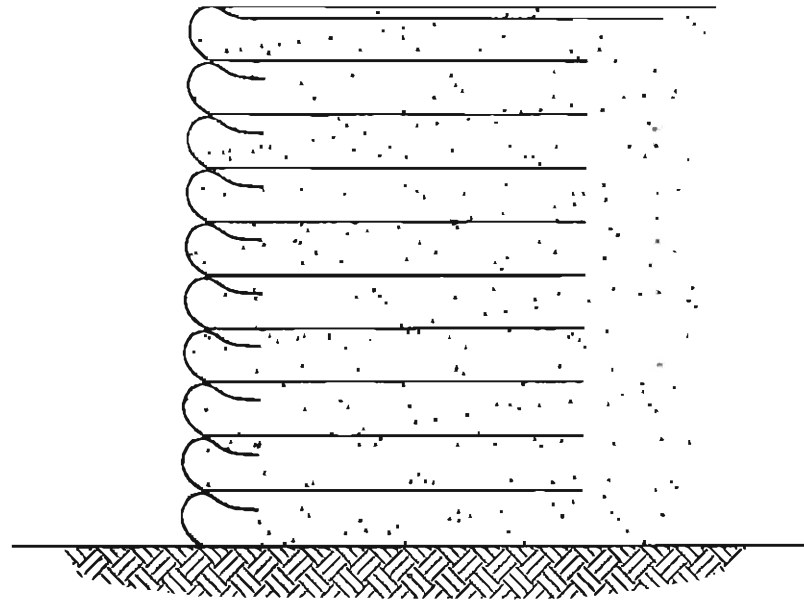


Figure 1.7 An internally stabilized wall versus an externally stabilized wall

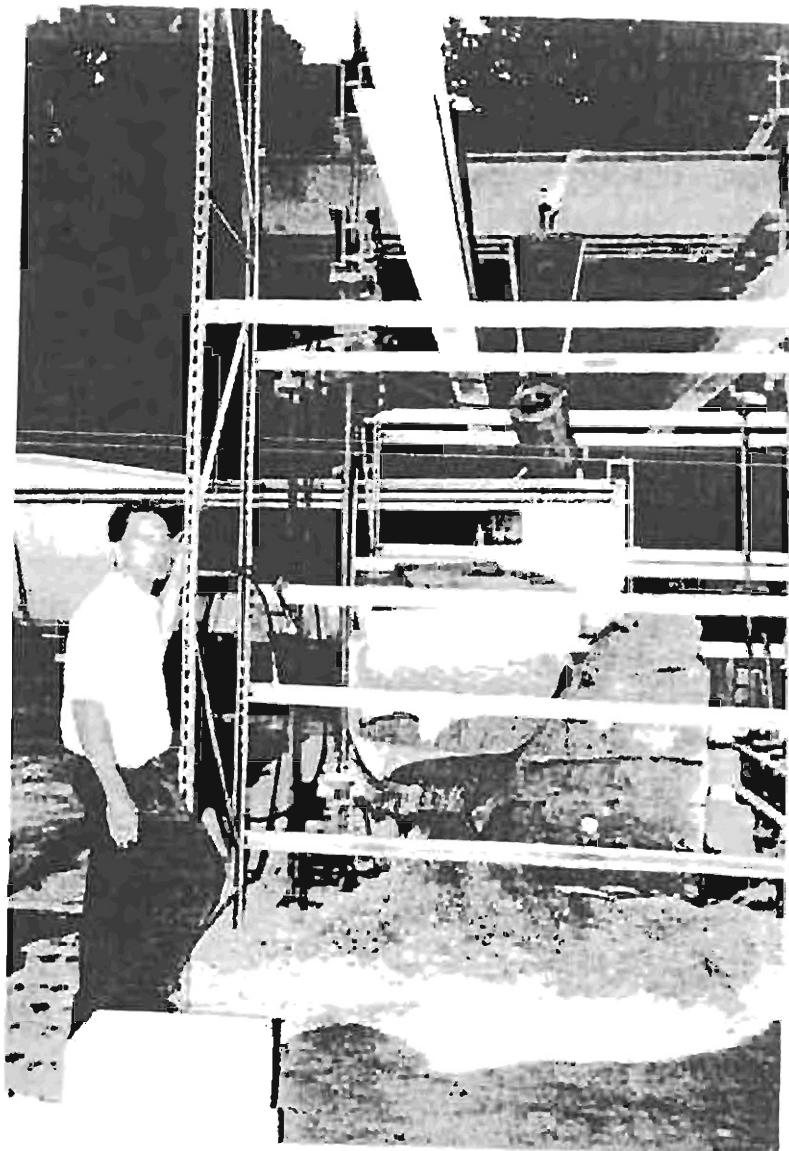


Figure J.8 A large-scale loading test of GRS mass (courtesy of M.L. Adams)

of 4 in. would produce a practically indestructible reinforced soil mass. The effect of reinforcement strength, on the other hand was of secondary importance.

The beneficial effect of smaller reinforcement spacing can also be seen from finite element analysis of a soil-reinforcement composite (Ketchart and Wu, 2001). Figure 1.9 shows the distribution of the minor principal stress ratio (the ratio of minor principal stress in a reinforced soil to the minor principal stress in a unreinforced soil) for a soil mass reinforced with three layers of reinforcement (at top, bottom and mid-height) at 12 in. vertical spacing. It is seen that the reinforcing effect does not propagate far from the reinforcement and that there is little interaction between the reinforcement layers at 12 in. reinforcement spacing. The implication is that vertical spacing less than 12 in. will have resulted in a stronger reinforcing effect.

### **1.3 Fundamental Deficiencies of the AASHTO Guidelines for Design and Construction of GRS Walls**

The AASHTO guidelines fail to account for the soil-reinforcement interaction and are fundamentally unsound. Three major fundamental deficiencies of the AASHTO guidelines are addressed below, including deficiencies concerning (1) the assumed failure mechanism, (2) the relationship between spacing and strength of reinforcement, (3) the assumed lateral earth pressure, and (4) the recommended safety factors.

#### **1.3.1 Failure Mechanism**

Stemming from the design methods for externally stabilized retaining walls, the AASHTO guidelines for design of GRS walls (referred to as one type of MSE walls by the AASHTO) as well as all other prevailing design methods are based on the concept of "tie-backs"; in other words the reinforcement extending beyond an assumed failure surface is considered as tension-resistant tie-backs for the assumed failure wedge.

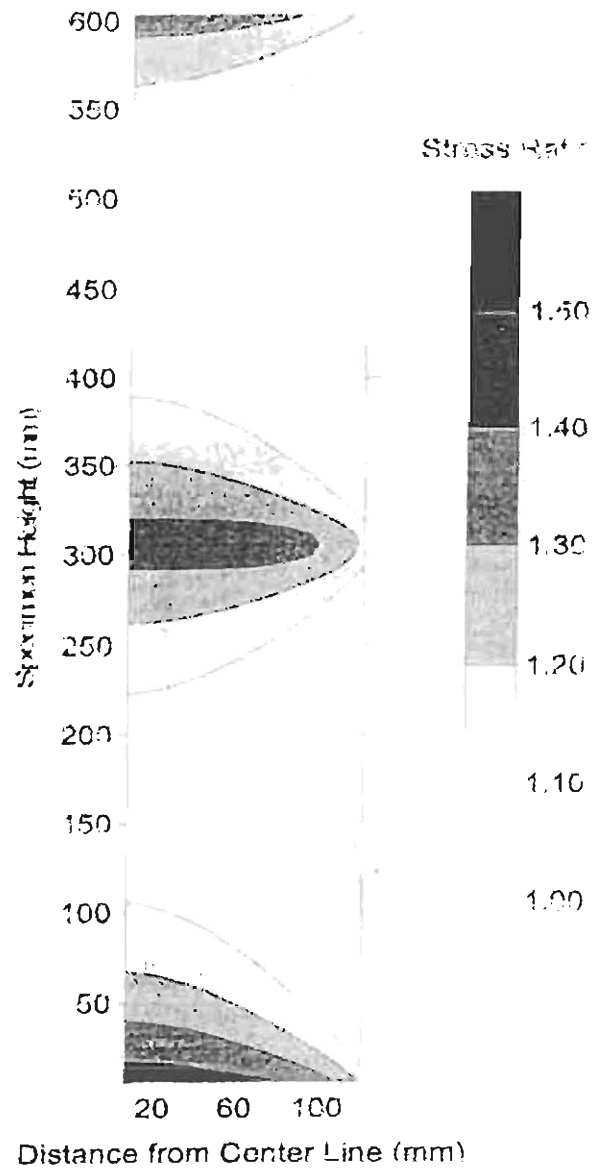


Figure 1.9 Distribution of minor principal stress ratio of a reinforced soil mass (after Ketchart and Wu, 2000)

Perhaps the best example to manifest the deficiency concerning the assumed failure mechanism is the experiment conducted by the Public Research Institute (PWRI) in Japan. The PWRI constructed a 6-m high GRS retaining wall in 1996. The wall face was concrete blocks and the backfill was a sandy soil reinforced with 6 layers of 3.5-m long polymer grid. The reinforcement in the test wall was also severed after construction. Figure 1.10 shows the sequence of cutting the reinforcements. Figure 1.10 also shows the maximum horizontal movement associated with the cutting of the reinforcements. It is seen that there was little movement due to the cutting of the reinforcements until Cut No. 55.

The AASHTO design guidelines will have predicted a failure condition to occur long before Cut No. 55. *The failure mechanism assumed in the design guidelines is clearly fallacious.*

From the standpoint of an internally stabilized retaining wall, the observed behavior is not at all "surprising." *A reinforcement sheet, whether continuous or not, can offer a similar restraining effect to lateral movement of soil and achieve a stable composite.* Note that the resulting stress distribution in the reinforcement is likely to be rather different for a continuous and a discontinuous reinforcement. The results of the PWRI experiment also suggest that long-term degradation of the reinforcement is not a design issue. The cutting of reinforcements can be considered as very severe degradation in that the reinforcement was degraded into pieces.

It should be noted that the above observations are supported by similar experiments constructed by John (1985) and by the AMOCO test wall (Ketchart and Wu, 1997), to be presented in Chapter 2.

### 1.3.2 Relationship between Spacing and Strength of Reinforcement

In the AASHTO design guidelines, reinforcement spacing is obtained by dividing the design strength (i.e., the allowable strength) by the lateral earth pressure,  $\sigma_h$  at a given depth, i.e.,

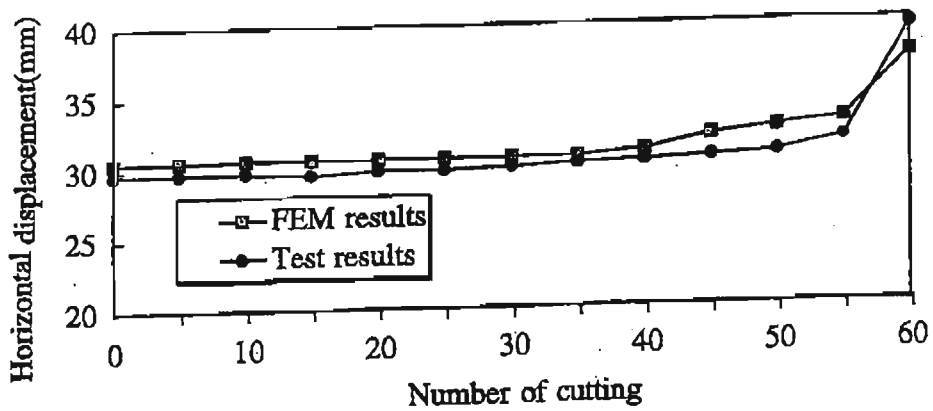
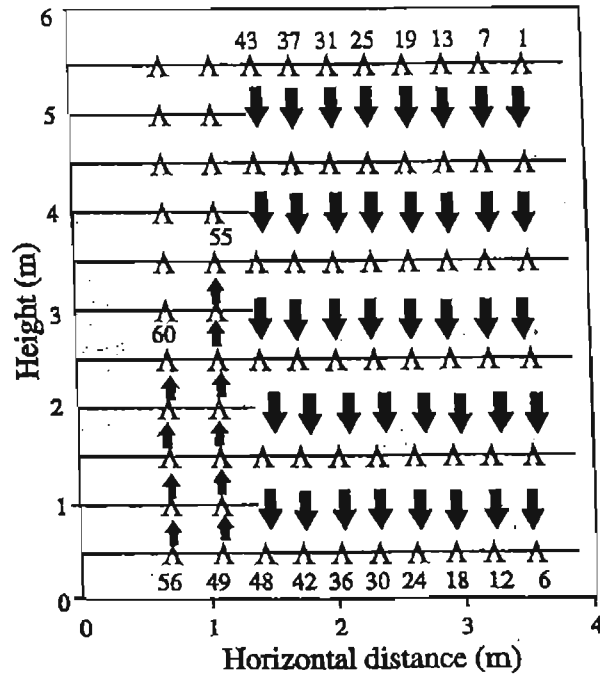


Figure 1.10 Sequence of cutting and the resulting maximum horizontal movement of the PWRI test wall

$$s = \frac{\sigma_{allow}}{\sigma_h} \quad \text{Equation 1.1}$$

The above Equation implies that for a given backfill (i.e., a given  $\sigma_h$ ), all GRS walls with their allowable strengths proportional to the spacing will behave the same. In other words, a GRS wall with a reinforcement of an allowable strength,  $\sigma_{allow}$ , at spacing,  $s$ , will behave the same as the one with a reinforcement of an allowable strength of  $2 * \sigma_{allow}$  at twice the spacing,  $2 * s$ .

In Michael Adams' large-scale experiments (see Section 1.2), a weak reinforcement at small spacing and a strong reinforcement (with several times strength of the weak reinforcement) at twice the spacing were load tested. The former reinforced soil mass was found to be much stronger than the latter. The experiment shows that the relationship between reinforcement strength and spacing given by Equation 1.1 is not correct.

It should be mentioned that Equation 1.1 encourages a designer to use stronger reinforcement at larger spacing, as larger spacing tends to minimize the efforts of reinforcement placement in construction. The fact, however, is that the use of a weaker reinforcement at smaller spacing will produce a much stronger reinforced soil mass.

### 1.3.3 Lateral Earth Pressure

The lateral earth pressure, the Rankine active earth pressure, assumed in the AASTO guidelines, is far from being true for an internally stabilized wall. This point will be addressed in detail in Chapter 2. An excellent case history to illustrate this deficiency in the AASHTO guidelines is the segmental GRS wall constructed in 1997 in Grand County, Colorado (see Figure 1.11). The backfill was a well-compacted granular soil. The reinforcement was woven polypropylene geotextiles. The facing of the wall was dry-stacked, common split-faced concrete blocks (of dimensions 8 in. by 8 in. by 16 in.) without any mechanical connections. The tallest section of the wall was 55-ft high. With the active Rankine earth pressure, a failure condition would have occurred.

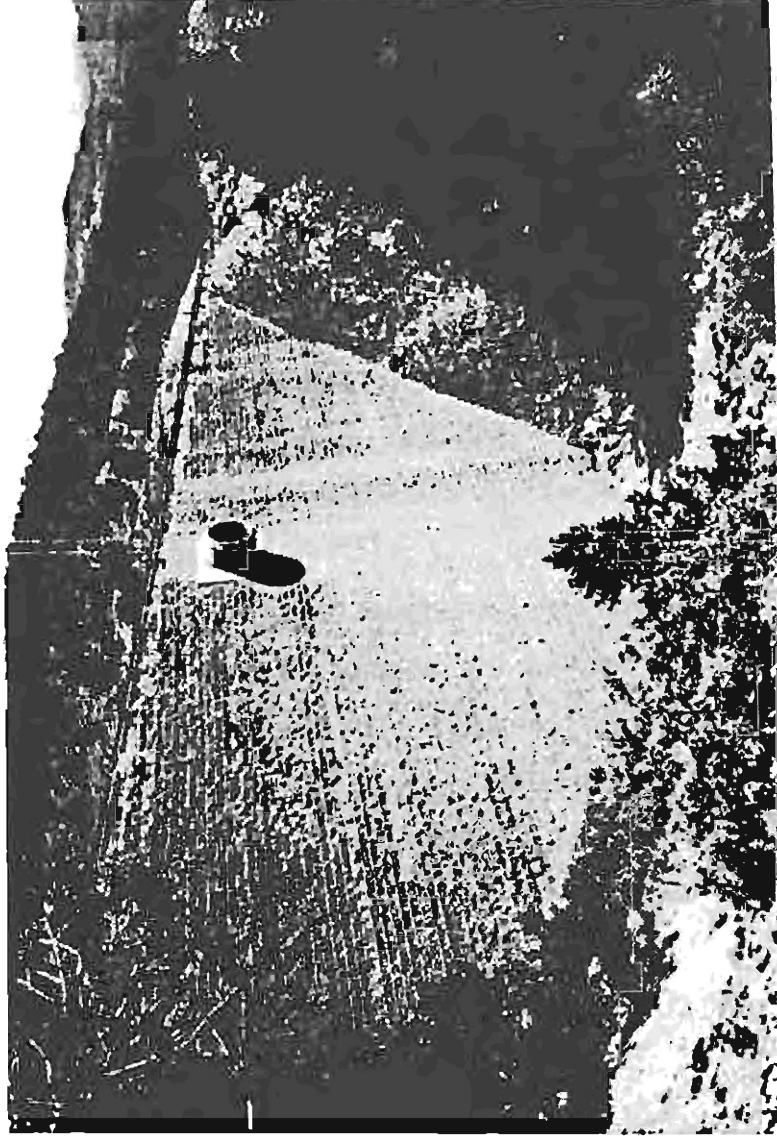


Figure 1.11 Grand county wall with largest height 55 ft (courtesy of R.K. Barrett)

However, the wall performed satisfactorily without any sign of distress or visible deformation.

#### 1.3.4 Safety Factors

As a result of the deficiencies described above, together with the use of somewhat arbitrary safety factors (as will be discussed later in Chapter 3 on proposed methods to account for long-term deformation), current design methods have typically been found to be overly conservative. A glaring example can be illustrated with the Denver Test Wall (Wu, 1992a).

Figure 1.12 shows the plane strain test facility in which the Denver test wall was conducted. The test frame was rigid and its sidewalls were lubricated near frictionless (friction angle less than  $1^\circ$ ). The test section can, therefore, be regarded as a typical "slice" of a very long wall. Great care was exercised to ensure that the soil in the test wall was as uniform as can be achieved. Figure 1.13 shows that the soil was being placed painstakingly using an air-pluviation technique. The air-pluviation technique has been known to produce the most uniform placement of a sand backfill. In addition, the soil properties were carefully determined by various methods. Therefore, any discrepancies between the measured and computed values can be attributed to the deficiencies of the computational (i.e., design) method.

The wall with a granular backfill was loaded to failure by incrementally increasing the surcharge pressure. Failure occurred at 29 lb/in<sup>2</sup> surcharge pressure. Table 1.1 shows the failure surcharge pressure from various design methods (Claybourn and Wu, 1992). Every design method gives a much lower failure load than the measured value.

It is important to point out that the failure surcharge pressures presented in Table 1.1 were computed based on a safety factor of one (1), although all these design methods require the use of various safety factors (Claybourn and Wu, 1991 and 1993). Had the safety factors suggested by each design method been adopted, the design load would have been much smaller. In other words,



Figure 1.12 The plane strain test facility for the Denver test wall (after Wu, 1992a)

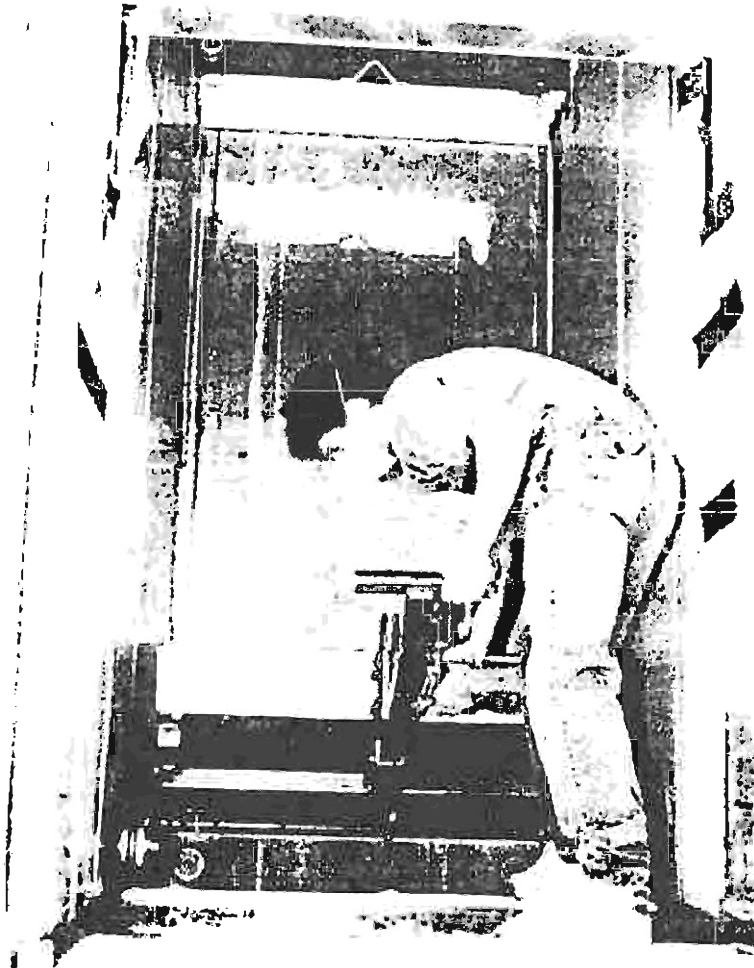


Figure 1.13 Placement of granular backfill with air-pluviation (after Wu, 1992b)

Table 1.1 Failure surcharge pressures obtained from various design methods (Claybourn and Wu, 1992)

		Failure Surcharge (measured value = 29 psi)
Design Method (with $F_s = 1$ )	U. S. Forest Service (Steward, et al., 1977& 1983)	0.7 psi
	Broms (1978)	6.2 psi
	Collin (1986)	7.3 psi
	Bonaparte, et al. (1987)	0.9 psi
	Leshchinsky and Perry (1987)	5.2 psi
	Schmertmann, et al. (1987)	6.0 psi
	GeoServices (1989)	0 (cannot be built)

the differences between the measured and calculated surcharge pressures shown above are a direct result of *the deficiencies of the design methods*. They are not an indication of any intended safety margins.

#### **1.4 Proposed Revisions of the AASHTO Guidelines**

Although there are fundamental deficiencies in the current AASHTO guidelines for GRS walls, a number of revisions can be made before a rational design method becomes available. This report presents four proposed revisions to the AASHTO guidelines for design and construction of GRS walls (AASHTO, 1996). The proposed revisions are regarding:

- (1) lateral earth pressure on wall facing
- (2) long-term deformation
- (3) truncated reinforcement at wall base and the CTI tails
- (4) embedment and leveling pad.

For each of the proposed revisions, the literature on research findings and measured performance is summarized. The limitations and practical implications are also discussed.

It is to be noted that the proposed revision for lateral earth pressure on wall facing applies only to segmental GRS walls (with facing comprising dry-stacked modular blocks). The other proposed revisions, on the other hand, apply to non-propped GRS walls in general. The GRS walls are considered to have the following features:

- The wall face is vertical or near-vertical (no less than 80° from horizontal).
- No prop (temporary bracing) is used in the construction of the wall.
- The backfill is predominantly granular (say, no more than 20% of fines, with liquid limit not greater than 35 and plasticity index not more than 8), with a maximum particle size of 3 in., and in a non-aggressive environment (say, a pH value between 5.0 and 9.5).
- The backfill is well compacted (i.e., at least 95% of the Standard

Proctor or 90% of the modified Proctor) and with placement moisture at  $\pm 2\%$  of the optimum.

- The maximum back slope is not more than  $\tan^{-1}(\tan \phi / 1.3)$ .
- The foundation soil is competent (i.e., undrained shear strength, in psf, greater than  $\{30 * \text{wall height in feet}\}$  for a clayey foundation, and standard penetration blow count greater than 8 for a granular foundation).

Note that *there is no theoretical limit on the wall height*, although there may be practical height limitations in considerations of economics and visual appearance.

## **Chapter 2**

### **LATERAL EARTH PRESSURE ON WALL FACING**

The active Rankine lateral earth pressure employed by the AASHTO guidelines for GRS walls was adopted from the lateral earth pressure developed for gravity or cantilever retaining walls, referred to as conventional retaining walls. The Rankine earth pressure assumes that the soil is uniform and that every point in the soil mass, including those in contact with the wall face, is “at failure”. The lateral earth pressure on the wall face of a segmental GRS wall is typically very different from the Rankine earth pressure because the mass behind the wall face is no longer “uniform” (due to the geosynthetic inclusion) thus the lateral earth pressure at wall face is typically very different from that in the reinforced soil mass. The following sections describe (a) a discussion of lateral earth pressure in a GRS wall, (b) literature related to the lateral earth pressure of GRS walls, (c) the proposed earth pressure diagram, and (d) the limitations and practical implications of the proposed earth pressure diagram. It is to be noted that this proposed revision applies only to segmental GRS walls.

#### **2.1 Lateral Earth Pressure on the Facing of a GRS Wall**

As described in Chapter 1, in the design of a GRS retaining structure (or a “pure” GRS retaining structure) the objective is to design a reinforced soil mass that will be sufficiently stable by itself without any means of external support. The facing of an internally stabilized retaining wall is to prevent sloughing of the reinforced soil mass. The facing also serves as a construction aid. It is, however, not a major load-carrying element.

When properly designed and constructed, the lateral earth pressure of an internally stabilized wall will approach nil at any depth where there is a reinforcement sheet. The lateral earth pressure at the wall face is, therefore, merely the sum of the earth pressures between adjacent reinforcement sheets

(called the "bin pressure"). Note that the bin pressure is practically independent of wall height and is strongly affected by the reinforcement spacing.

The fact that a reinforced soil mass, with small reinforcement spacing, will only exert a small earth pressure on the facing element can be explained by considering the following scenario -- Visualize a body that produces no lateral deformation under self-weight and external loads (see Figure 2.1), if a facing element is placed in front of this body, the facing element will not experience any lateral pressure from the body. If the reinforcement can effectively restrain lateral deformation of a soil mass, the lateral earth pressure will be nearly zero at the depths of all the reinforcements. The lateral earth pressure acting on the wall face will then be the "bin" pressure induced between adjacent reinforcement sheets. The magnitude of this lateral earth pressure will depend largely on the rigidity of the facing. The greater the facing rigidity, the larger the lateral pressure will be. If the facing rigidity allows the active condition to be developed, the lateral earth pressure will be fairly small for closely spaced reinforcements.

There is a concern with internally stabilized walls that the deformation of these structures may be too large due to the flexibility of the system. Theories and experiences for design of conventional earth retaining structures suggest that this will not be a problem. With a well-compacted granular backfill, the movement required to mobilize the active condition is typically on the order of  $0.001H$  ( $H$  = wall height) and always less than  $0.005H$ . For a 15-ft high wall, the typical wall movement to develop the active condition will be around 0.2 in., and always less than 0.9 in.

The AASHTO design guidelines for GRS walls are in fact for a "hybrid" system -- a mix of externally stabilized and internally stabilized wall. The "hybrid" wall employs geosynthetic reinforcement to create a reinforced soil mass and at the same time uses a high resistance facing to resist the earth pressure. The design method "borrowed" from the design concepts for externally stabilized retaining walls (i.e., the Rankine earth pressure theory),

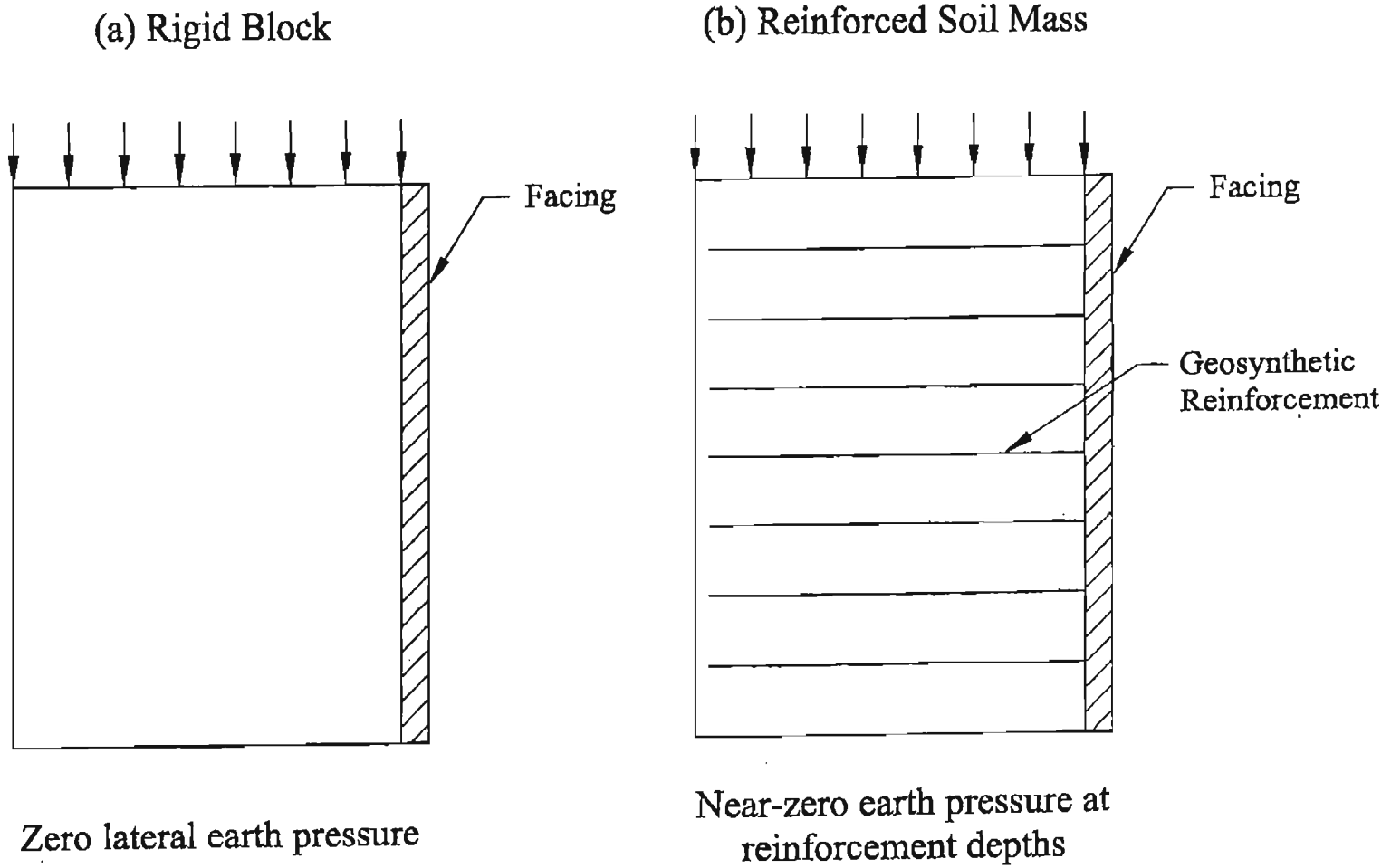


Figure 2.1 (a) A rigid block with no lateral deformation, versus (b) a reinforced soil mass

and considers the reinforcement sheets as tie-backs. Such a design method encourages the use of heavy facing blocks and the use of pins and lips to increase resistance to lateral earth pressure. The stronger the resistance, the higher is the earth pressure that needs to be overcome. As a result, thousands of “connection strength” tests have been conducted.

## **2.2 Literature on Lateral Earth Pressure of GRS Walls**

Owing to the fact that lateral earth pressure is very sensitive to movement and the fact that measurement of lateral earth pressure has often been found to be somewhat unreliable, most of the literature on the lateral earth pressure of GRS walls described below involves only indirect implication rather than direct measurement of the lateral earth pressure.

For finite element analysis of the lateral earth pressure, it is a common mistake to take the lateral stress in the soil elements adjacent to the facing as the lateral earth pressure on the wall. This procedure gives a good approximation for analysis of conventional retaining walls, but can be drastically misleading for segmental GRS walls. For the latter, the lateral earth pressure acting on the wall facing can be much smaller than the horizontal stresses in the soil. A good approximation of the lateral earth pressure can be obtained by dividing the reinforcement force at the wall face by the vertical spacing of the reinforcement, assuming there is little interaction between the reinforcements.

### ***2.2.1 Reinforced Soil Mass Loading Experiments, McLean, Virginia (Adams, 1997b)***

From 1996 to 1997, Michael Adams conducted a series of field experiments to demonstrate the concept of reinforced soil at the Turner-Fairbank Highway Research Center in McLean, Virginia. Figure 2.2 shows a soil mass reinforced with layers of weak cheese cloth carrying 10 solid concrete blocks. In contrast, the same soil mass without any reinforcement collapsed as the second concrete block was placed on top of the soil mass (see Figure 2.3).

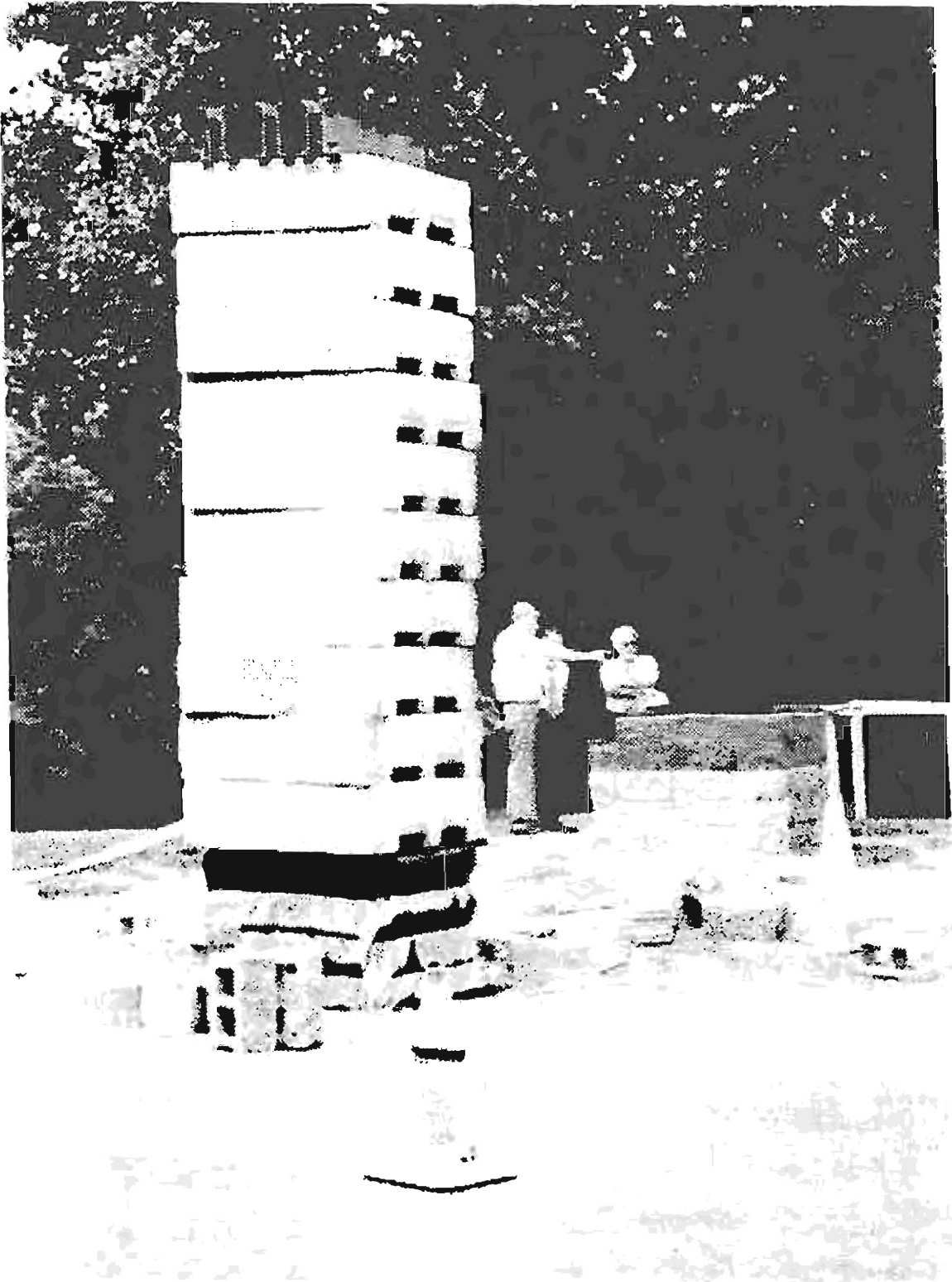


Figure 2.2 A soil mass reinforced with cheese clothes carrying loads of 10 concrete blocks (after Adams, 1997b)

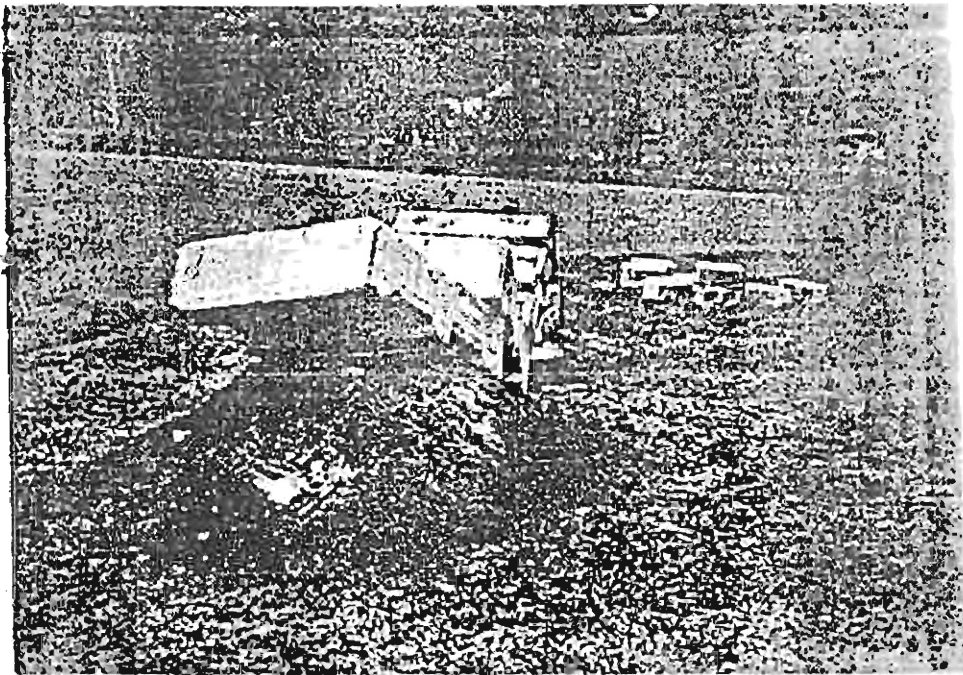


Figure 2.3 A unreinforced soil mass collapsed under loads of two concrete blocks (after Adams, 1997b)

It is evident that the reinforced soil mass can withstand its self-weight and significant external loads in the absence of any facing elements. The presence of the cheese cloth (the reinforcement), although of very low strength, was able to restrain the lateral deformation of the soil mass. If a "flexible" facing is placed in front of the soil mass, there will be little lateral earth pressure.

### *2.2.2 Bed Sheet Reinforcement Loading Test, Rifle, Colorado (Barrett, 1996)*

In 1996, Robert Barrett of the Colorado Department of Transportation conducted a demonstration project to show the load-carrying capacity of a reinforced soil mass. The soil mass was approximately 6 ft by 6 ft by 6 ft and was reinforced with layers of bed sheet at 8-in. vertical spacing. The bed sheet has a wide-width strength of less than 20 lb/in. The backfill was a silty gravelly sand, known locally as road base. The reinforced soil mass was constructed with Jersey barriers as forming elements, which were removed after construction. Jersey barriers were used as deadweight to load the reinforced soil mass. There was no visible lateral deformation of the reinforced soil mass carrying 21 Jersey barriers (see Figure 2.4). The demonstration indicates that the reinforced soil mass can safely assume a vertical face without external support. Again, any "flexible" facing placed over the fill will experience very small lateral earth pressure.

### *2.2.3 Commerce City Walls, Commerce City, Colorado*

In 1994, the Colorado Department of Transportation constructed a 15-ft high GRS wall in Commerce City, Colorado (see Figure 2.5). The backfill was a road base material. Two types of concrete blocks were used as facing: Amastone block and Keystone block. Amastone block is an 8 in. by 16 in. face by 10 in. deep split-faced concrete block with 2 in. wall thickness. The Amastone blocks were not filled during construction. Keystone block is an 8 in. by 16 in. face by 12 in. deep solid split-faced concrete block. The reinforcement was Tensar UX1400 geogrid. The reinforcement was placed at 12 in. vertical

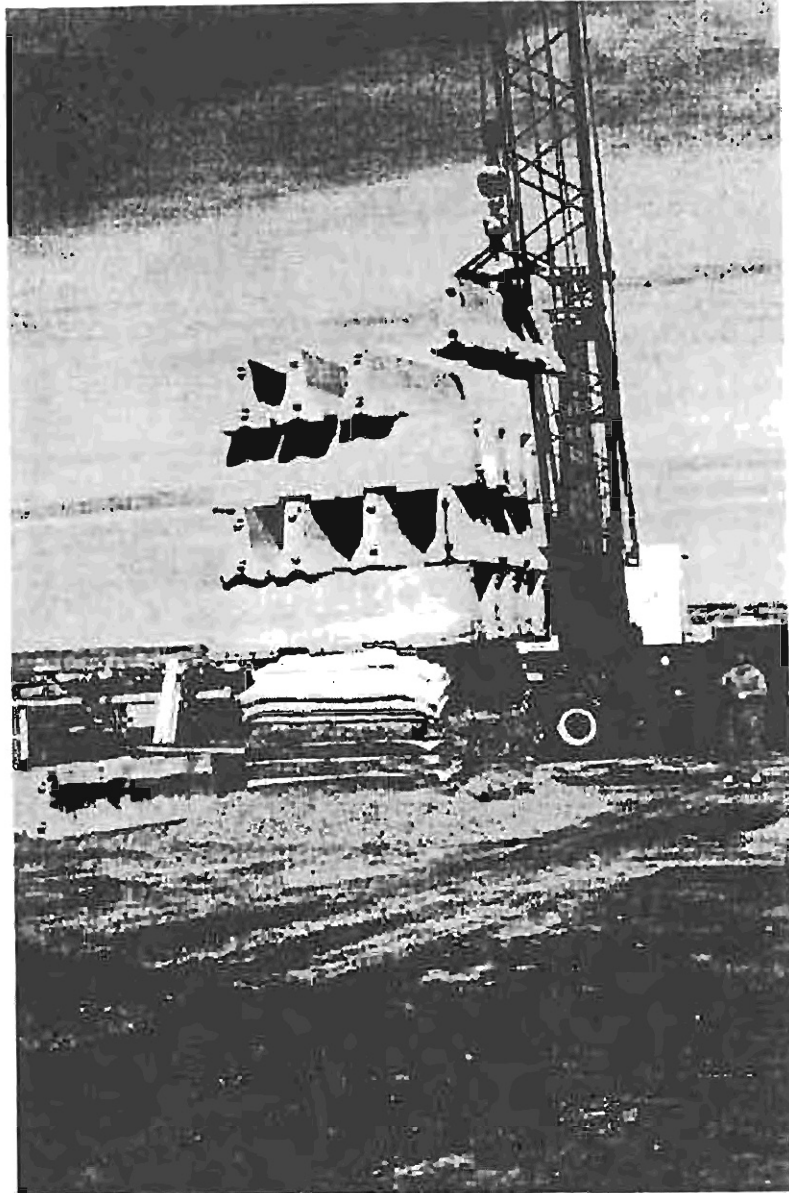


Figure 2.4 Loading test of a soil mass reinforced with bed sheets (courtesy of R. K. Barrett)



Figure 2.5 Loading test of the Commerce City wall

spacing and was not attached to the block facing. Instead, the block facing was attached to the reinforced soil mass by means of a "tail" of Trevira 1125 (a weak needle-punched geotextile) placed between blocks and extended 3 ft into the reinforced soil mass. Figure 2.6 shows the cross section at the middle of the wall. Note that the wall was not embedded and that the reinforcement was in a truncated configuration.

Metal wires were taped securely to the Trevira geotextile at the connection to the facing block (immediately behind the facing block) prior to placement of backfill. After the wall was constructed, a surcharge load of approximately 40,000 lb, in a cantilevered configuration, was placed on top of the wall. The load was applied to the reinforced soil mass and did not rest on the facing blocks. The wires were then heated to cut the geotextile and sever all connection between the facing blocks and the reinforced soil mass. Several facing blocks were removed afterwards to allow access to verify that the geotextile connections had indeed been severed (see Figure 2.7).

The wall was instrumented with linear potentiometers and measurement hook points to monitor the lateral movement of the facing. Four potentiometers were mounted along the height of the wall. Each potentiometer was enclosed in a 1 in. diameter PVC pipe with the stylus extended and attached to the facing blocks to measure the movement of the facing relative to the reinforcement. Two 3 in. by 3 in. by 0.25 in. angle iron posts were set in front of the wall to measure horizontal movement of the wall at seven hook points on the wall face.

The measured results indicated that there was no increased rate of movement as the geotextile connections were severed and that the maximum lateral movement of the wall, when extrapolated over 100 years, would be between 1.3 and 1.6 in. The tests indicated that the lateral earth pressure on the facing was likely to be small.

#### 2.2.4 AMOCO Test Wall (Ketchart and Wu, 1997) and UK Test Wall (John, 1985)

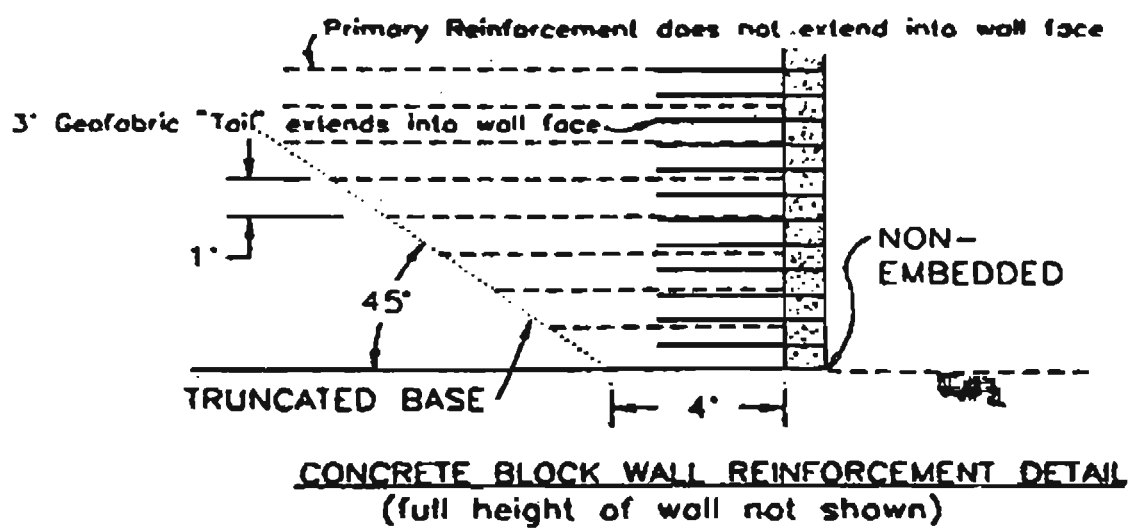
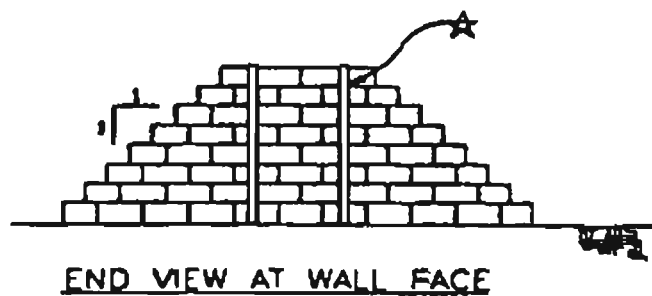


Figure 2.6 Cross-section of the Commerce City wall



Figure 2.7 Inspection of severed geotextile connection to wall face

A loading test of a GRS wall was conducted in 1997 at the University of Colorado at Denver. The test wall was 9.5 ft high and constructed inside the Denver test wall plane strain loading facility described in Section 1.3. The GRS wall was reinforced by four layers of Amoco 2044 woven polypropylene geotextile. The reinforcement was 60 in. long and placed at 30-in. vertical spacing (see Figure 2.8). The backfill was a road base material. The facing blocks comprised fairly heavy “diamond blocks” with a built-in lip at the edge.

A unique feature of this test wall was that four nichrome wires were attached to the geosynthetic reinforcement at selected locations along its length, including one wire immediately behind the wall face (i.e., near the connection), as depicted in Figure 2.8. These nichrome wires, when connected to a power source, can produce high heat and sever the reinforcements inside the GRS wall.

A rubber bladder, installed over the top surface of the wall, was employed to apply surcharge pressure. After the wall was constructed, surcharge pressure was applied in increments until it reached 15 psi. A maximum lateral movement of 0.35 in. was measured at approximately 9 ft above the base. The pressure was maintained for 45 days. The creep movement was less than 0.2 in. The reinforcement sheets were then severed by heating the nichrome wires. The additional movement due to severance of the reinforcement was negligible.

Based on the results of the test, the following conclusions can be made:

- The lateral earth pressure on the wall face is likely to be small, even with the fairly heavy facing blocks. The lateral earth pressure was apparently not high enough to move the facing blocks.
- A reinforcement sheet, whether continuous or not, offers a similar effect of restraining lateral movement of soil, although the resulting stress distribution is likely to be rather different.
- Long-term degradation of the reinforcement is not a design issue.

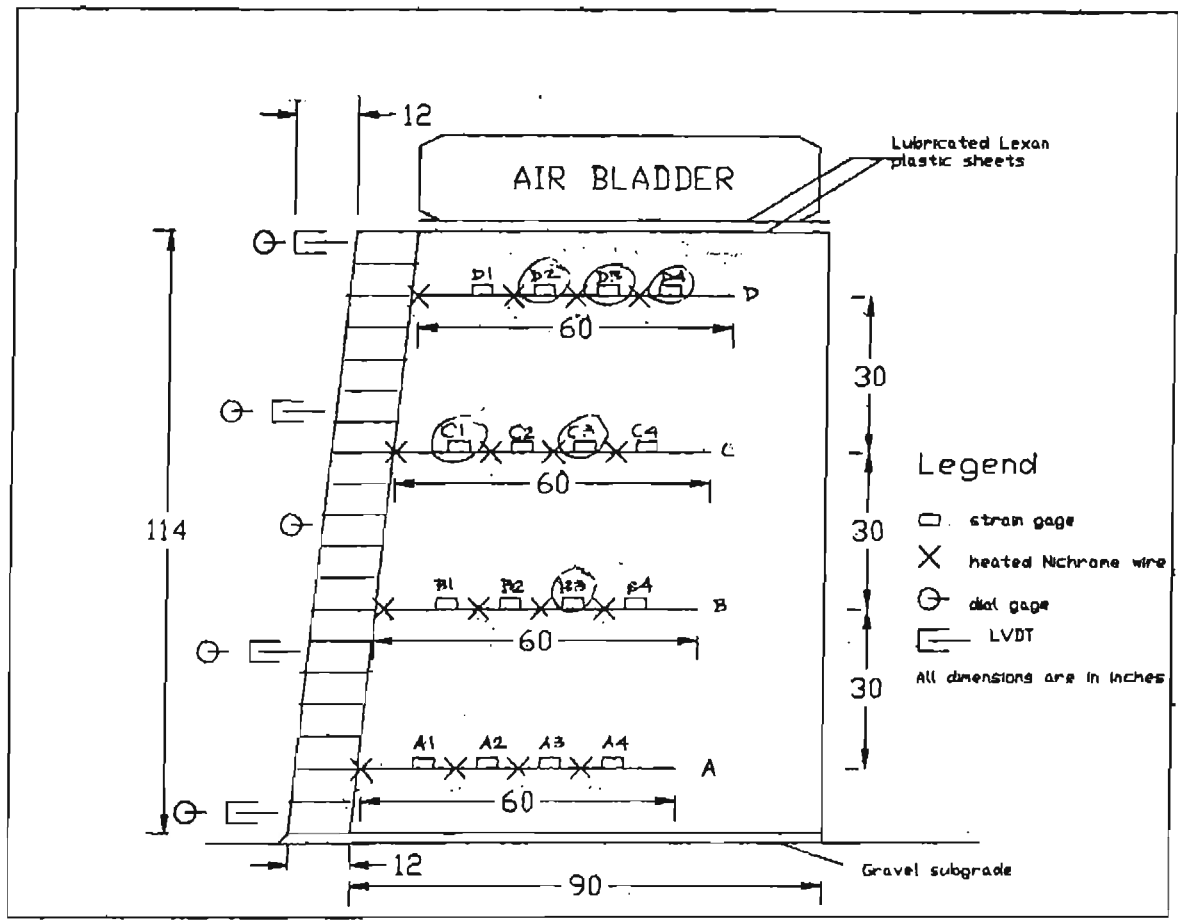


Figure 2.8 Cross-section of the Amoco test wall (after Ketchart and Wu, 1996)

Note that the tests simulated a very severe degradation state in that the reinforcement was degraded into pieces.

- *The failure surface assumed in nearly every prevailing design method, including the AASHTO design method, is fallacious.*

The above conclusions are supported by the tests constructed by John (1985) and by the tests conducted at the PWRI in Japan (see Section 1.3). John (1985) cut the reinforcement length in stages and measured the connection loads between the reinforcement and the facing panels. Figure 2.9 shows the connection loads at week-70 of the test, with the associated reinforcement configuration depicted in the Figure. It is seen that the retaining wall was stable despite the severed reinforcements.

#### 2.2.5 *Full-Scale Loading Test of an IFF Reinforced Soil Retaining Wall (Wu at al., 1993)*

A new reinforced soil retaining wall system, referred to as the Independent Full-height Facing (IFF) reinforced soil retaining wall was developed by the Colorado Department of Transportation in 1992. To examine the feasibility and performance of this new retaining wall system, a full-scale loading test was conducted at the University of Colorado at Denver.

As shown in Figure 2.10, the IFF reinforced soil wall system has three major components: full-height reinforced concrete panels (to serve as facing), reinforced soil mass (comprises the backfill and layers of reinforcement), and face anchors (to attach the facing panel to the reinforced soil mass). Note that the face anchor can take many different forms. The face anchor shown in Figure 2.10 takes the form of straight shaft with round anchor plates.

To construct an IFF reinforced soil retaining wall, the facing panel was first erected with the aid of temporary bracing. The reinforced soil mass was then constructed behind the facing by installing layers of the reinforcement in compacted fill at prescribed vertical spacing. The face anchors were installed at selected heights to connect the facing panel to the reinforced soil mass. The

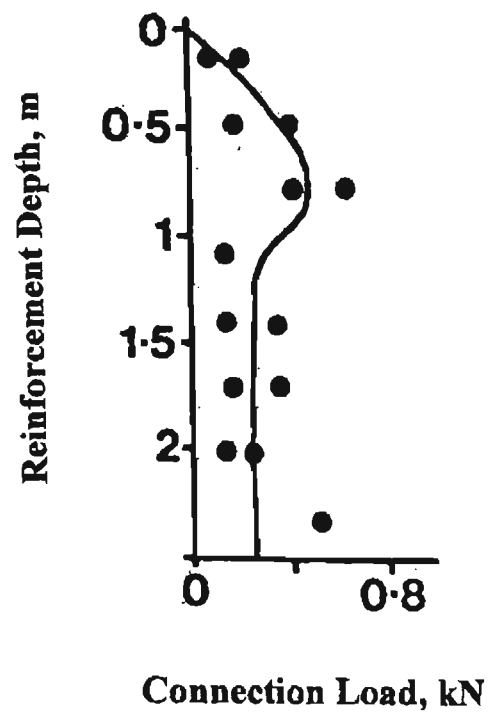
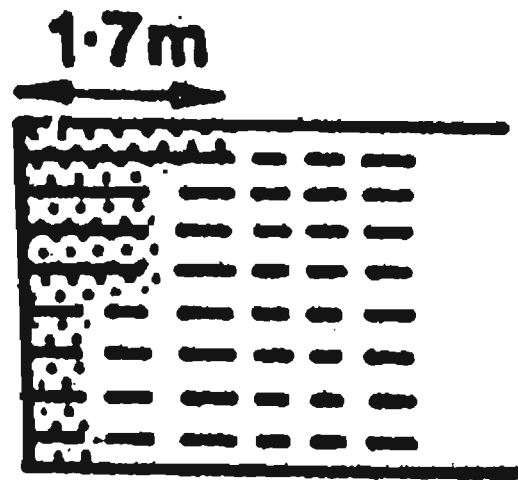


Figure 2.9 Connection loads with severed reinforcements at different depths (after John, 1985)

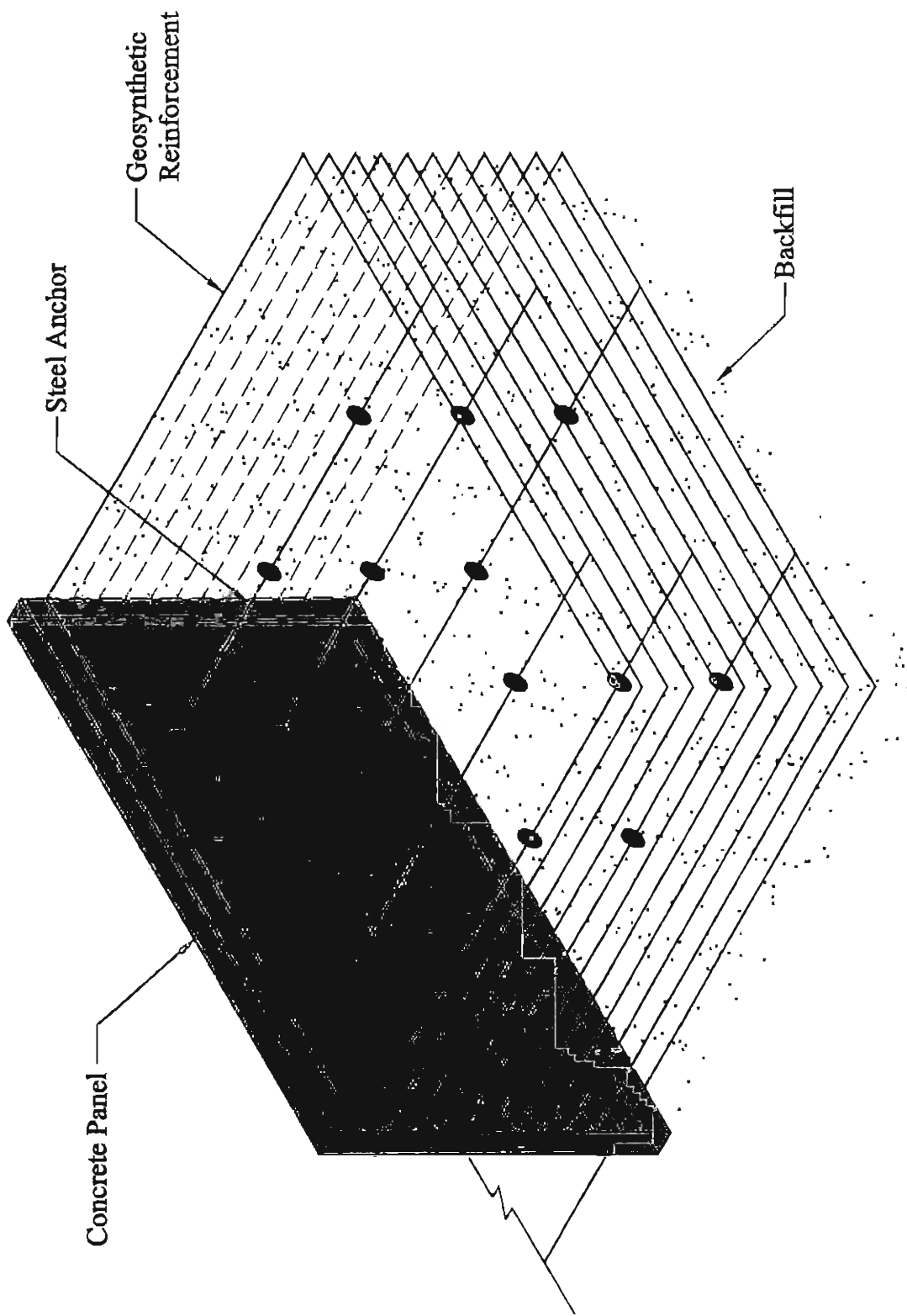


Figure 2.10 An IFF reinforced soil wall (after Wu, et al., 1993)

temporary bracing was removed after the facing was securely attached to the reinforced soil mass.

The IFF wall system has a number of distinct characteristics over the conventional cantilever reinforced concrete retaining wall. They are:

- Construction of the IFF wall is rapid and relatively easy. Construction typically requires little or no over-excavation. Construction does not require on-site concrete formwork.
- The IFF wall, although constructed with rigid concrete facing, is more flexible than the conventional reinforced concrete wall; therefore, it can withstand larger foundation settlement. The facing panel rests directly on the ground (or on a narrow footing if the ground is "weak"). The "deformable" connection between the anchor and facing panel allows movement of the facing panel when the lateral thrust becomes "excessive." The final position of the facing panel can be adjusted to achieve proper alignment.
- The IFF wall is low in total cost. The total cost of the MSB wall may be as low as 1/3 or even 1/2 of that of a comparable cantilever reinforced concrete retaining wall.
- The IFF wall can potentially accommodate large settlement of highly compressible backfill without causing distress in the facing panel.

A full-scale loading test was conducted inside the Denver wall loading facility (see Section 1.3.4) to investigate the performance of an IFF wall. In order to achieve better control of the test conditions, the loading test was conducted inside the Denver test wall testing facility at the University of Colorado at Denver (see Section 1.3). The wall was 3 m high and 1.2 m wide in a plane strain condition. A uniform Ottawa sand was used as backfill. The backfill was reinforced with 10 layers of heat-bonded nonwoven geotextile at 30 cm vertical spacing. The reinforcements were not attached to the facing panel. They were simply laid horizontally against the facing at prescribed heights. Four steel anchors were employed to attach the facing panel to the reinforced soil mass

through sliding-yielding "D-connections" (see Figure 2.11 for the close-up of the "D-connection"). The D-connection not only allows the anchor to slide downward with the fill, but also allows outward deformation when the lateral earth pressure becomes excessive. After construction of the wall was completed, four equal increments of surcharge, 34.5 kPa (5 psi) each, were applied to the top surface of the wall.

A number of instruments were installed to monitor the performance of the wall during and after construction. The instruments include six two-component load cells, high-elongation strain gages, digital dial indicators, and a lubricated latex grid system.

The measured behavior indicated that the lateral thrust acting on the facing panel was very small. Under a surcharge pressure of 138 kPa (20 psi), the average tensile forces were 3.43 kN (770 lb) in the top two anchors and 1.49 kN (335 lb) in the bottom two anchors. In the Rankine active condition, the lateral thrust would have been 145.9 kN (32,800 lb).

It should be mentioned that another loading test with road base as backfill was subsequently conducted (Helwany, 1994). The lateral thrust on the wall face was, again, found to be very small. After the test was completed, the facing panel was removed and the exposed face of the reinforced soil mass was spray-painted to examine surface integrity. The soil mass remained stable during the next 42 days until the test was disassembled (see Figure 2.12).

#### **2.2.6 Fox Wall, Denver, Colorado (Ma and Wu, 2000)**

A new retaining wall was designed and constructed by the Colorado Department of Transportation in 1996 for the ramp connecting Northbound Interstate-25 and Interstate-70. The retaining wall, referred to as "Fox wall", employed the Independent Full-height Facing (IFF) reinforced soil retaining wall system described in Section 2.2.5. This retaining wall system was adopted primarily because it did not require over-excavation in front of the wall, which allowed the traffic to remain open during construction and alleviated the need to

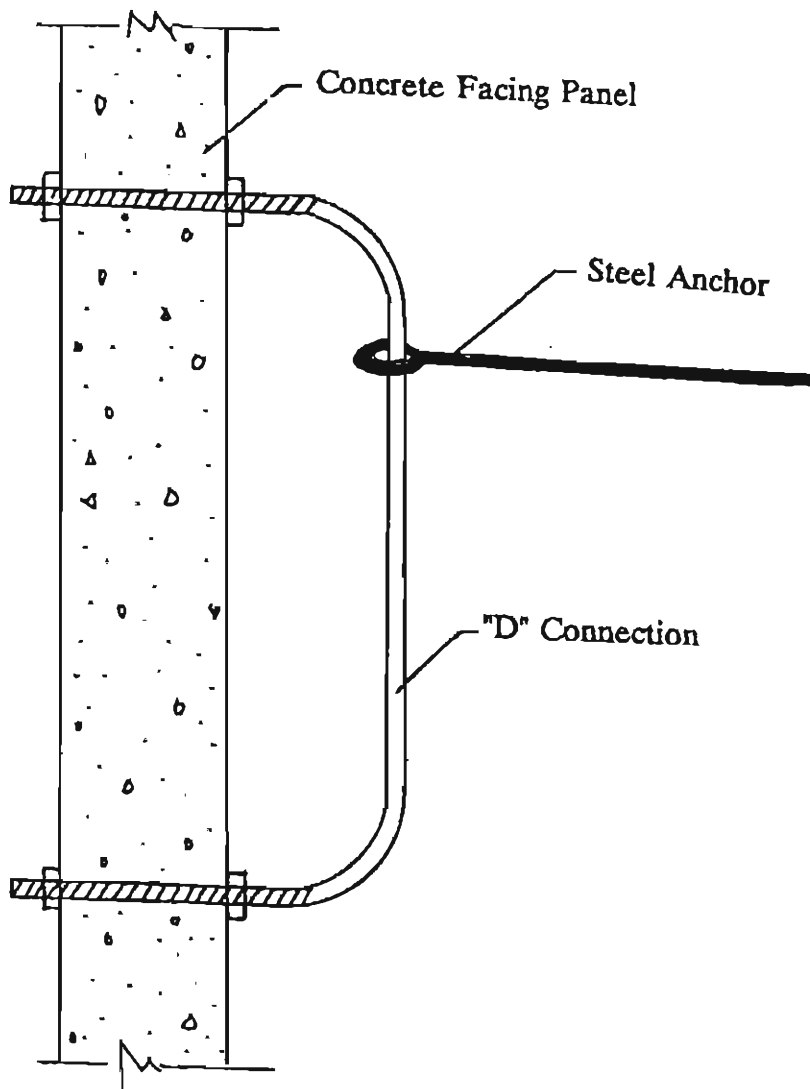


Figure 2.11 The sliding and yielding D-connection (after Wu, et al., 1993)

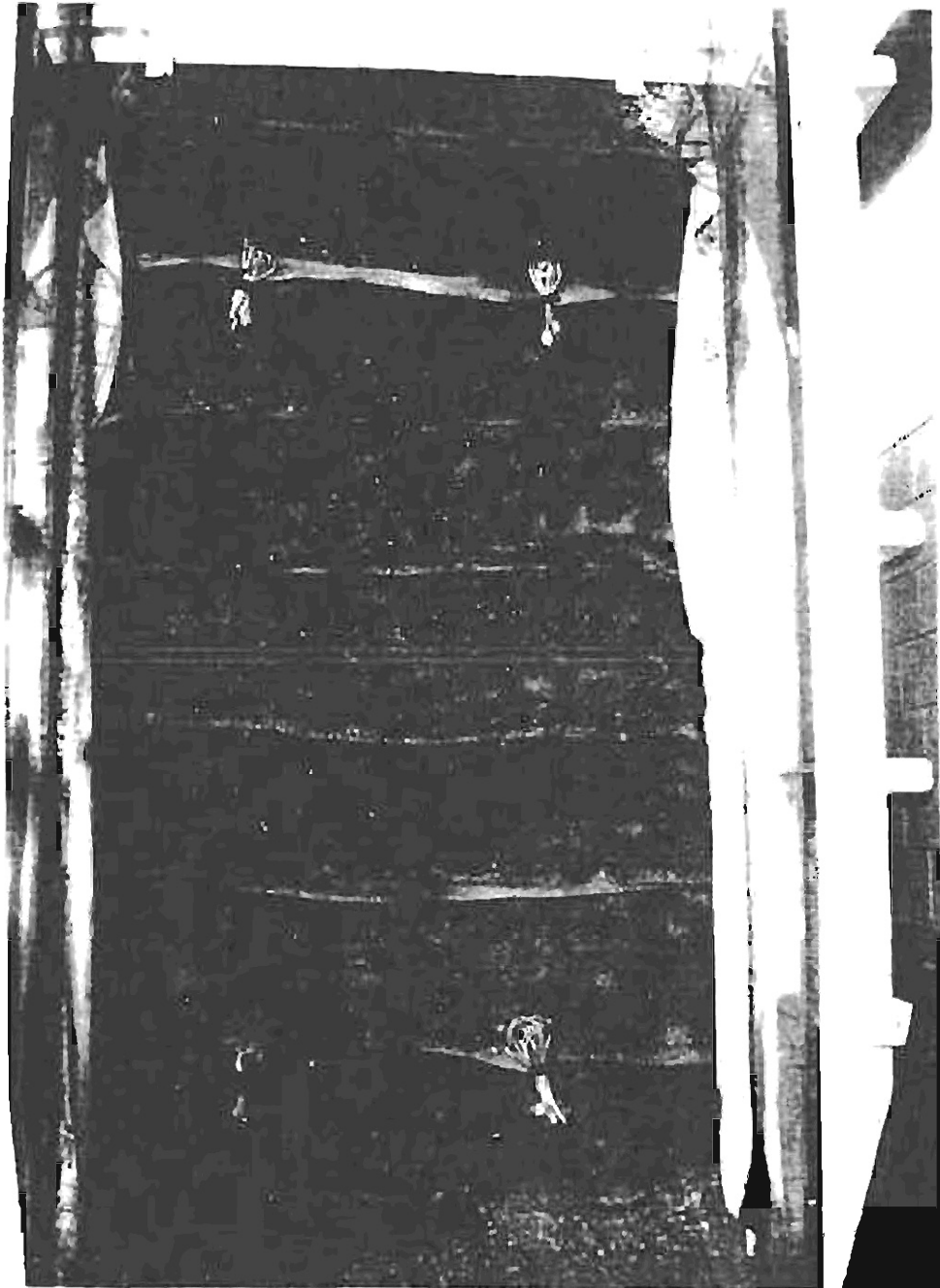


Figure 2.12 Exposed facing of an IFF reinforced soil wall 42 days after removal of facing panel (after Helwany, 1994)

deal with excavation and disposal of the contaminated subsoil.

The wall height varied from 5.7 ft at the north end to 18.8 ft at the south end. The total wall length was over 1,400 ft. Mr. Mike McMullen of the CDOT, the primary inventor of the IFF wall, designed the retaining wall. A typical cross section of the retaining wall is depicted in Figure 2.13. As described in Section 2.2.5, the wall system has three major components: full-height reinforced concrete facing panels, reinforced soil mass (i.e., backfill reinforced with layers of reinforcement), and face anchors (to attach the facing panel to the reinforced soil mass). In this project, the facing panels were 4-ft or 8-ft wide reinforced concrete panels. The reinforcement used was a welded wire mesh, 8 ft by 20 ft in size. The wire was 3/16-in. diameter epoxy-coated steel. The grid size of the mesh was 1 ft by 1 ft. The face anchors were #5 epoxy-coated rebars, shaped as one half of a 12-sided symmetric polygon. The rebars were attached to the facing panels (with threaded screws and nuts) in the gaps between adjacent facing panels. The nuts can be backed off to adjust the alignment of the facing panels during and after construction. The completed structure is shown in Figure 2.14.

Two sections of the retaining wall, referred to as Stations 3116 and 3119, were instrumented to monitor the performance during and after construction. A number of instruments were employed, including survey targets, inclinometers, wire mesh strain gages, rebar strain meters, and thermistors.

The construction procedure of the retaining wall can be described in the following steps:

1. Excavate a trench at the planned location of facing panel. The trench should be at least 2 ft in depth.
2. Position facing panel in the trench with a required setback, and use flow fill (a mixture of concrete sand, cement and water in a flowable consistency) and temporary bracing (in front of facing panel) to brace the panel in position in the trench.
3. Place backfill behind wall facing, compact the fill to the specified density,

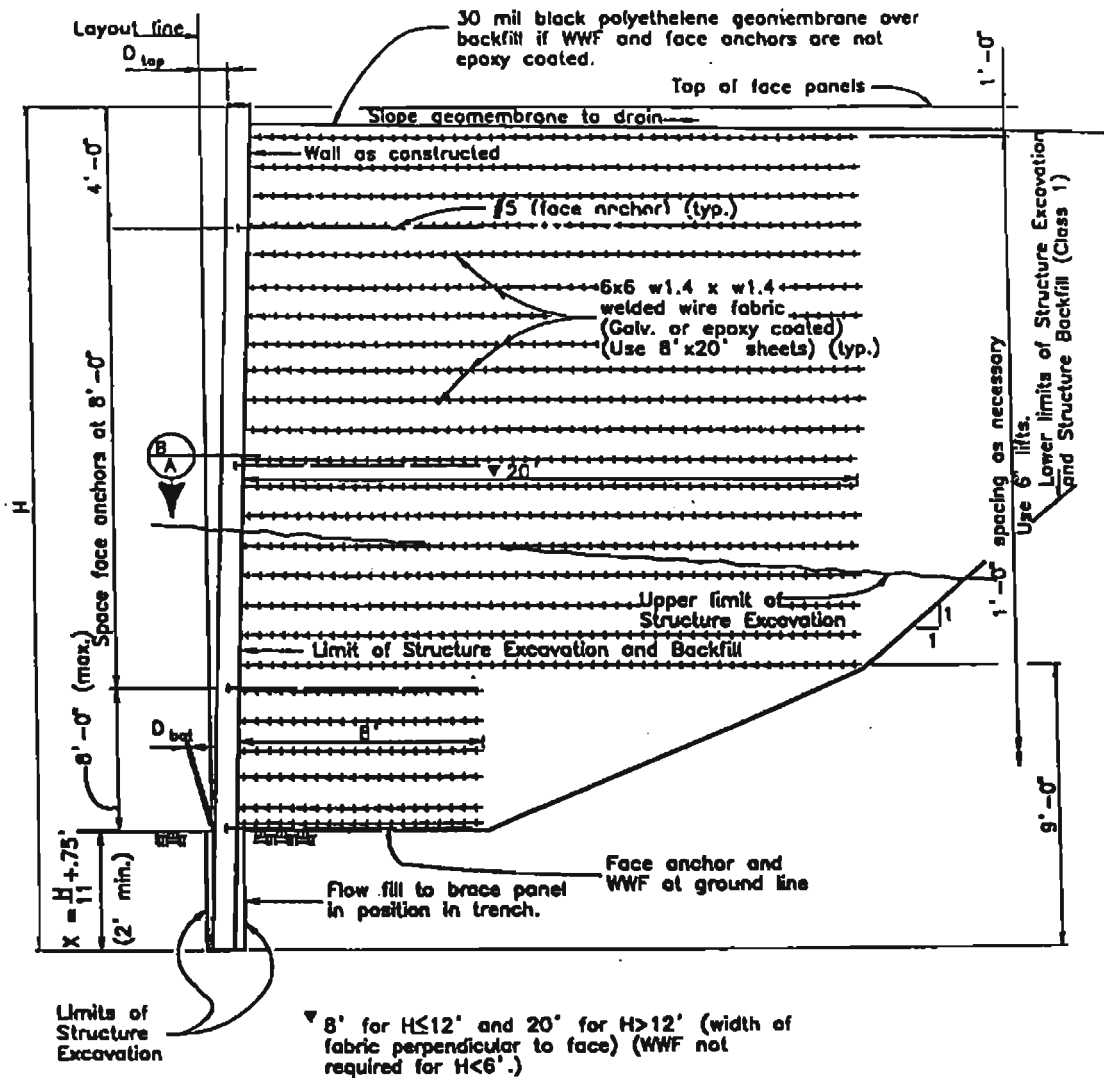


Figure 2.13 Typical cross-section of the IFF Fox wall

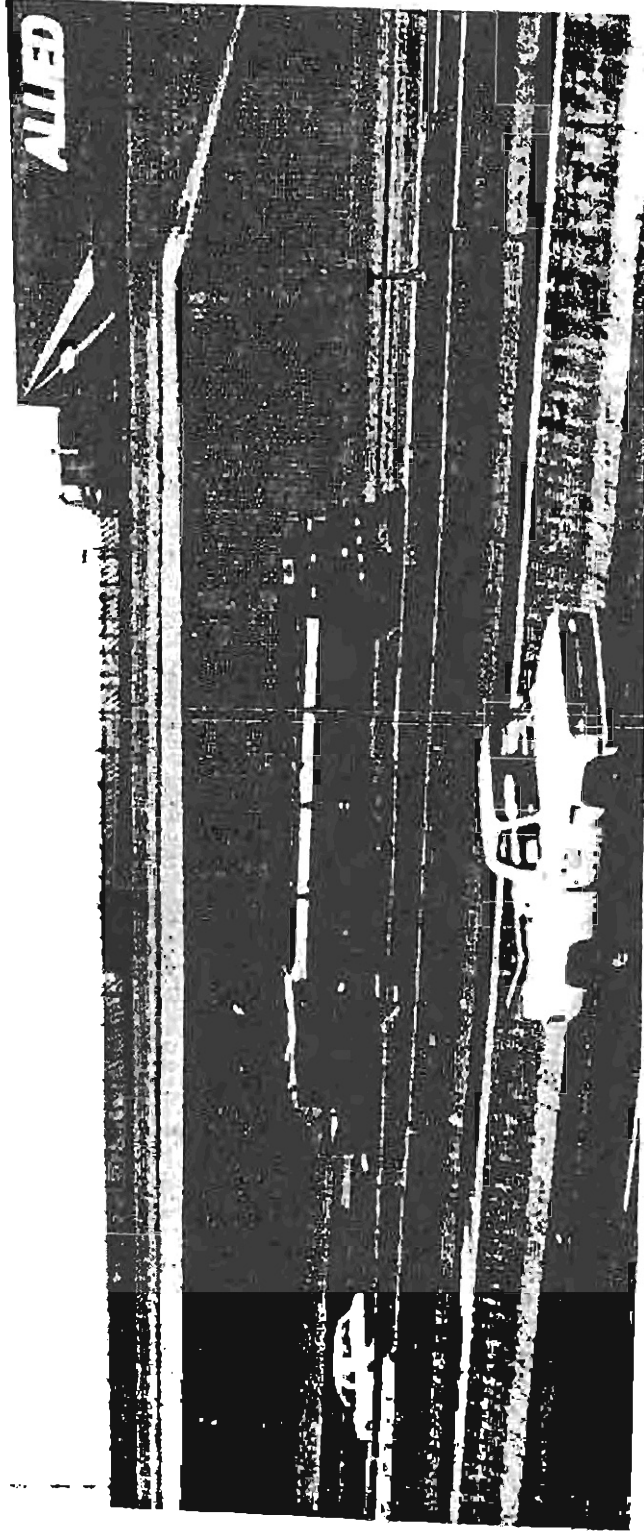


Figure 2.14 Completed wall structure of the IFF Fox wall

and lay reinforcement at every prescribed interval (i.e., prescribed vertical spacing).

4. Install the face anchors (rebars) at selected elevations, and continue the placement of reinforced fill until the design height is reached.

It is to be noted that the vertical spacing of the reinforcement prescribed in this project was 1.0 ft. The mesh was laid tightly against the back of the facing panels. The rebar face anchors were installed at  $H = 0$  (ground surface), 6 ft, and 11 ft above the ground surface for Station 3116, and  $H = 0$  (ground surface), 3 ft, and 7 ft above the ground surface for Station 3119.

The forces in the rebars of Station 3116 were in the range of 0.36 kips (tension) and  $-0.39$  kips (compression). The average forces in the rebars at  $H = 0$ , 6 ft and 11 ft were 0.10 kips, 0.06 kips, and  $-0.13$  kips, respectively. All the forces in the rebars were very small, implying that the lateral earth pressure exerted by the reinforced soil mass on the facing panels was also very small.

In Station 3119, the forces in the rebars ranged from 0.02 kip (tension) to  $-1.42$  kips (compression). The average forces in the rebars at  $H = 0$ , 3 ft, and 7 ft were  $-0.55$  kips,  $-0.86$  kips and  $-0.52$  kips, respectively. The compressive forces were due to the restraints to outward movement of the facing panel. The larger compressive forces (compared with Station 3116) were probably because the panels were shorter and the instrumented rebars were at lower elevations. The lateral earth pressure was apparently not large enough to “push” the facing panels outward and turn the rebars into tension.

Compared with the lateral thrust of 51.2 kips for the  $K_0$ -condition and 32.8 kips for the  $K_a$ -condition (both with assumptions that  $c = 0$ ,  $\phi = 34^\circ$  and  $\gamma = 125$  psf), the measured rebar forces are smaller by nearly two orders of magnitude.

### 2.2.7 Grand County Walls, Grand County, Colorado (1997)

As mentioned in Section 1.3.3, Grand County built four geosynthetic-reinforced soil walls in 1997. The tallest of these walls was 55 ft high (see

Figure 1.11). The walls used common split-faced concrete blocks (of dimensions 8 in. by 8 in. by 16 in.) as facing. The backfill was well-compacted granular soil. The wall performed satisfactorily without any sign of distress or visible deformation. According to the Rankine earth pressure theory, the lateral earth pressure at the base of the wall would be over 1,800 psf, and the facing would be subject to a lateral thrust over 50,000 lb/ft. Yet there were no cracked blocks on any of the four walls. For an externally stabilized retaining wall to support such a lateral thrust, the wall would have been very massive and would require a large space for the construction. The Grand County walls offer perhaps the clearest evidence that the lateral earth pressure in a "pure" internally stabilized wall is indeed very small.

#### *2.2.8 Large-Scale Tests at University of Strathclyde, Glasgow (Yogarajah and Saad, 1996; Yogarajah and Andrawes, 1994)*

Two large-scale tests were conducted to examine the behavior of GRS walls with single-segment facing and multi-segment facing at the University of Strathclyde, U.K. The walls were 2.0 m high and reinforced with three layers of Tensar SR80 geogrid reinforcements at 0.63 m vertical spacing. Leighton Buzzard sand consisting of rounded sands with a small amount of silt was used as backfill. The fill was compacted in lifts of 1.35 m to 1.75 m thickness. The dry unit weight of the fill was approximately 16.4 kN/m<sup>3</sup>. A representative peak angle of friction of the soil was 47° and the constant angle of friction was 34°. For the single-segment wall, the facing was fully propped during construction. For the multi-segment wall, the panels were propped only until the fill reached the top of each panel; thereafter, the props were released.

Figure 2.15 shows the lateral earth pressures at various stages of construction for both walls. It is seen that prior to the removal of the props, the lateral earth pressures were larger than the at-rest pressure. However, after the removal of the props, the earth pressures become very small, especially for the single segment wall. The lateral earth pressures in both walls, after all the

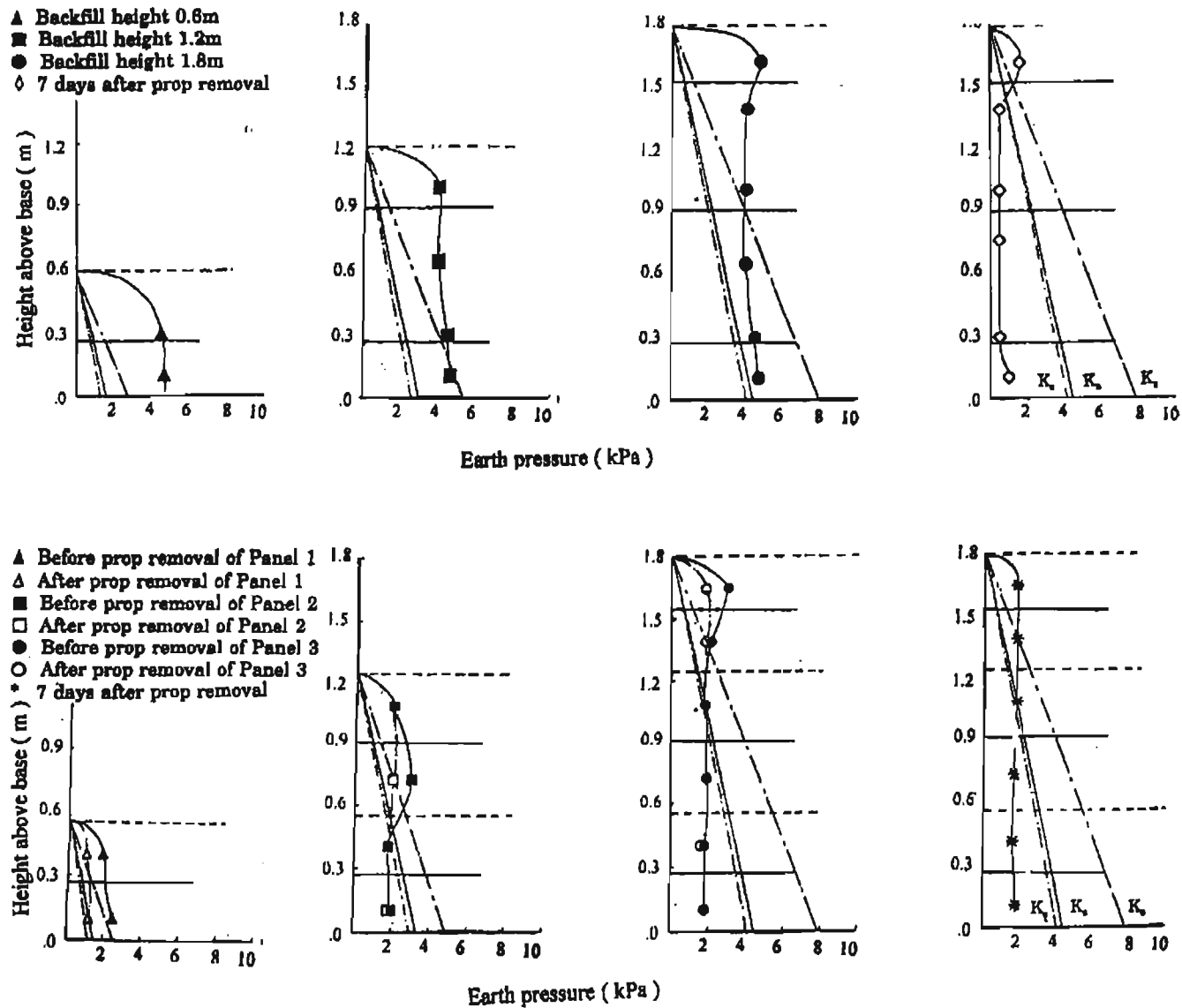


Figure 2.15 Lateral earth pressure of (a) a single-segment wall and (b) a multi-segment wall (after Yogarajah and Saad, 1996)

props were removed, are nearly constant with depth.

Figure 2.16 shows the results of another study, also conducted at the University of Strathclyde, on lateral earth pressure of an incremental panel wall (Yogarajah and Andrawes, 1994). It is seen that, other than near the top of the wall, the lateral earth pressure is smaller than the active earth pressure and that the lateral earth pressure is practically constant with depth.

### *2.2.9 Finite Element Analysis (Chou and Wu, 1993)*

Chou and Wu (1993) conducted a study to investigate the performance of geosynthetic-reinforced soil retaining walls by the finite element method of analysis. They started the study with an in-depth evaluation of available finite element computer models. A comparative study of four finite element codes (SSCOMP, CRISP, CON2D, and DACSAR) indicated conclusively that DACSAR is the best overall finite element code for the analysis.

The computer code DACSAR (Deformation Analysis Considering Stress Anisotropy and Reorientation) was developed by Ohta and Iizuka (1986) at the University of Kyoto, Japan. It can be used to perform finite element analysis of plane strain and axi-symmetric geotechnical engineering problems. DACSAR has three constitutive models: linear elastic model, modified Duncan model (Duncan et al., 1980), and Sekiguchi-Ohta (1977) model. The Sekiguchi-Ohta model is a generalized Cam-clay model. The code employs a “coupled” formulation that makes it well suited for time-dependent analysis.

Each component of the computer code DACSAR was validated through comparisons with laboratory tests of soils, reinforcements, and facing. The overall algorithm of DACSAR was then validated through comparisons with another finite element computer code, SSSCOMP. The applicability to GRS walls was validated through comparisons with two full-scale test walls.

Using the analytical model, a parametric study was undertaken to investigate the effects of various factors on the performance of GRS walls. The factors investigated include: wall height, wall shape, backfill type, foundation

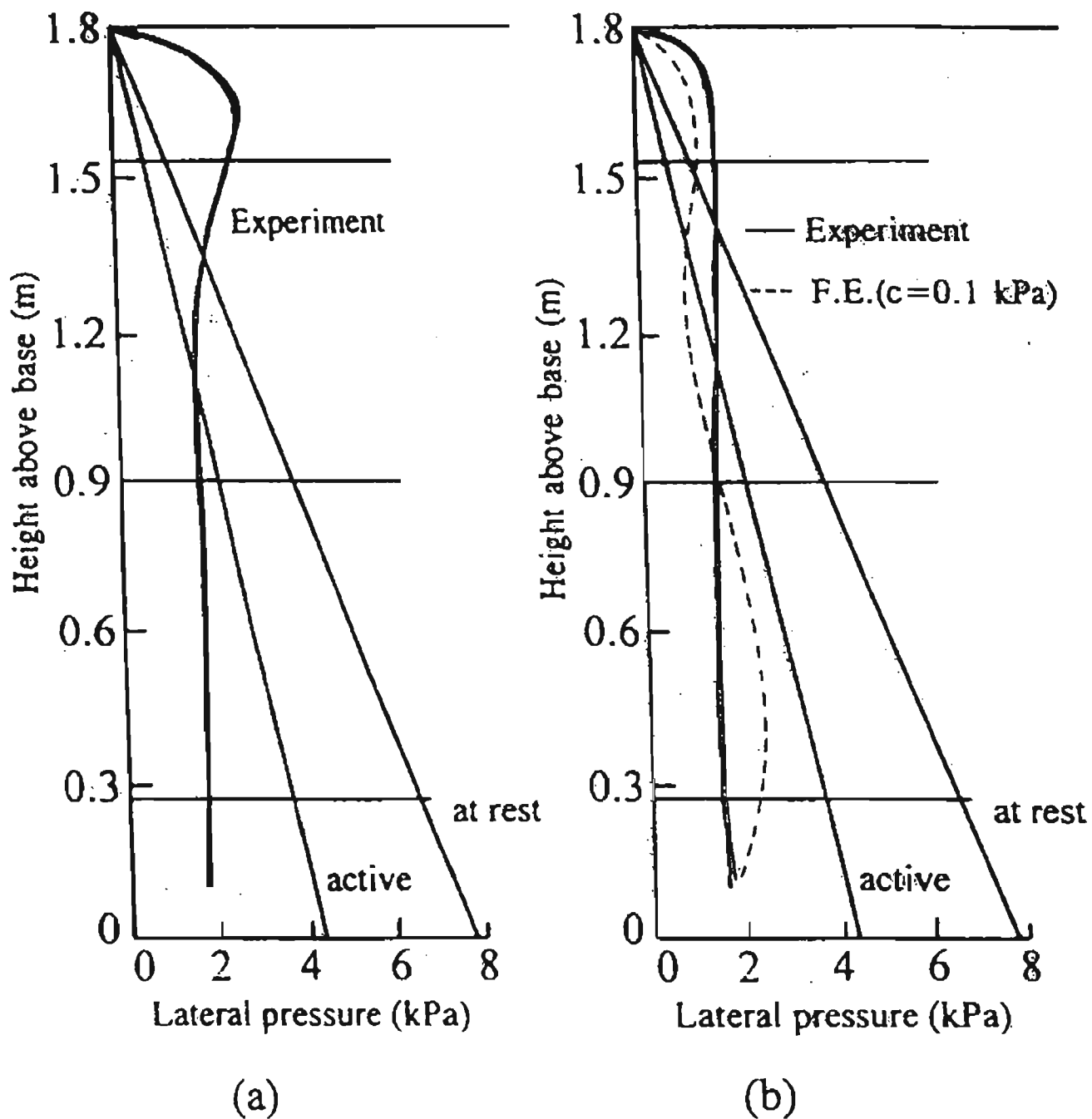


Figure 2.16 Measured and analytical lateral earth pressures of two GRS walls (after Yogarajah and Andrawes, 1994)

stiffness, facing rigidity, reinforcement stiffness, and fill compaction.

The “control” wall used in the parametric study is shown in Figure 2.17. The wall was 12 ft high and reinforced with 11 sheets of geosynthetic reinforcement at 12 in. vertical spacing. The facing was a flexible timber/plywood facing. The backfill was a silty sand and gravel. The backfill was placed and compacted in 12 equal lifts, 12 in. thick each. The wall was assumed to situate over a “deformable” foundation: a medium stiff sandy clay (the most common overburden soil in Colorado). The water table was assumed to be 3 ft below the ground surface.

Figure 2.18 shows the lateral earth pressures of the “control” wall. The earth pressures along three locations are shown in the Figure: earth pressure against the wall face, earth pressure against the reinforced soil mass, and earth pressure along the plane of maximum tensile force in the reinforcement. It is seen that the lateral earth pressure against the wall face was the smallest of all and is practically constant with depth except near the wall base.

Figure 2.18 also shows that the earth pressure along the plane of maximum tensile force in the reinforcement -- the earth pressure commonly used to determine the required tensile strength in design -- takes a shape similar to the earth pressure against the wall face, although its magnitude is somewhat larger.

It should also be noted that the earth pressure against the reinforced soil mass -- the earth pressure commonly used to evaluate external stability of GRS walls -- does not deviate significantly from the Rankine active earth pressure. This suggests that the current practice of using Rankine lateral earth pressure to evaluate external stability of a GRS wall with level crest is well warranted.

### **2.3 Proposed Lateral Earth Pressure Diagram**

The literature has conclusively indicated that GRS walls constructed with close reinforcement spacing can assume a stable state with a vertical or near-vertical face without external facing acting as a load-carrying element. For a wall facing that does not offer much resistance to the lateral movement of the

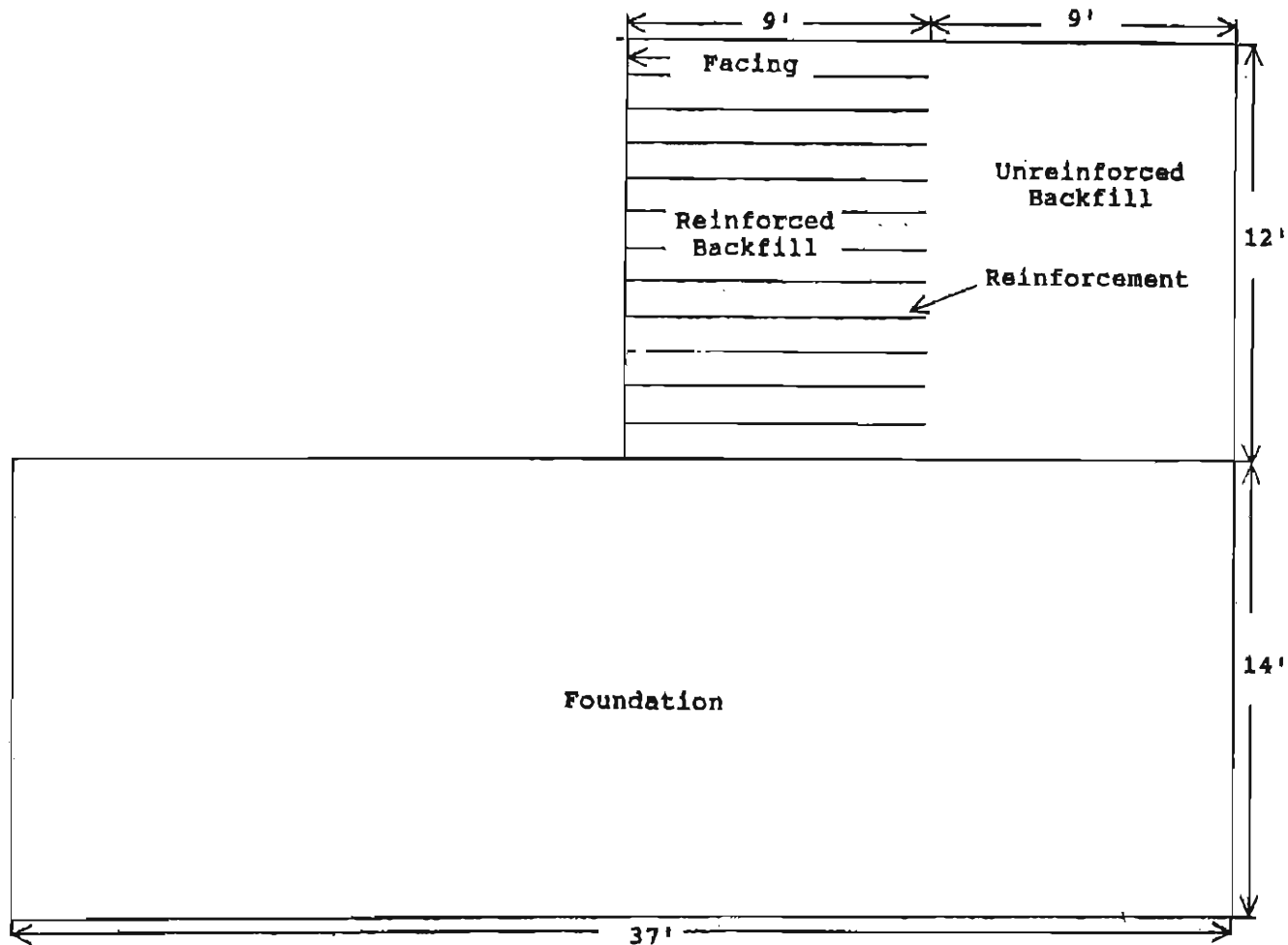


Figure 2.17 The control wall used in the parametric study (after Chou and Wu, 1993)

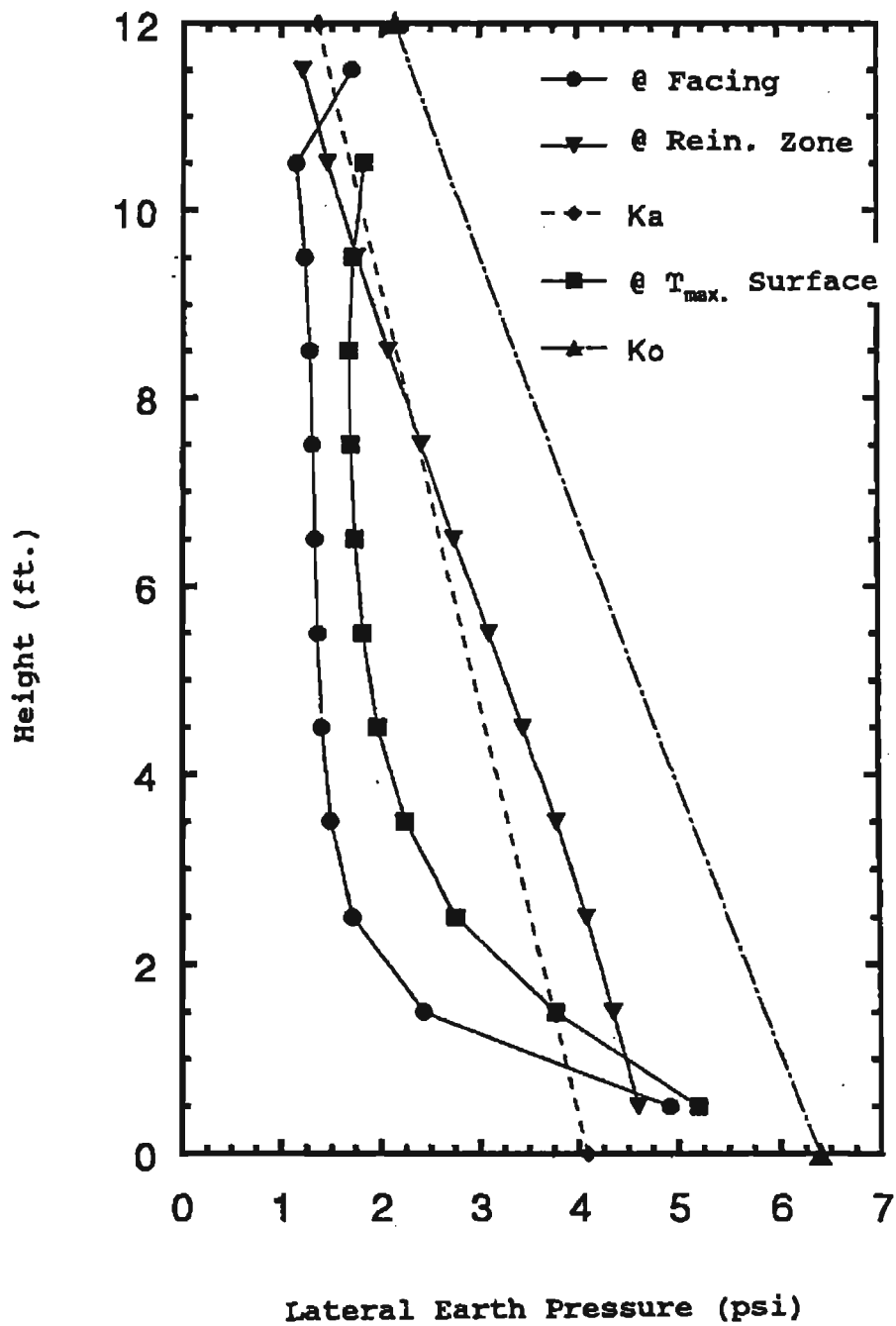


Figure 2.18 Lateral earth pressure of the control wall at three locations (after Chou and Wu, 1993)

wall, the lateral thrust on the wall face will be very small, provided that the reinforcement can effectively restrain lateral deformation of the surrounding soil.

In an idealized bin pressure diagram (recall: bin pressure is the lateral earth pressure between adjacent reinforcement layers), the pressure is zero at the depth of any reinforcement layer within a "bin," the lateral earth pressure will increase linearly with depth before decreasing to zero at the next reinforcement layer. Because reinforcement may deform slightly and the interface between soil and reinforcement may not be perfectly bonded, the bin pressure shown in Figure 2.19 is proposed. It should be noted that the bin pressure is not a function of wall height. Rather, the bin pressure is a function of reinforcement spacing and the strength parameters of the soil. Assuming  $\phi = 34^\circ$ ,  $c = 0$ ,  $\gamma = 125 \text{ lb/ft}^3$ , and a safety factor of 2, the bin pressures for different values of reinforcement spacing are shown in Table 2.1.

The proposed design lateral thrusts as a function of the vertical reinforcement spacing are plotted in Figure 2.20 for a backfill with  $\phi = 34^\circ$ ,  $c = 0$ , and  $\gamma = 125 \text{ lb/ft}^3$ . The nonlinear increase of the design thrust with increasing reinforcement spacing is evident.

## 2.4 Limitations and Practical Implications

The bin pressure presented in Section 2.3 is subject to the following limitations:

- The facing should offer only small resistance to lateral movement of the wall such that the active condition can be developed between reinforcement layers (i.e., the segmental GRS wall approaches a "pure" internally stabilized wall, as described in Section 2.1).
- Bonding at soil-reinforcement interface should be maintained at the designed load.
- The reinforcement needs to be sufficiently stiff.

The practical implications of the proposed bin pressures are as follows:

$$\begin{aligned}\sigma_h &= \gamma S \tan^2(45^\circ - 34^\circ/2) \\ &= 35.4 S \text{ (psf)}\end{aligned}$$

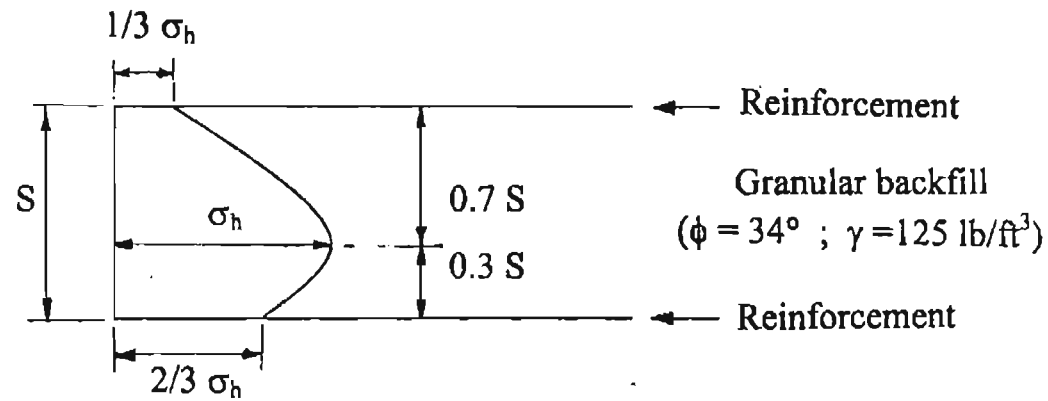


Figure 2.19 The proposed bin pressure diagram

Table 2.1 Lateral thrusts on wall facing: bin pressure (for backfill with  $\phi = 34^\circ$ ,  $c = 0$ , and  $\gamma = 125 \text{ lb/ft}^3$ )

Reinforcement spacing	Lateral thrust (lb/ft) between any two adjacent reinforcements	Design bin thrust (lb/ft) (with $F_s = 2$ )
8 in.	11.3	22.6
12 in.	25.4	50.8
16 in.	45.2	90.4
24 in.	101.6	203.2
36 in.	228.6	457.2

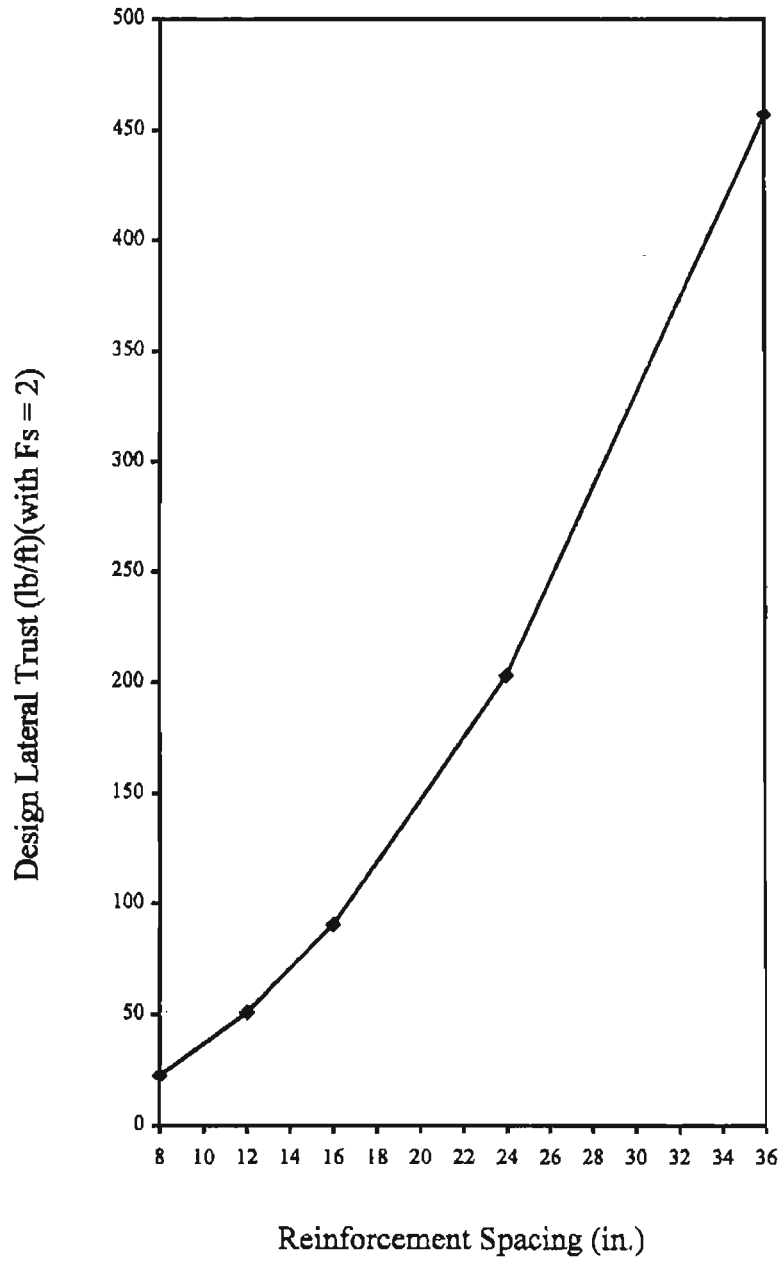


Figure 2.20 Proposed lateral thrust as a function of reinforcement spacing

- The lateral earth pressure will be very small provided that the reinforcement spacing is small and that the global facing rigidity is low. To achieve sufficiently low global facing rigidity, one may use split-faced, hollow-cored concrete blocks and suspend the use of connection pins and keys between vertically adjacent blocks. The hollow core of the concrete blocks may be filled with gravels to increase stability before the next course of blocks is laid.
- For facing that uses heavy concrete blocks, the earth pressure at the height of a reinforcement layer will still be fairly small. The resulting total thrust will still be much smaller than the thrust based on the Rankine active earth pressure.
- To ensure that there will be sufficiently high frictional resistance between vertically adjacent facing blocks at all depths, it may be necessary to join the top two to four courses of blocks using cement between vertically adjacent blocks or fill the hollow-core with cement (combining with steel bars for high surcharge loads). This is because the normal forces on the horizontal contact surfaces of these blocks may not be sufficiently high to ensure adequate frictional resistance. The use of chemical adhesives (e.g., epoxies) is not recommended as they may deteriorate with time.
- The concrete facing blocks should be sufficiently strong in compression (say, with a minimum compressive strength of 4,000 psi).
- The connection strength is not a design issue when reinforcement spacing is small (say,  $\leq 12$  in.), and lightweight facing blocks are employed.
- Since the bin pressure is not a function of wall height, the total lateral thrust will be small, even for tall retaining walls (say, wall height  $> 40$  ft).

It is important to mention that the proposed lateral earth pressure only applies to the wall face, and does not apply to the evaluation of required reinforcement tensile strength or evaluation of external stability of reinforced soil mass. It is recommended that Rankine lateral earth pressure be used for both these situations, although the required reinforcement tensile strength determined by the Rankine earth pressure is likely to be rather conservative (see discussions in Section 2.2.9).

## Chapter 3

### LONG-TERM DEFORMATION

Geosynthetics, manufactured with polymers such as polypropylene, polyethylene, polyester and polyamide (nylon), are generally considered creep-sensitive. The long-term design strength of a geosynthetic reinforcement employed in the AASHTO design guidelines is determined by performing laboratory creep tests or by applying long-term reduction factors to short-term tensile strength of the geosynthetic reinforcement.

The laboratory tests have been performed by applying uniaxial tensile forces to a geosynthetic specimen (in confined or unconfined condition) without any regard to the soil-geosynthetic interaction. Laboratory tests and field measurement have indicated that the results obtained in this manner are overly conservative when granular backfill is employed.

The use of default values of the partial factors of safety, on the other hand, result in very small cumulative reduction factors,  $k$ . In fact, the values of  $k$  are so small that geotextiles have practically been precluded for use in GRS walls. Field observation has repeatedly indicated that the default values are overly conservative.

The following sections give brief summaries of (a) long-term creep behavior of geosynthetics, (b) long-term pullout behavior of geosynthetics, (c) soil-geosynthetic interactive creep tests, (d) finite element analysis of long-term performance, (e) in-service GRS walls and field measurement. The creep rates as determined from in-service walls and the CTI performance tests are then discussed. The proposed protocol to account for long-term creep in a design is presented.

#### **3.1 Long-Term Creep Behavior of Geosynthetics**

Many researchers have investigated the long-term creep behavior of

geosynthetics using laboratory tests. Findings of the tests are summarized as follows:

- Stress level and polymer type significantly affect creep potential of a geosynthetic (Hoedt, 1986). Polypropylene and polyethylene generally exhibit larger creep deformation than polyester and polyamide. For geotextiles that are loaded *in-isolation* for prolonged periods of time (10 to 100 years) at ambient temperature, the permissible load is about 20% to 25% of tensile strength for polypropylene and polyethylene, and about 40% to 50% for polyester and polyamide (Koerner, 1998).
- Since temperature is known to affect the rate of creep of geosynthetics, creep tests of geosynthetics should be conducted to cover a range of temperatures in the anticipated in-service condition of the earth structure. This does, however, require extensive testing at different temperatures over considerable time periods. In absence of such information, time-shifting techniques may be utilized, with caution, to account for the temperature effect.
- McGown, et al. (1982) employed a fairly sophisticated uniaxial tension test device to measure creep behavior of geotextiles under soil confinement. In the test, a constant force is exerted to both ends of a geotextile test specimen that is sandwiched between two soil cakes and subjected to a confining pressure. Figure 3.1 depicts the test apparatus. The tests indicated that soil confinement generally reduced creep deformation of geosynthetics. Figure 3.2 shows comparisons of the load-deformation-time behavior of two geotextiles tested under unconfined and confined conditions.
- Many researchers have conducted so-called "confined tests" of geosynthetics (e.g., Leshchinsky and Field, 1982; Siel, Wu and Chou, 1987; Kokkalis and Papacharisis, 1989; Juran and Christopher, 1989). In these tests, a geosynthetic specimen is

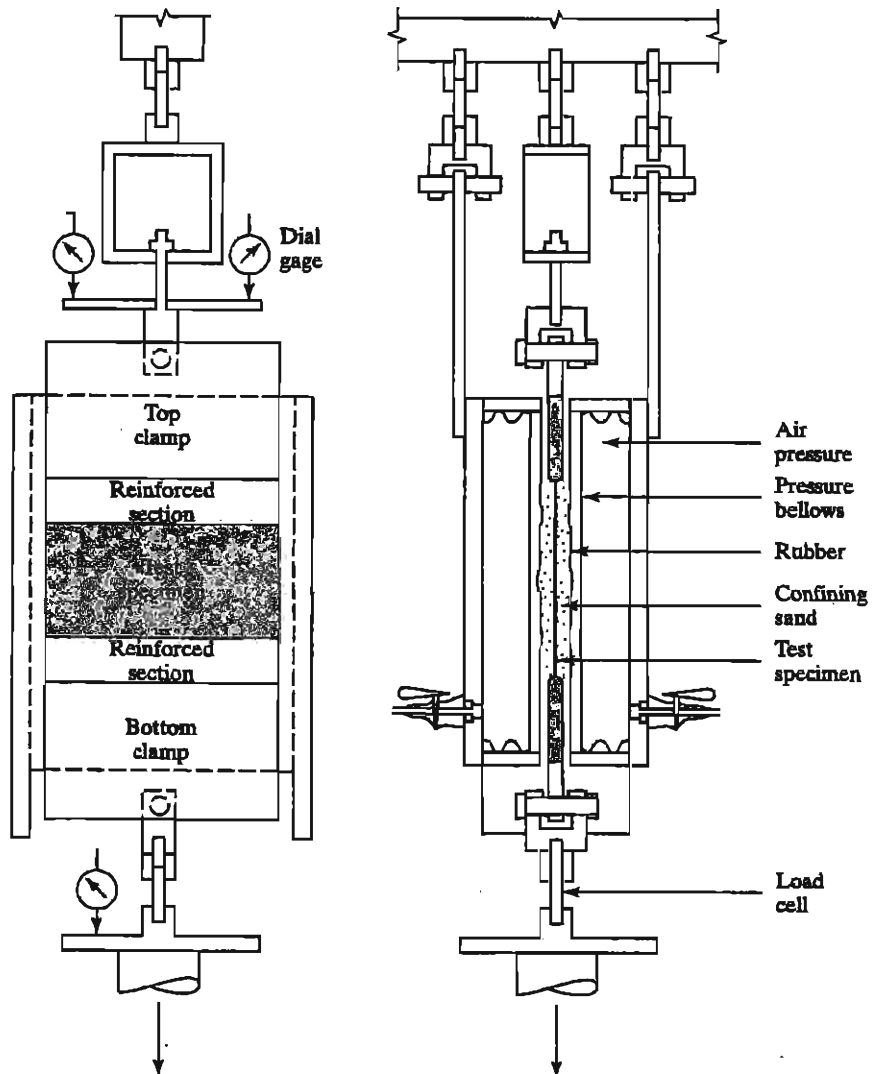
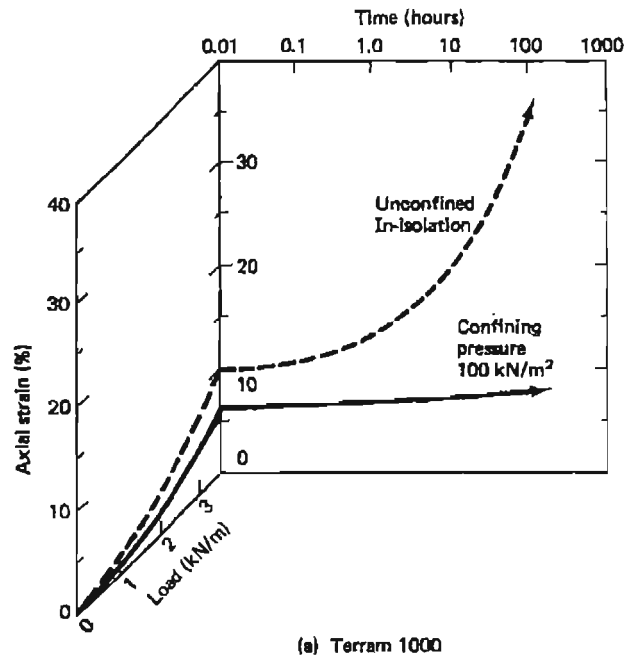
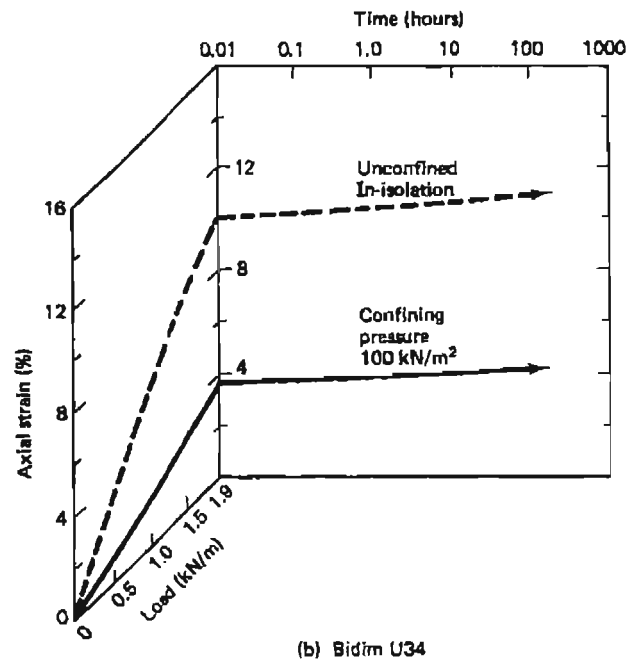


Figure 3.1 A confined creep test (after McGown et al., 1982)



(a) Terram 1000



(b) Bidim U34

Figure 3.2 Load-deformation-time relationships of two geotextiles (after McGown, et al., 1982)

- confined in soil and subjected to a certain normal stress. Uniaxial tensile forces are then applied to the geosynthetic specimen. Note that the deformation of the geosynthetic specimen is resisted by both the inherent structure of the geosynthetic (under the confined condition) and the frictional resistance at the soil-geosynthetic interface. The implication of the test is that the soil will remain “stationary” while the geosynthetic reinforcement deforms. The load-deformation properties obtained from this type of test will be on the unconservative side (Wu, 1991; Wu and Tatsuoka, 1992).
- Wu (1991), Ling et al. (1992), and Ballegeer and Wu (1993) developed an improved confined creep test, in which a constant sustained tensile force is applied to a membrane-confined geosynthetic specimen without inducing soil-geosynthetic interface friction (see Figure 3.3). The confining pressure is exerted on the surface of the test specimen by suction during the test. Figure 3.4 shows a comparison of a soil-confined test and a membrane-confined test. In the soil-confined test, the soil is allowed to deform with the geosynthetic. It is seen that the membrane-confined test yields essentially the same results as the soil-confined test. A number of different geotextiles under various confining pressures were tested. The results indicated that pressure confinement gave various degrees of improvement in creep behavior for different geotextiles. The greatest improvement was in needle-punched nonwoven geotextiles, while the improvement in woven geotextiles and heat-bonded nonwoven geotextiles was negligible.
- Geosynthetics subject to “constant” deformation (e.g., when deformation of a wall ceases or the rate of deformation becomes very small) are likely to experience stress relaxation, i.e., there will be a reduction of force with time in the geosynthetic. All the geosynthetics that have a tendency to undergo creep deformation

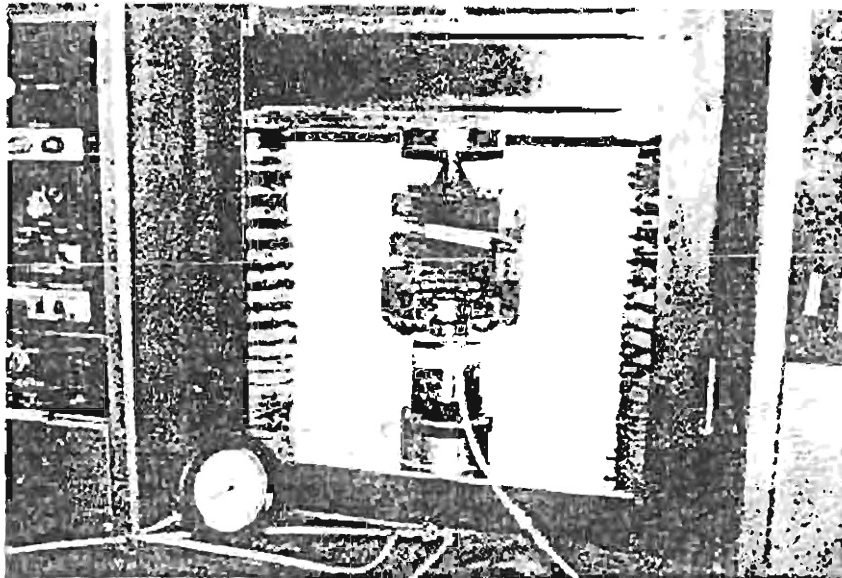
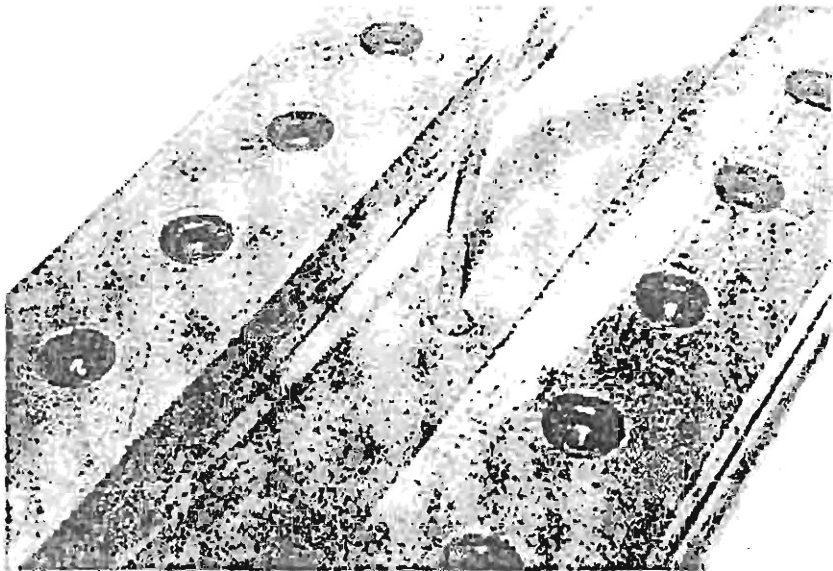


Figure 3.3 Membrane-confined load-deformation test of geosynthetic (after Balleger and Wu, 1993)

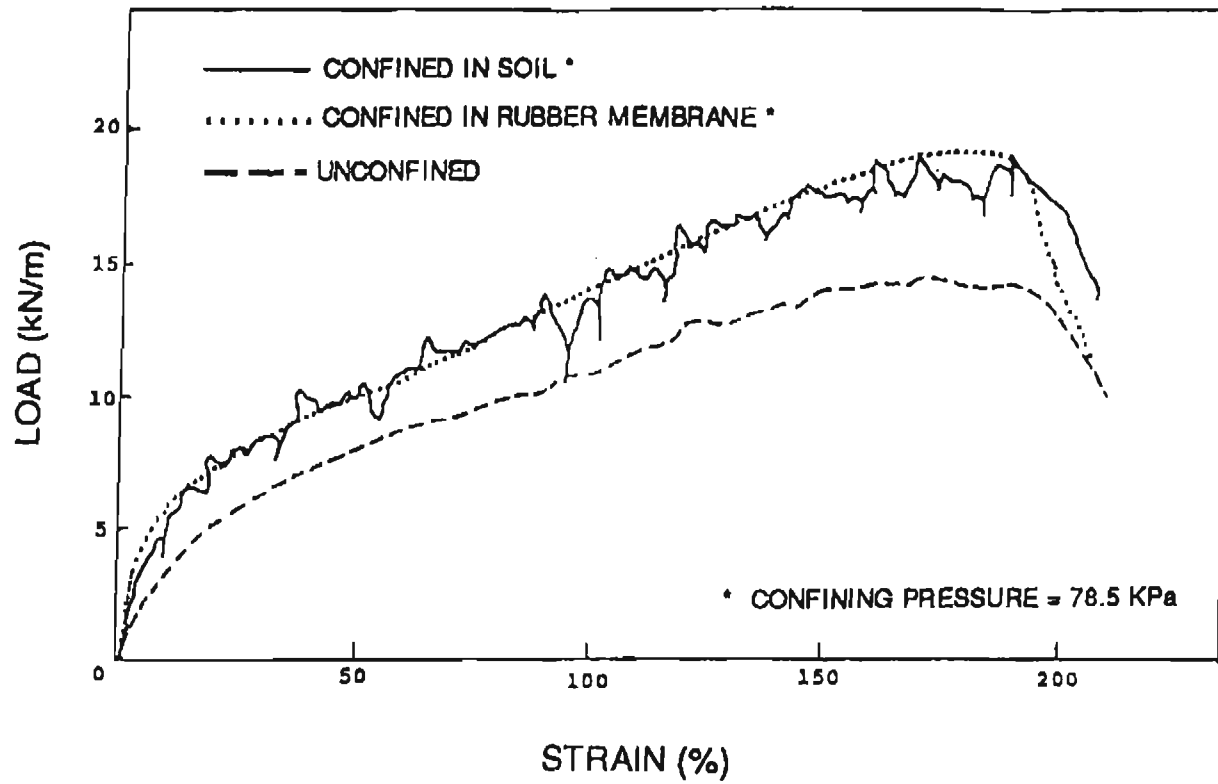


Figure 3.4 Comparisons of load-deformation behavior of geosynthetic under in-soil, in-membrane and unconfined conditions (after Wu, 1991)

will have the same tendency to undergo stress relaxation.

### **3.2 Long-Term Pullout Behavior of Geosynthetics**

Long-term pullout behavior of geosynthetics has been the subject of a limited number of studies. Long-term pullout tests have been performed on various geogrids in granular soil (e.g., Kutara, et al., 1988; Wilson-Fahmy, et al., 1995). The tests indicated that for practical purposes, the long-term pullout strength could be assumed to be equal to the short-term pullout strength provided sufficient anchorage length is available. It appears reasonable to accept this premise in design of GRS structures.

### **3.3 Soil-Geosynthetic Interactive Creep Tests**

It can be misleading to evaluate the long-term creep potential of a GRS structure based on the results of long-term load-deformation tests performed by applying a sustained tensile force to the geosynthetic reinforcement alone. If the confining soil has a tendency to deform faster than the geosynthetic reinforcement along the direction of elongation, the geosynthetic will impose a restraining effect on the time-dependent deformation of the soil through the interface bonding resistance. Conversely, if the geosynthetic reinforcement in isolation tends to deform faster than the confining soil, then the confining soil will restrain creep deformation of the reinforcement. This restraining effect is a direct result of soil-reinforcement interaction wherein redistribution of stresses in the confining soil and changes in axial forces in the reinforcement occur over time in an interactive manner.

#### **3.3.1 Soil-Geosynthetic Interactive Performance Test (Wu, 1994a; Wu and Helwany 1996)**

Recognizing that it is the composite behavior of a reinforced soil (not the behavior of its components in isolation) that must be the basis for rational design of GRS structures, Wu (1994a) developed a *soil-geosynthetic interactive*

*performance (SGIP) test*. A schematic diagram of the test device is shown in Figure 3.5, in which a reinforced soil unit was placed inside a rigid container with smooth transparent plexiglass sidewalls. The reinforced soil unit comprises a geosynthetic reinforcement sheet, confining soil and two flexible steel plates. The reinforcement is securely attached to the vertical flexible plates at their mid-height. The transverse direction of the reinforced soil unit is fitted between two lubricated plexiglass side walls in such a manner that the reinforced soil unit is restrained from movement in the direction perpendicular to the plexiglass side walls (i.e., in a plane strain configuration). On the top surface of the reinforced soil unit another geosynthetic reinforcement sheet is used to attach the top edge of the vertical flexible plates.

The test has two important features. First, the stresses applied to the soil are transferred to the geosynthetic in a manner similar to the typical load transfer mechanism in a typical GRS structure. Second, both the soil and the geosynthetic are allowed to deform in an interactive manner under self-weight and externally applied loads.

Wu and Helwany (1996) reported the results of two carefully conducted SGIP tests, one used a clayey backfill and the other a granular backfill. Compared with *element tests* conducted on the geosynthetic alone, the element test under-estimated the maximum strain by 250% in the clay-backfill test, and over-estimated the maximum strain by 400% in the sand-backfill test. It should be noted that creep deformation essentially ceased within 100 minutes after the sand-backfill test began; whereas the clay-backfill test experienced creep deformation over the entire test period (18 days, at which time shear failure occurred in the soil).

### 3.3.2 A Modified Long-Term Performance Test (Ketchart and Wu, 1996)

Ketchart and Wu (1996) developed a modified version of the SGIP test presented in Section 3.3.1. The test apparatus is shown schematically in Figure 3.6. This test differs from the original performance test in several aspects,

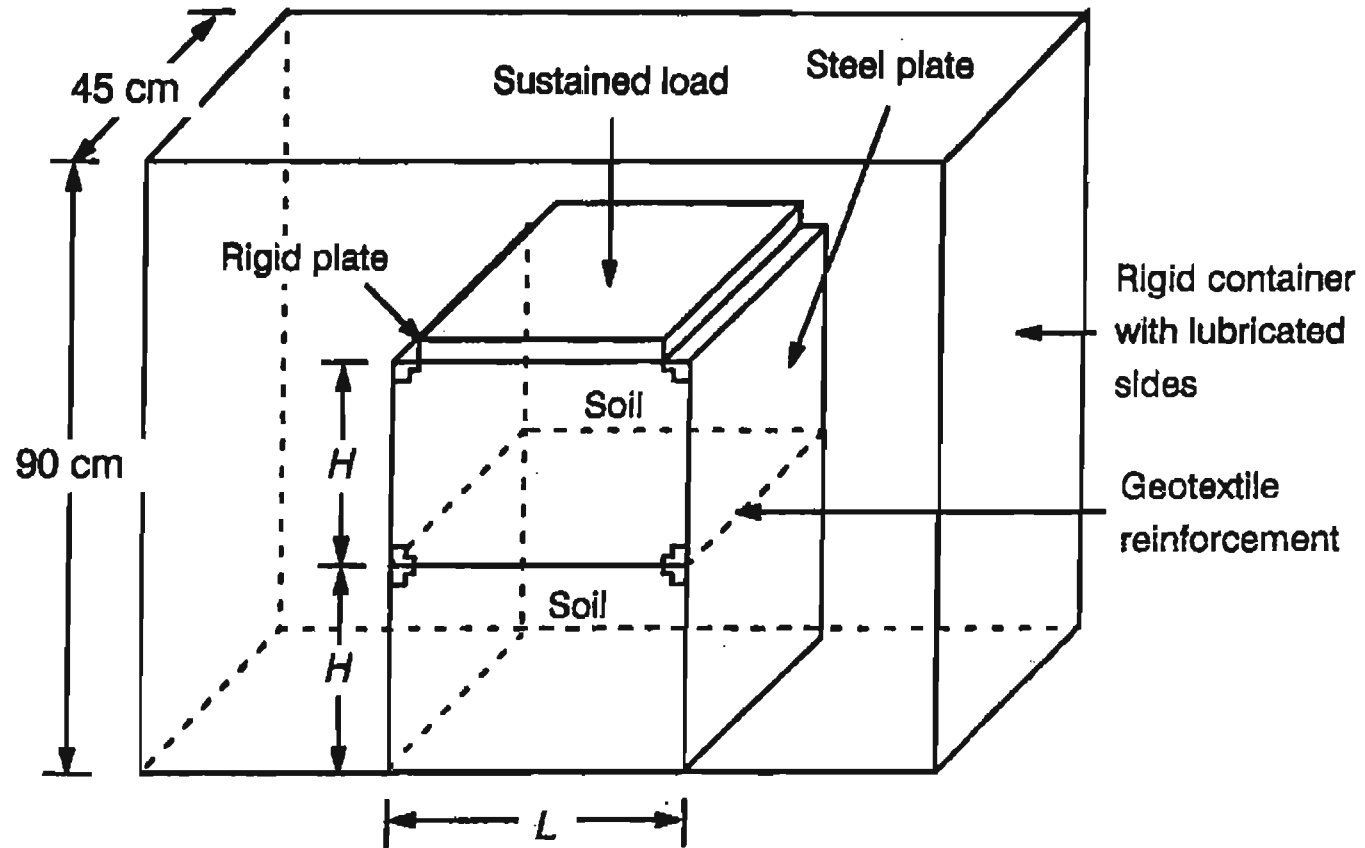


Figure 3.5 Schematic diagram of the soil-geosynthetic interactive performance test (after Wu and Helwany, 1996)

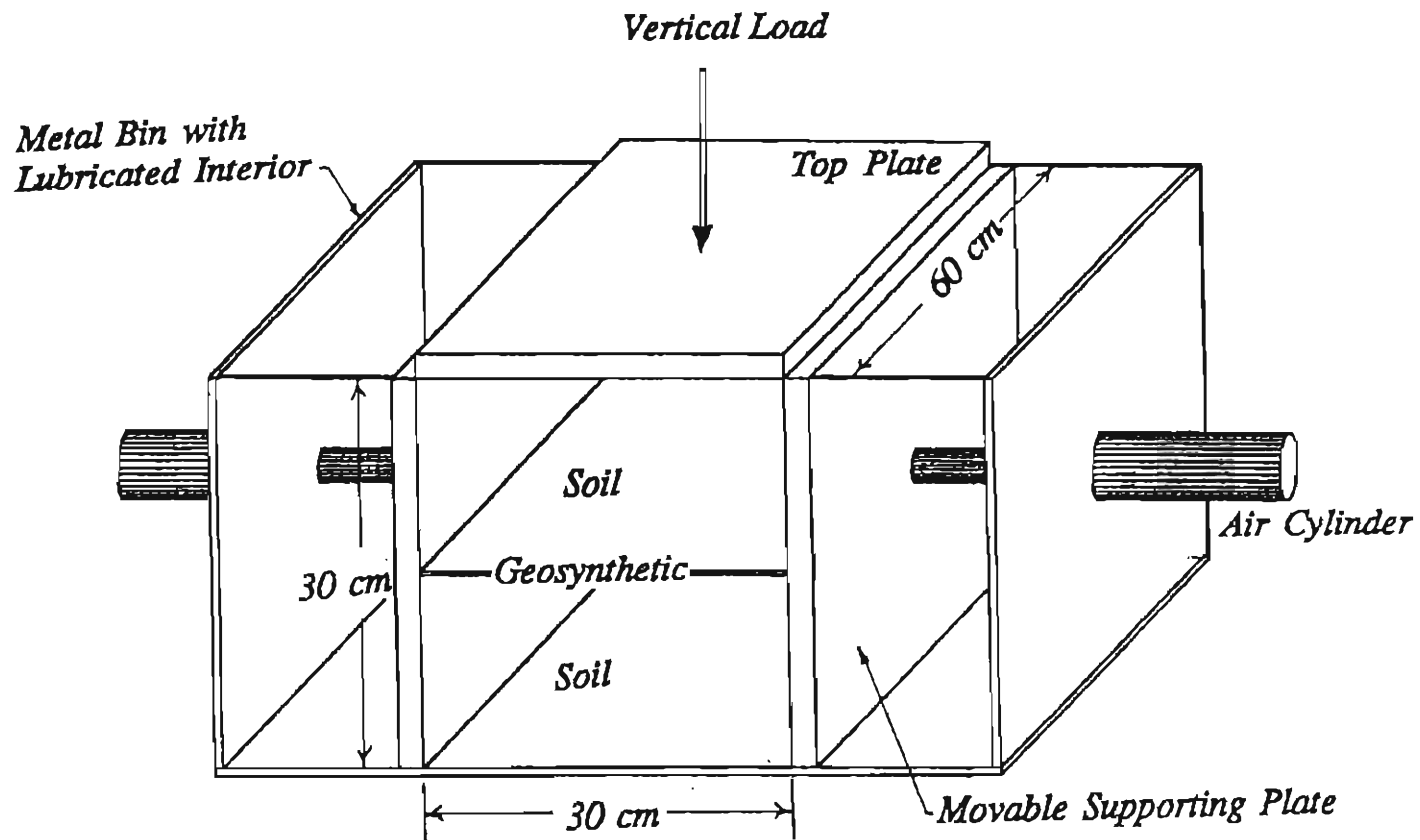


Figure 3.6 Schematic diagram of the CTI long-term performance test (after Ketchart and Wu, 1996)

including dimensions, lateral confinement (there is no confinement in the modified performance test), attachment to geosynthetic reinforcement (geosynthetic reinforcement is not attached at the ends in the modified performance test), and load application mechanism. Note that the loads can be applied in a self-contained manner using Conbel pneumatic loading device (see Figure 3.7) or through a universal testing machine (see Figure 3.8).

The SGIP test has been employed to predict the performance of a full-scale GRS pier experiment conducted by Adams (1997a) at the Turner-Fairbank Highway Research Center of FHWA in McLean, Virginia (see Figure 3.9). The pier was 5.4 m high. Dry-stacked split-faced cinder blocks were used as facing elements. The backfill was a crushed Diabase. The backfill was reinforced with layers of a woven polypropylene geotextile at 0.2 m vertical spacing. The pier was preloaded to 900 kPa, unloaded to zero and subsequently reloaded. A SGIP test was conducted, prior to construction of the pier, using the same soil and reinforcement as those used in the pier. The SGIP test accurately predicted the effects of the preloading: it decreased the vertical settlement by a factor of two for load level  $\leq 0.5$  (load level = applied load / ultimate load), and there was little effect on the lateral movement (see Figure 3.10).

A number of geosynthetic/granular road base composites have been tested using the SGIP test device (Ketchart and Wu, 1996). Figure 3.11 shows the lateral and vertical displacements versus time relationship of a soil-geosynthetic composite comprising a road base material and a woven polypropylene geotextile (Amoco 2044). For comparison, the behavior for the road base without the reinforcement is also shown in the Figure. It is seen how the geosynthetic reinforcement can effectively reduce time-dependent deformation of a soil mass. It is interesting to note that in a test of which a clayey soil was reinforced with Amoco 2044 and subject to an average vertical pressure of 15 psi, the soil-geosynthetic composite exhibited negligible creep in the lateral direction over the entire test period of 30 days. Creep deformation in the vertical direction, however, was significant and continued to increase at the end of the

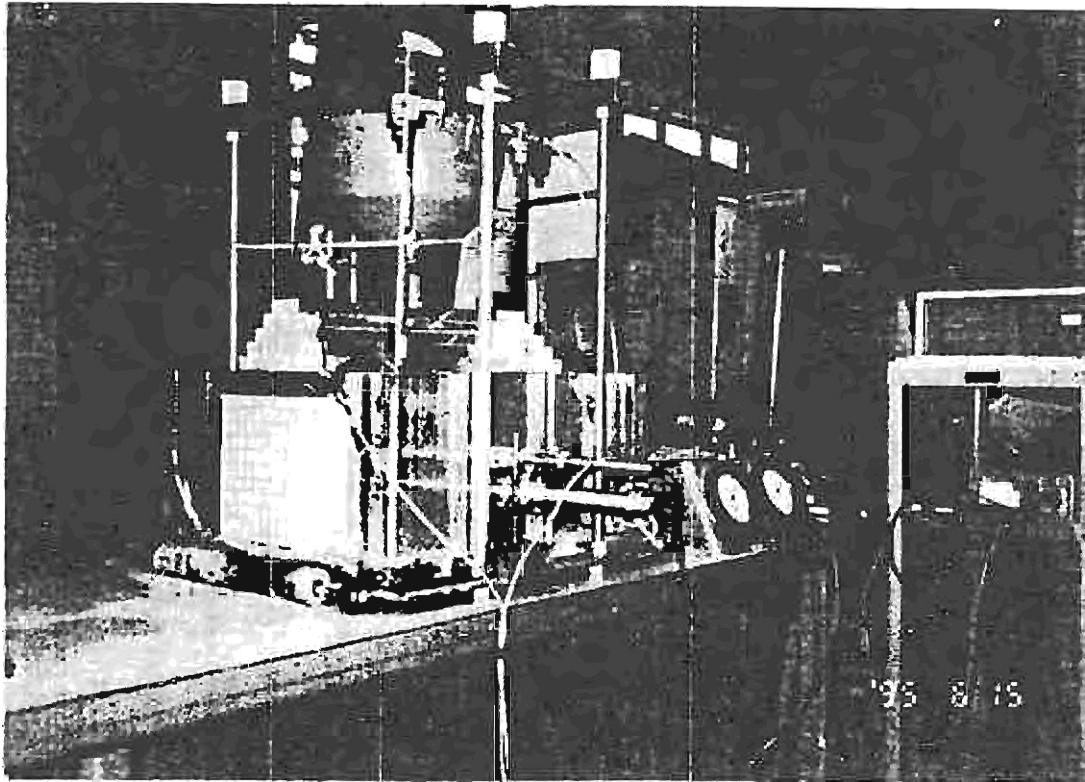


Figure 3.7 CTI long-term performance test loaded with Conbel pneumatic loading device

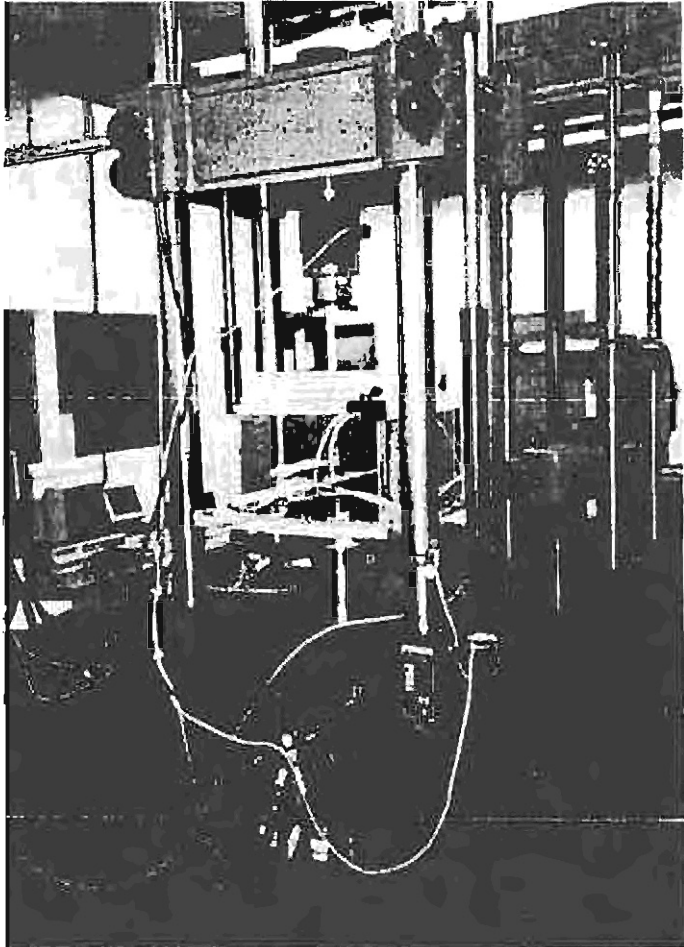


Figure 3.8 CTI long-term performance test loaded with a universal testing machine

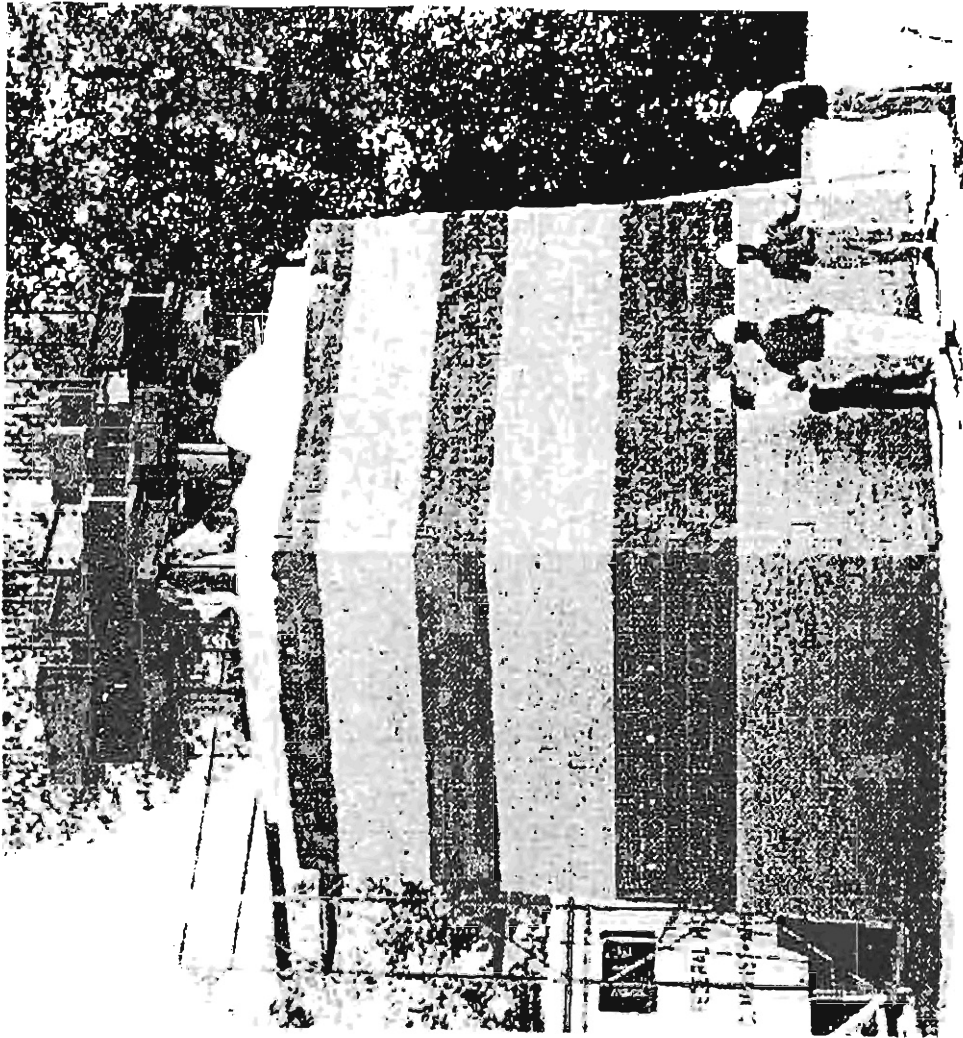


Figure 3.9 The FHWA pier experiment

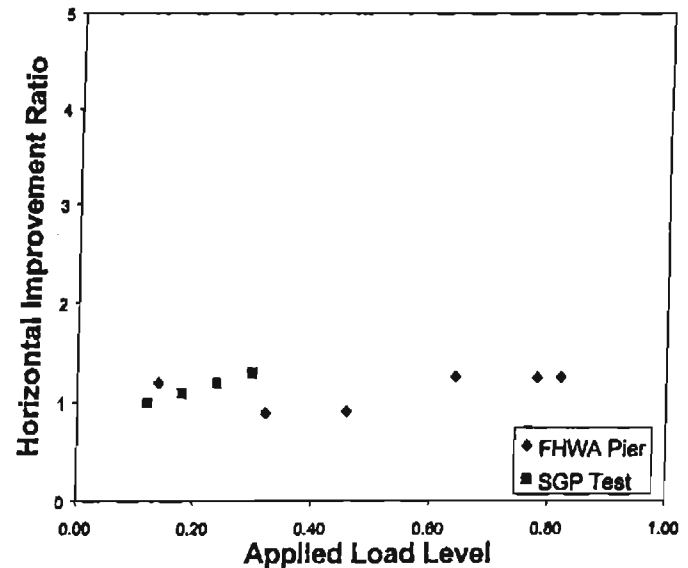
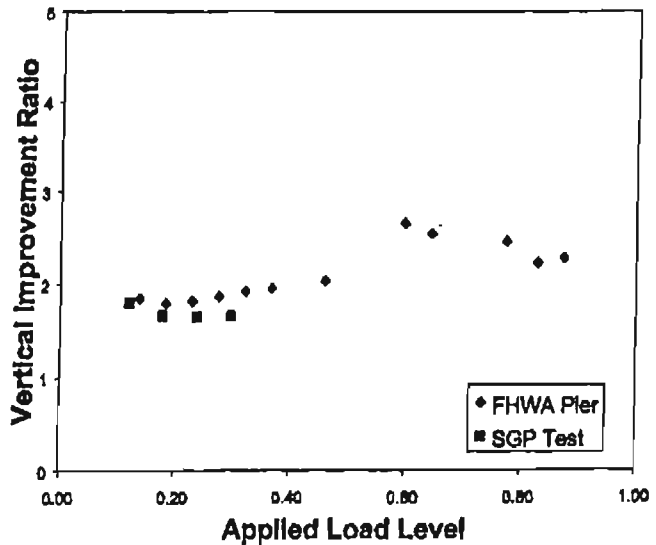


Figure 3.10 Effects of preloading: measured values versus predicted values by the CTI performance tests (after Ketchart and Wu, 2001)

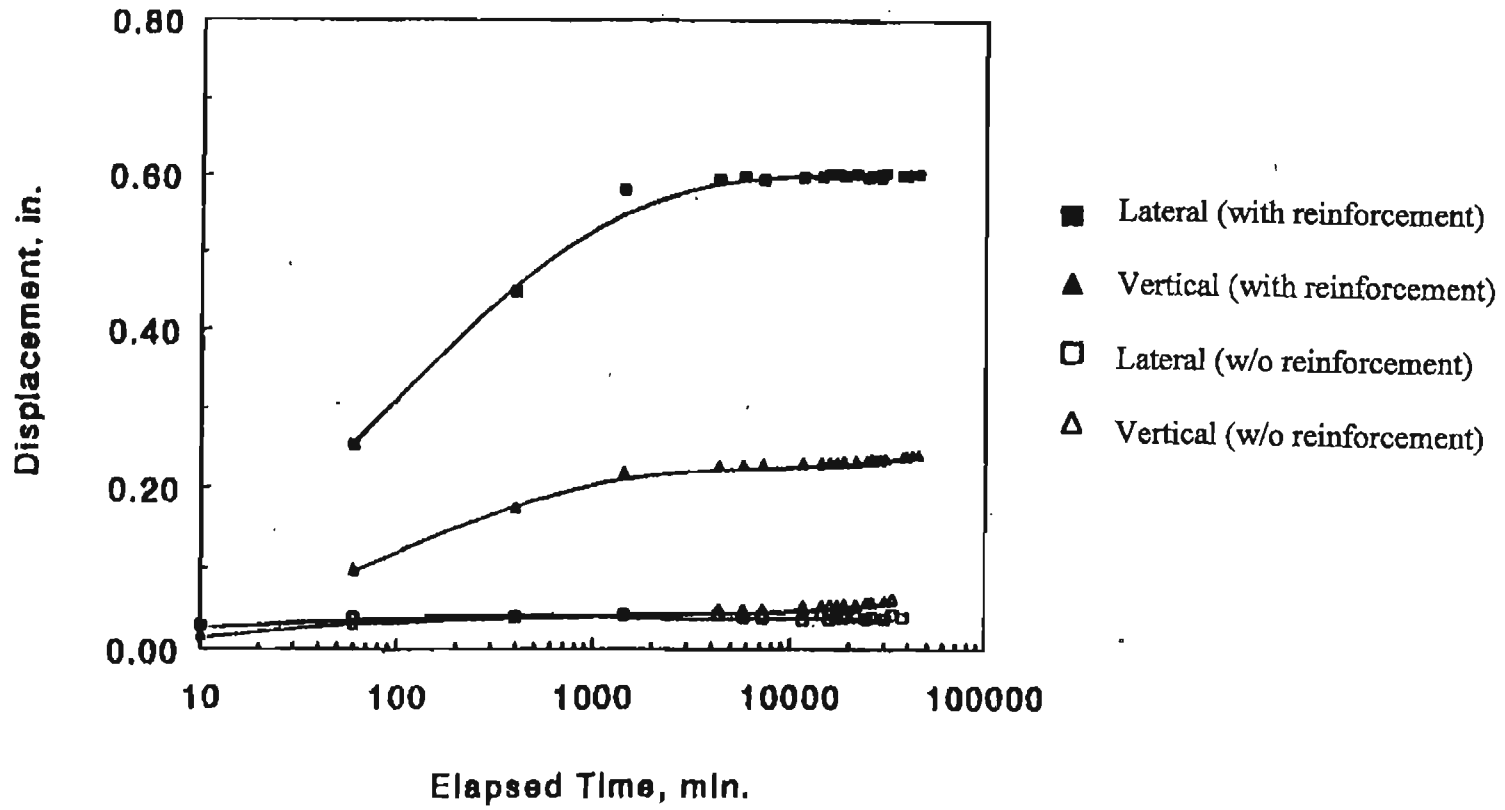


Figure 3.11 Vertical and lateral movements versus time relationships of a soil-geosynthetic composite and the soil mass without reinforcement (after Ketchart and Wu, 1996)

test. The clayey soil without any reinforcements, in otherwise the same test conditions, "collapsed" within merely 17 minutes after the test began.

As the creep rate of a soil-geosynthetic composite becomes very small, stress relaxation in the geosynthetic reinforcement is likely to occur. Figure 3.12 shows how the maximum forces in a geosynthetic reinforcement sheet decrease with time at various locations in the reinforcement. These forces were deduced from the strains measured along the length of the reinforcement (by the use of isochronous creep curves of the reinforcement). The reinforcement employed in the test was a heat-bonded geotextile (Tygar 3301) and the soil was a road base material.

Many SGIP tests have been conducted *under elevated temperatures* to accelerate creep of the geosynthetics (Ketchart and Wu, 1996). Figure 3.13 shows a SGIP test being conducted inside a temperature incubator. Figure 3.14 shows the vertical and lateral displacements versus time curve of a soil-geotextile composite at a temperature of 125°F. The composite was a nonwoven geotextile embedded in a road base material (with 20% of fines, prepared at 95% R.C. and 2% wet-of-optimum moisture) and subject to an average surcharge of 15 psi. Tests conducted by the fabric manufacturer have indicated that the creep rate of the geotextile at 125°F would be about 150 times faster than at the ambient temperature. Figure 3.14 indicated that the creep deformation of the soil-geotextile composite was very small and decreased rapidly with time. Creep deformation ceased completely after 12 days and gave an accumulative average strain of 0.58%. Similar behavior was observed for other reinforcements and surcharge pressures in that the creep deformation was small and reduced with time at a decreasing rate.

### 3.3.3 Unit Cell Test (Boyle, 1995) and ASPR Test (Whittle, et al., 1991 and 1992)

Boyle (1995) manufactured a unit cell device for soil-geosynthetic composites (see Figure 3.15). The device is similar to the Automated Plane

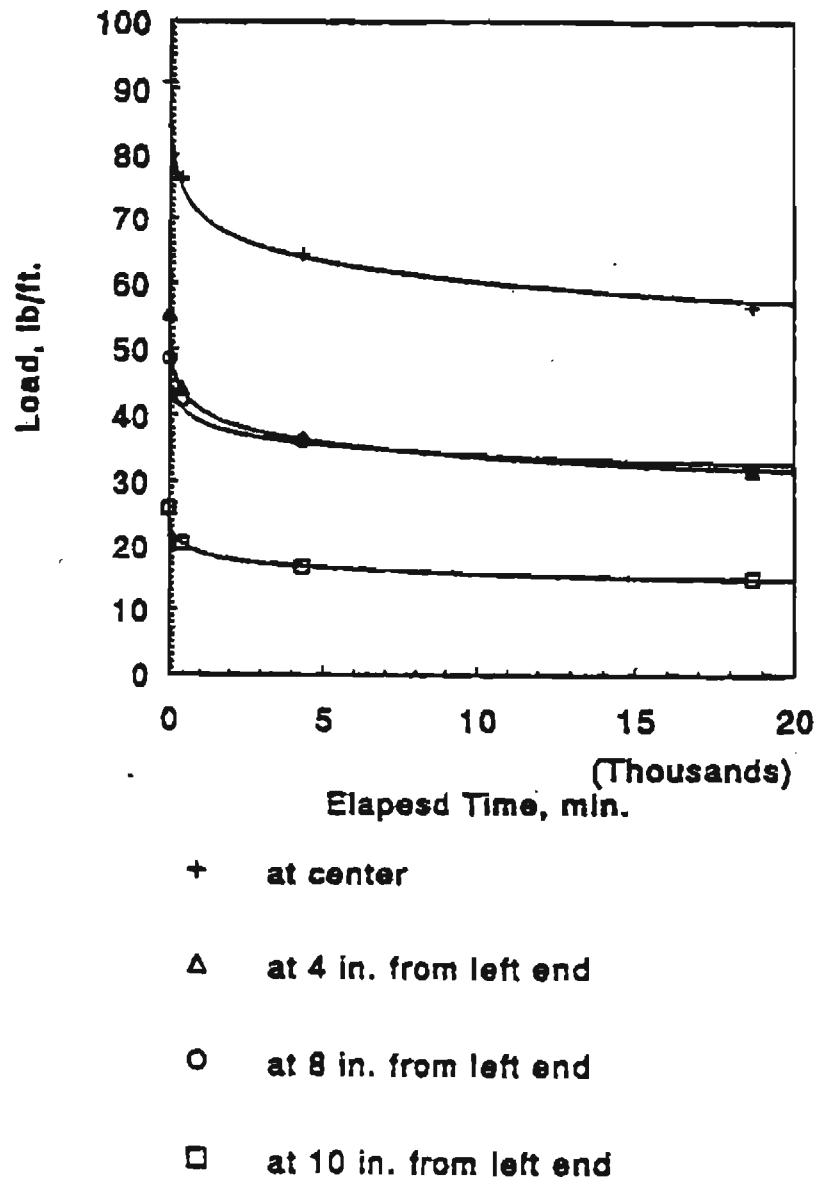


Figure 3.12 Relationship between forces in reinforcement and time (after Ketchart and Wu, 1996)

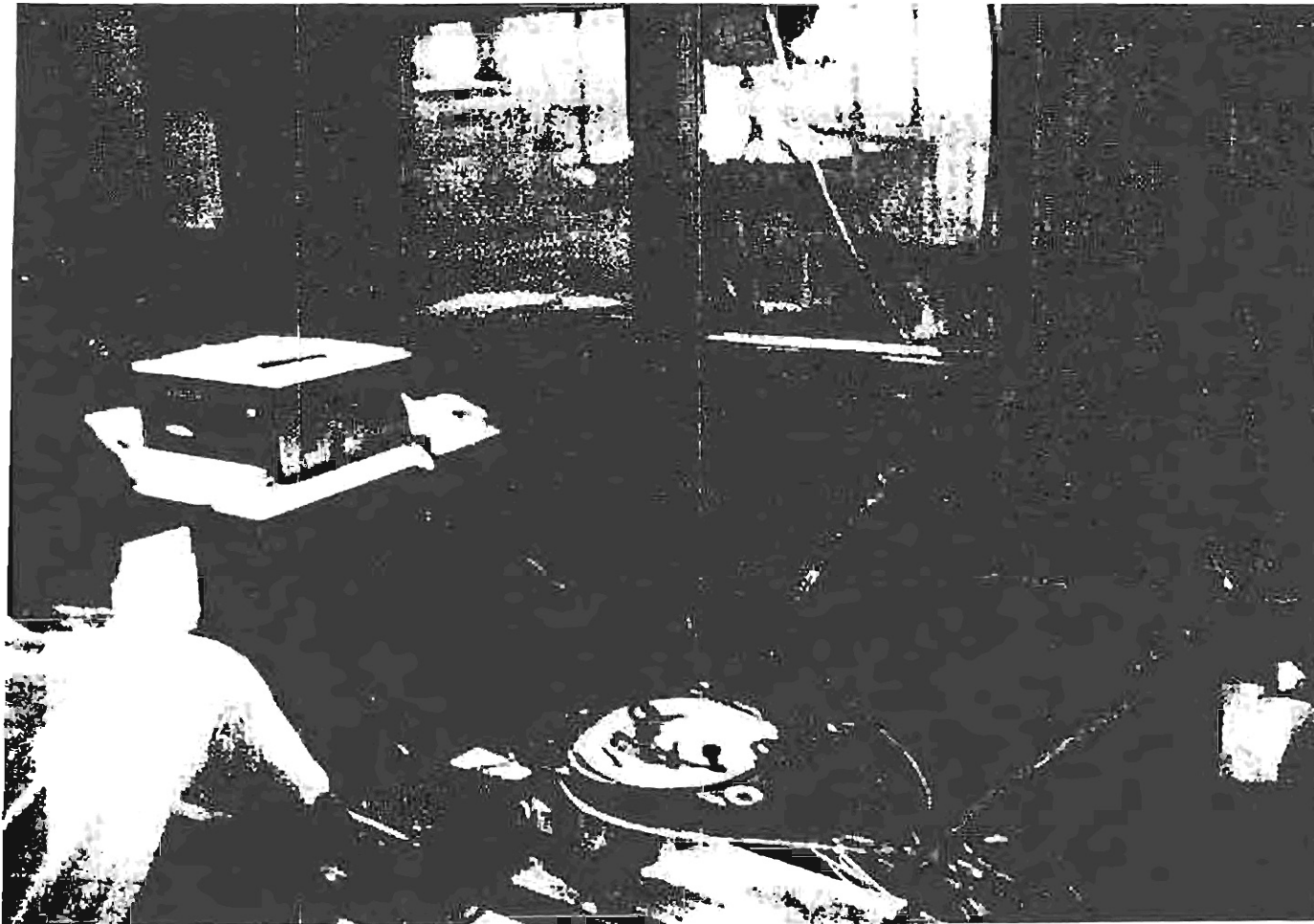


Figure 3.13 A CTI performance test being conducted inside a temperature incubator

Reinforcement : a polypropylene woven geotextile  
Soil: a "road base" (@ 95% R.C. & 2% wet of optimum)  
Overburden: 15 psi  
Temperature: 125° F

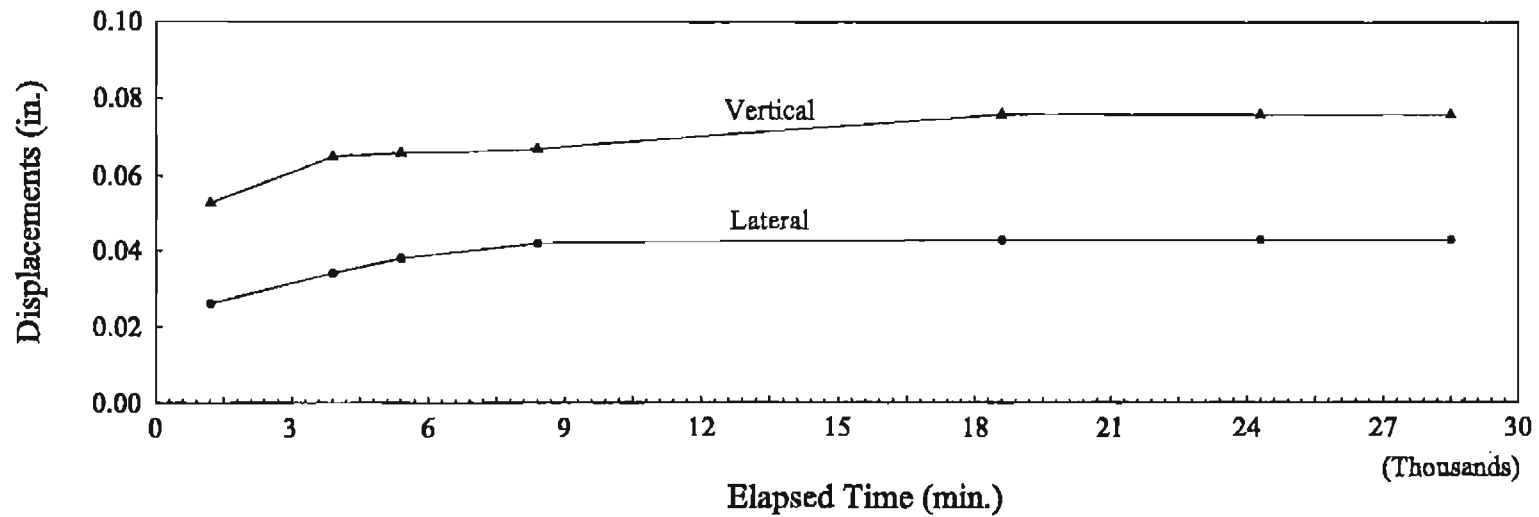


Figure 3.14 Vertical and lateral creep behavior of a soil-geosynthetic composite under 125° F (after Ketchart and Wu, 1996)

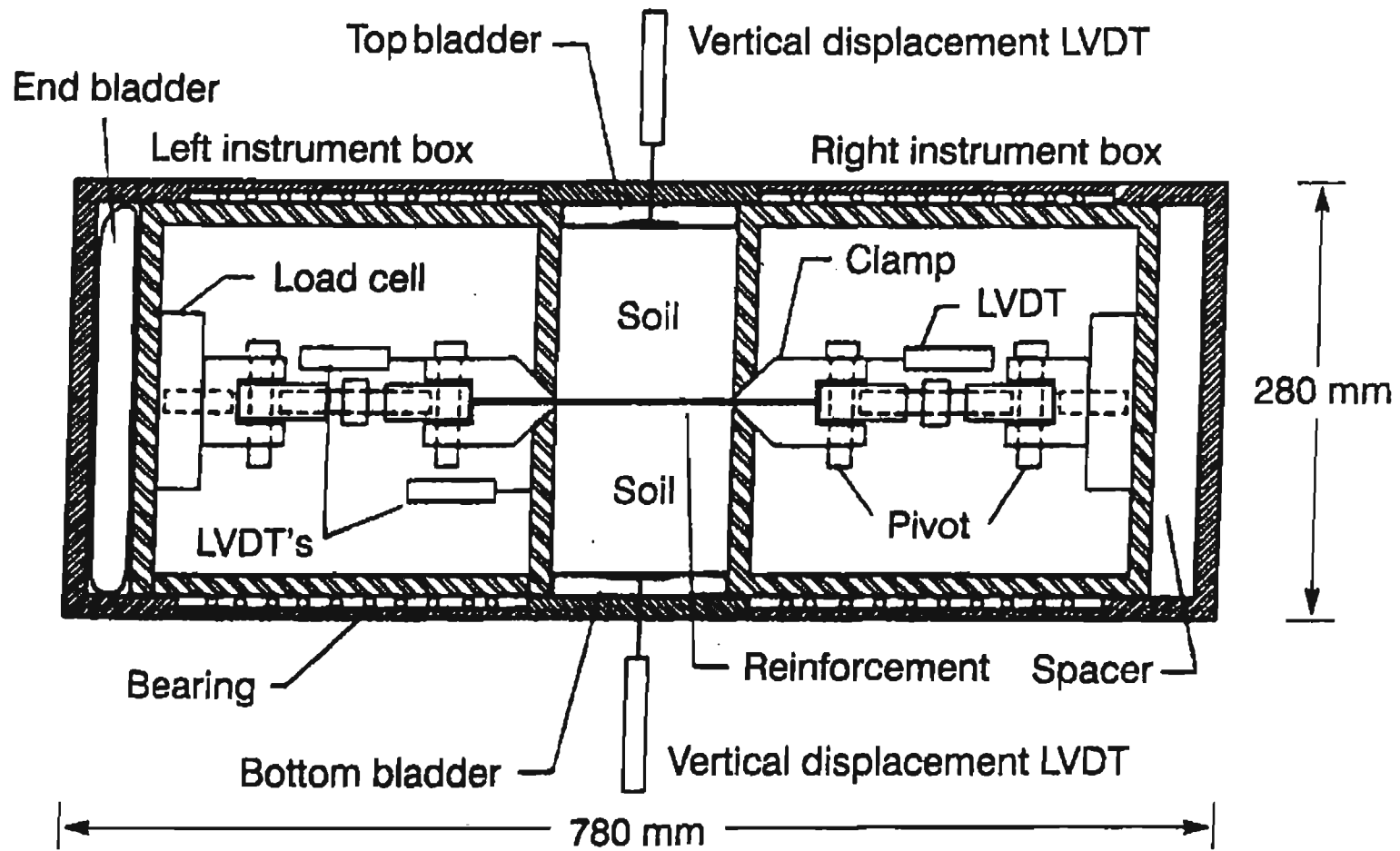


Figure 3.15 The unit cell device for soil-geosynthetic composites (after Boyle, 1995)

Strain Reinforcement (APSR) cell developed at MIT (see Figure 3.16) by Whittle and his associates (Whittle, et al., 1991 and 1992). In the test, a geosynthetic specimen was embedded in soil and was subjected to a plane strain loading condition. The loads at both ends of the geosynthetic were measured. Creep tests using sand as confining soil indicated that the geosynthetic experienced stress relaxation. In other words, after the creep deformation had become very small, the force in the geosynthetic began to reduce with time. The implication is that a GRS structure will have an increasing safety margin as time progresses.

### **3.4 Finite Element Analysis of Long-Term Performance**

Finite element analysis of the soil-geosynthetic interactive performance tests, as described Section 3.3.1, has also indicated that the backfill played the most important role in creep deformation of the soil-geosynthetic composites (Helwany and Wu, 1995). With a clayey backfill, creep deformation may be very significant, while the creep deformation will typically be negligible with a granular backfill.

Helwany and Wu (1995) conducted finite element analysis on two 3-m high geosynthetic-reinforced retaining walls. The walls were identical in every respect except that one wall was with a clayey backfill and the other with a granular backfill. In the clay-backfill wall, the maximum strain in the geosynthetic reinforcement at the end of construction was 8.5%. Due to the interaction between the clay and reinforcement, the maximum strain increased to 12.0% after 15 years. In the granular-backfill wall, the maximum strain at the end of construction was 2.5%. The strain showed negligible change over the next 15 years. Figure 3.17 shows the displacement fields for the two walls. The difference in the creep behavior due to the difference of the backfill is abundantly clear.

### **3.5 In-Service GRS Walls and Field Measurement**

Crouse and Wu (1996) conducted a study to examine seven actual GRS

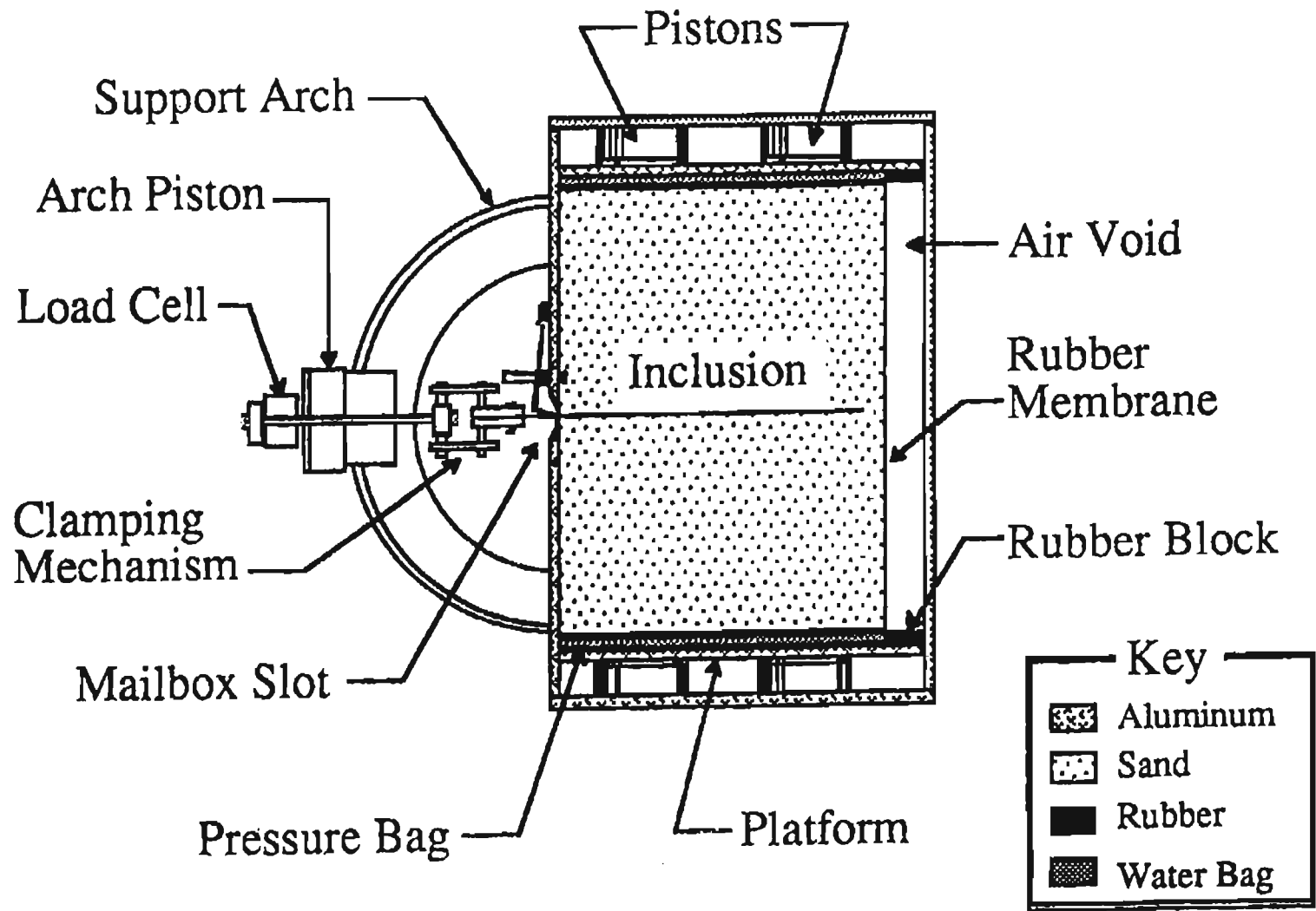


Figure 3.16 The automatic plane strain reinforcement (APSR) cell (after Whittle, et al., 1992)

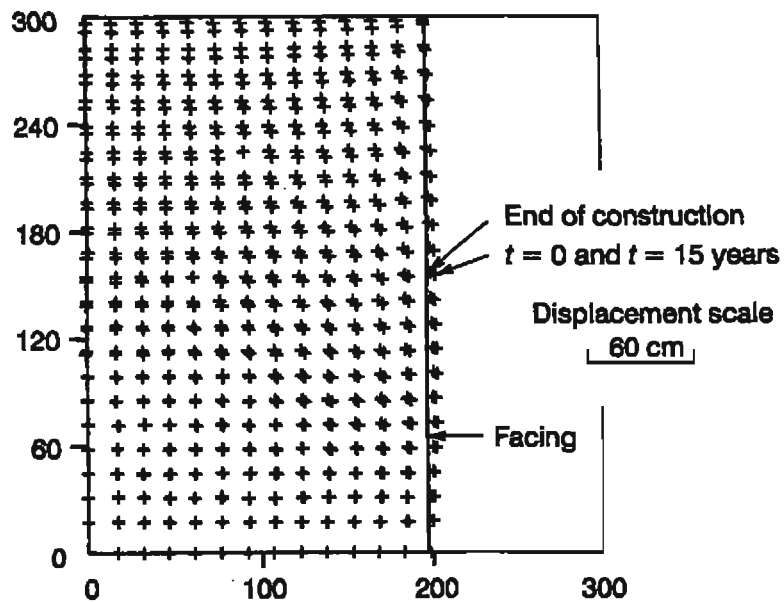
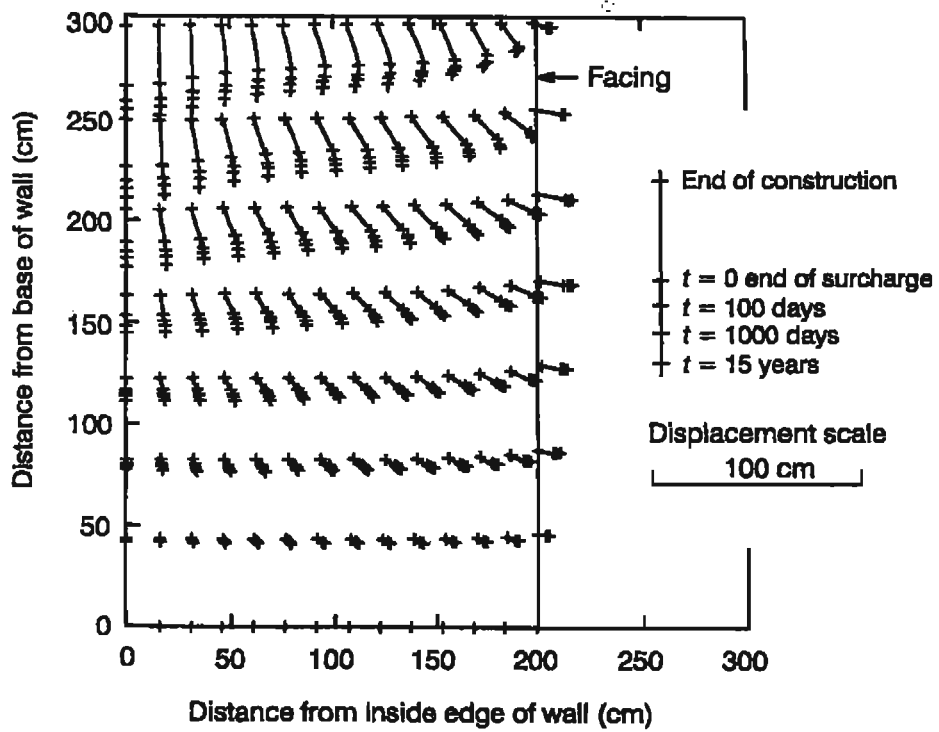


Figure 3.17 Displacement fields for a clayey backfill wall and a granular backfill wall (after Helwany and Wu, 1995)

walls that have sufficient measured data of long-term performance. These walls were selected because they have been monitored for extended periods of time (greater than six months) and typically with well-documented long-term reinforcement strain data, wall deformation data, and design information.

The seven GRS walls are (1) Interstate Highway 70 through Glenwood Canyon GRS wall project, *Glenwood Canyon wall* (Bell, et al., 1983; Derakhashandeh and Barrett, 1986; Bell and Barrett, 1995), (2) Tanque Verde - Wrighttown - Pantano Roads project, *Tucson wall* (Berg, et al., 1986; FHWA, 1989; Fishman, et al., 1993; Collin, et al, 1994; Bright, et al., 1994), (3) Norwegian Geotechnical Institute project, *NGI wall* (Fannin and Hermann, 1990 and 1992), (4) Japan Railway Test Embankment project, *JR wall* (Tatsuoka, et al., 1992), (5) Highbury Avenue, London Ontario project, *Highbury wall* (Bathurst, 1992), (6) Federal Highway Administration Research Algonquin Test Wall project, *Algonquin wall* (Simac, et al., 1990; Christopher, et al., 1994), and (7) Seattle Preload Fill project, *Seattle wall* (Allen, et al., 1992). These projects are summarized in Table 3.1. The walls range from 15 ft to over 40 ft in height and typically include surcharge loads comprising earth fills or highway loads. The geosynthetic reinforcement consisted of polypropylene or polyester geogrids and geotextiles ranging in short-term strength from 400 lb/ft to over 12,000 lb/ft. The facing used on the walls consisted of concrete modular blocks and panels or exposed surfaces. Some of the walls were constructed on weak foundations while others were constructed on competent foundations. The environmental conditions vary from freezing temperatures in Ontario, Canada, to temperatures up to 110° F for walls built in Arizona, USA.

In the following sections, a brief description of each project is presented, followed by a description and discussion of the long-term performance measurement of each project. A comparison of the measured creep rates and those obtained from the CTI interactive performance tests, as described in Section 3.3.2, is also presented.

Table 3.1 Selected In-Service GRS Walls (Crouse and Wu, 1996)

Project	Year Constructed	Monitoring Duration	Location	Representative Reference
Interstate-70 through Glenwood Canyon (Glenwood Canyon wall)	1982	7 months	Glenwood Springs, Colorado, USA	Bell, et al., 1983
Tanque Verde-Wrightstown-Pantano (Tucson wall)	1985	7 years	Tucson, Arizona, USA	Berg, et al., 1986
Norwegian Geotechnical Institute (NGI wall)	1987	4 years	Oslo, Norway	Fannin and Hermann, 1990
Japan Railway Test Embankment (JR wall)	1987	2 years	Tokyo, Japan	Tatsuoka, et al., 1992
Highbury Avenue (Highbury wall)	1989	2 years	London, Ontario, Canada	Bathurst, 1992
Federal Highway Administration (Algonquin wall)	1989	1.3 years	Algonquin, Illinois, USA	Simac, et al., 1990
Seattle Preload Fill (Seattle wall)	1989	1 year	Seattle, Washington, USA	Allen, et al., 1992

### 3.5.1 Glenwood Canyon Wall

#### A. Project Description

In April of 1982, the Colorado Department of Highways designed and constructed a geotextile-reinforced soil retaining wall through Glenwood Canyon. The wall was the first instrumented full-scale GRS walls constructed in the USA.

Figure 3.18 shows a typical cross-section of the Glenwood Canyon GRS wall. The wall was 15 ft high and 300 ft long and was divided into ten 30 ft long test sections. The subsoil at the construction site consisted of 10 to 60 ft of lacustrine deposits of highly compressible silt and clay layers. The backfill was a free-draining pit-run, rounded, well-graded, clean sandy gravel. Compaction of the backfill was carried to 95% of the modified Proctor (AASHTO T180). The wall was purposely designed to evaluate the lower stability limits of a GRS wall. Geotextiles having relatively low tensile strengths (400 to 900 lb/ft) were used for the reinforcement.

#### B. Measured Performance and Discussions

The performance of the Glenwood Canyon GRS wall was observed for several years; however, quantitative performance data was documented for only the first seven months of service (Bell, et al., 1983). As low strength reinforcement was employed, it was anticipated that the reinforcement would exhibit very large strains, on the order of 55%, yet little movement within the reinforced soil mass was observed. Approximately one year after the wall was constructed, a surcharge load was applied to the top in an attempt to create failure conditions. The surcharge consisted of a 15 ft high soil embankment applying a pressure of approximately 1,950 lb/ft<sup>2</sup>. However, failure never occurred.

Since the wall was constructed on a weak foundation soil, it did experience significant movement over time. The retaining wall experienced over 1.4 ft of differential settlement from one end of the wall to the other, 11 years after construction. The settlement was mostly due to consolidation of underlying clays.

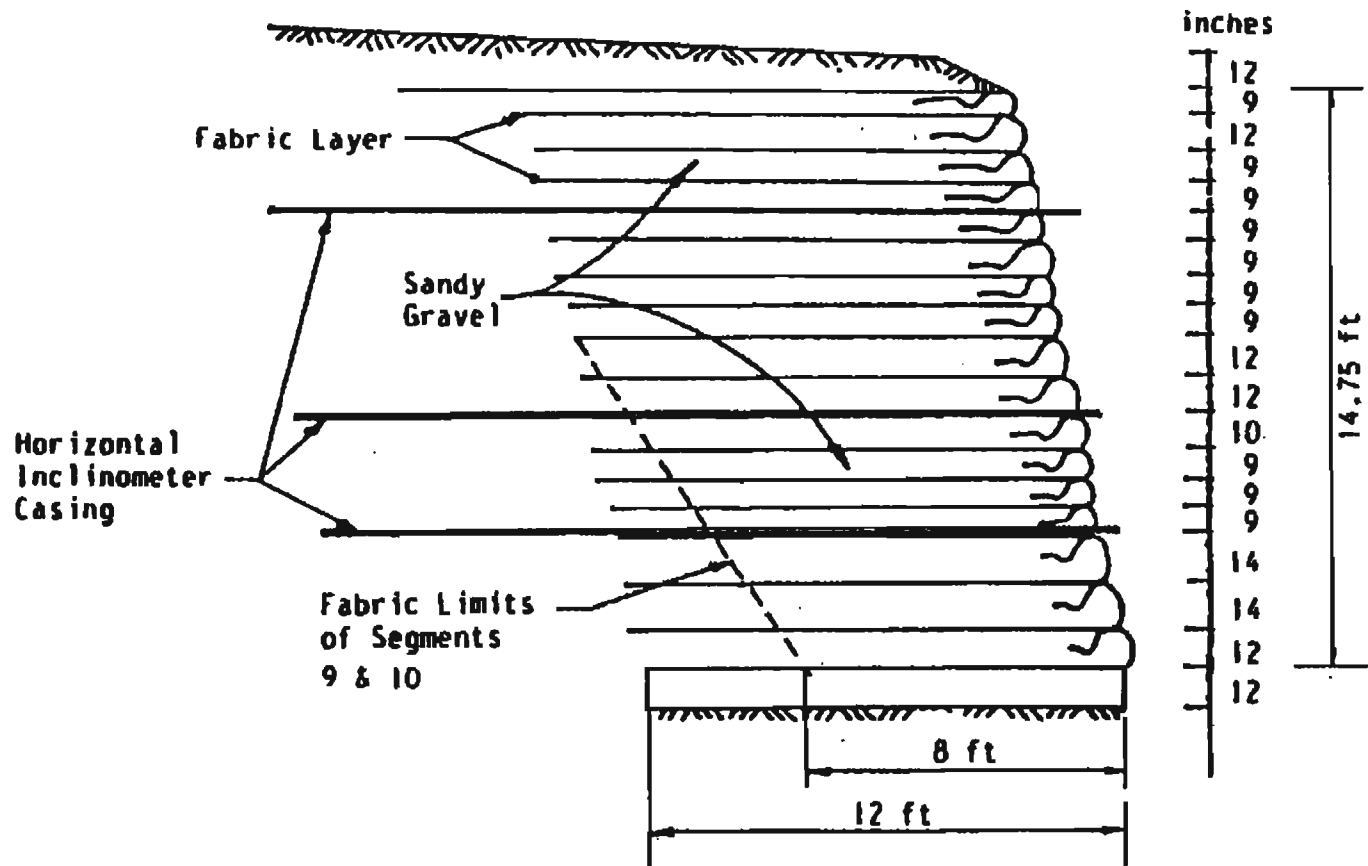


Figure 3.18 Typical cross-section of the Glenwood Canyon GRS wall (after Bell, et al., 1983)

Despite the large differential settlements, little distress of the wall was detected (Derakhashandeh and Barrett, 1986).

In 1984, a vertical cut measuring 15 ft x 15 ft x 15 ft was made in the wall to exhume geotextile samples for survivability/durability testing. The cut was left unprotected for the next seven years, yet the integrity of the wall was maintained (see Figure 3.19). Samples of geotextiles were again exhumed and tested in 1993. It was found that there was no loss of strength in samples obtained and tested in 1993 and 1984, indicating that durability of geotextiles was not a problem for this wall (Bell and Barrett, 1995).

### 3.5.2 Tucson Wall

#### A. Project Description

In 1984 and 1985, forty-six (46) GRS walls were constructed in the city of Tucson as part of the Tanque Verde Grade Separation Project (Collin, et al., 1994). A typical cross-section of the wall is shown in Figure 3.20. In September of 1985, two of the walls were instrumented (Panels 26-30 and 26-32) to monitor their performance during and after construction. Wall Panel 26-30 was 15.6 ft high and Wall Panel 26-32 was 16.1 ft high. Approximately seven years of performance data have been published for the instrumented walls (Collin, et al., 1994). The original design and instrumentation information is contained in a Federal Highway Administration (FHWA) report entitled "Tensar Geogrid-Reinforced Soil Wall" (FHWA, 1989). Other papers describing the construction and performance of the walls have also been published by Berg, et al. (1986) and Fishman, et al. (1993).

The city of Tucson is located in the southern part of the state of Arizona, USA, in the Sonora desert where summer temperatures can reach as high as 111° Fahrenheit. Soil temperatures within the wall can reach as high as 97° Fahrenheit. Elevated temperature environments for geosynthetics were a design concern since the high temperatures may accelerate mechanisms of long-term degradation. Similar to the Glenwood Canyon wall project,

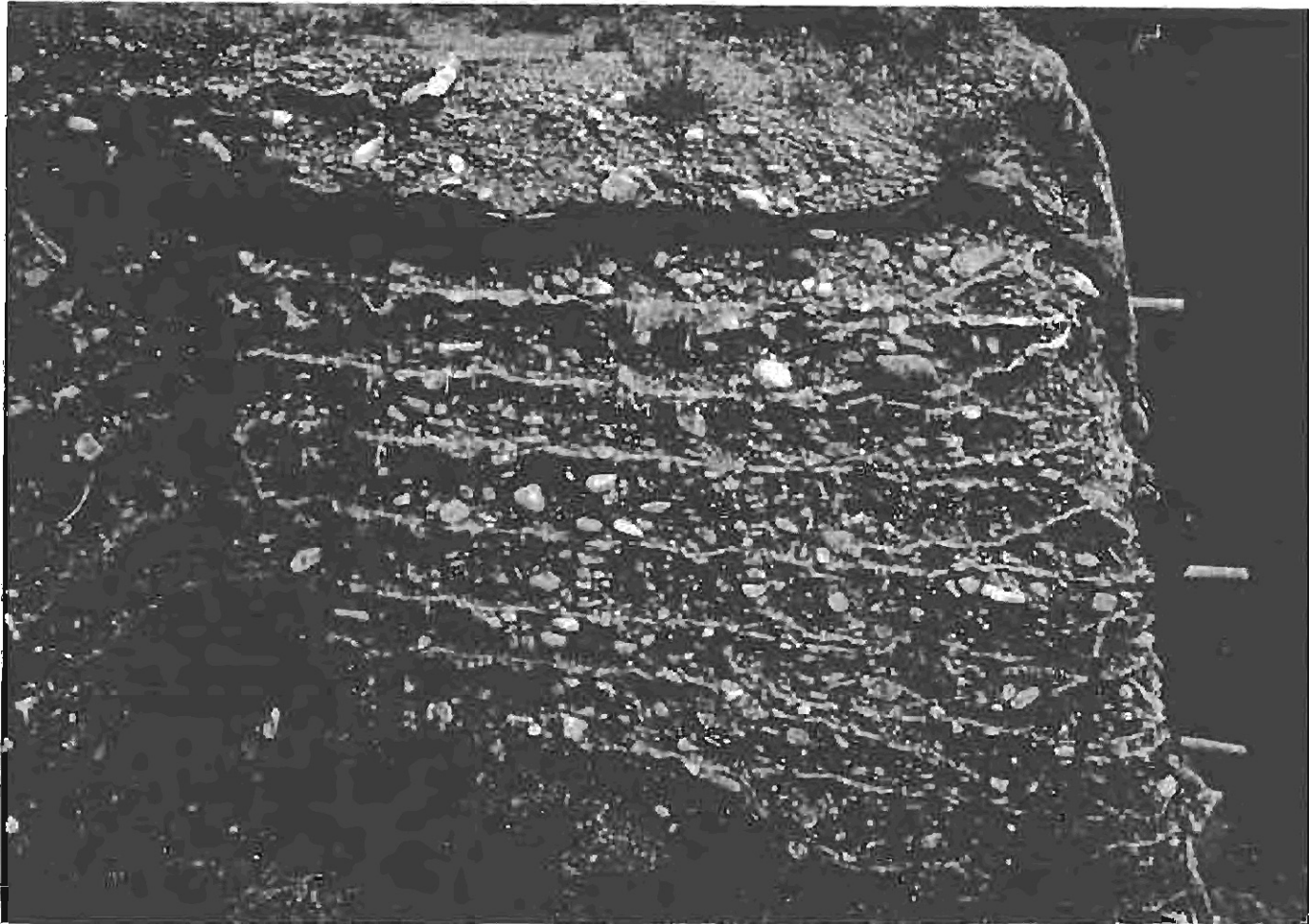
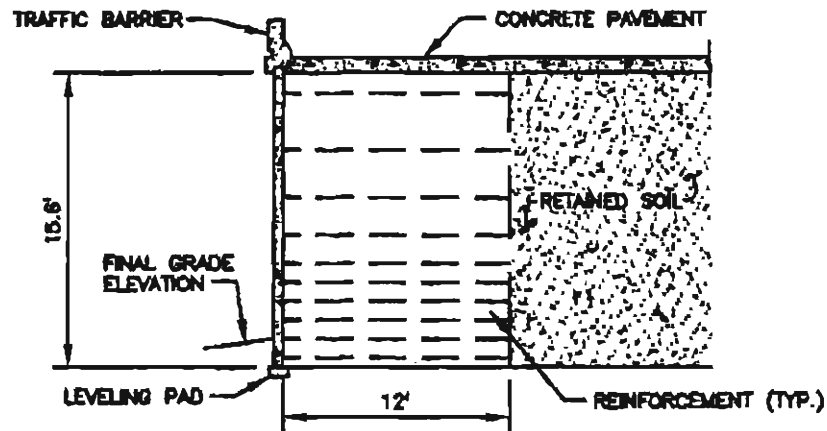
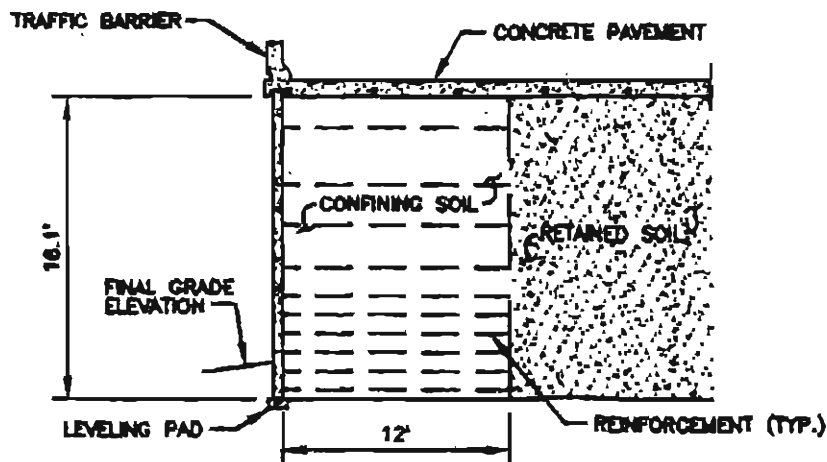


Figure 3.19 A cut made in the Glenwood Canyon wall left unprotected for seven years (courtesy of R.K. Barrett)



Wall Panel 26-30



Wall Panel 26-32

Figure 3.20 Typical cross-section of the Tanque Verde-Wrightstown-Pantano Roads wall (after Collin, et al., 1994)

reinforcement samples were exhumed after 11 years of service to examine the durability of the reinforcement (Bright, et al., 1994).

#### B. Measured Performance and Discussions

The performance of Wall Panels 26-30 and 26-32 was monitored for approximately seven years after construction. Geogrid reinforcement strains were measured in the bottom, middle and top layers of the two wall panels using resistance strain gages and inductance coils. Strain readings from the inductance coils had a large variance due to low strains in the reinforcement; therefore the results were believed to be unreliable (FHWA, 1989) so only the readings from the strain gauges were analyzed in this study.

Reinforcement strains were measured during construction, two weeks after construction and thereafter on an annual basis. The post-construction strain measurements were adjusted to account for pre-tensioning and compaction during construction so that strains measured after construction would be the result of creep.

The lateral movement of the walls was measured by surveying points at the top of the walls. The points were surveyed during construction and up to one month after construction. During construction, the top of both walls moved laterally approximately 3 in. while the bottom of the walls remained stationary. Little movement was observed after construction.

The mean total creep strain in the reinforcement after construction is shown in Figure 3.21. As can be seen from the Figure, the strain increased in the reinforcement during the first year of service. The creep deformation, however, was very small. The maximum creep strain was 0.4% (Panel 26-32) to 0.6% (Panel 26-30) in the first year. Thereafter, the creep strain remained practically unchanged, indicating that the walls had stabilized with time and the additional creep deformation was negligible.

It is to be noted that the exhumed samples exhibited little degradation over 11 years from the time the geosynthetic reinforcement was first installed.

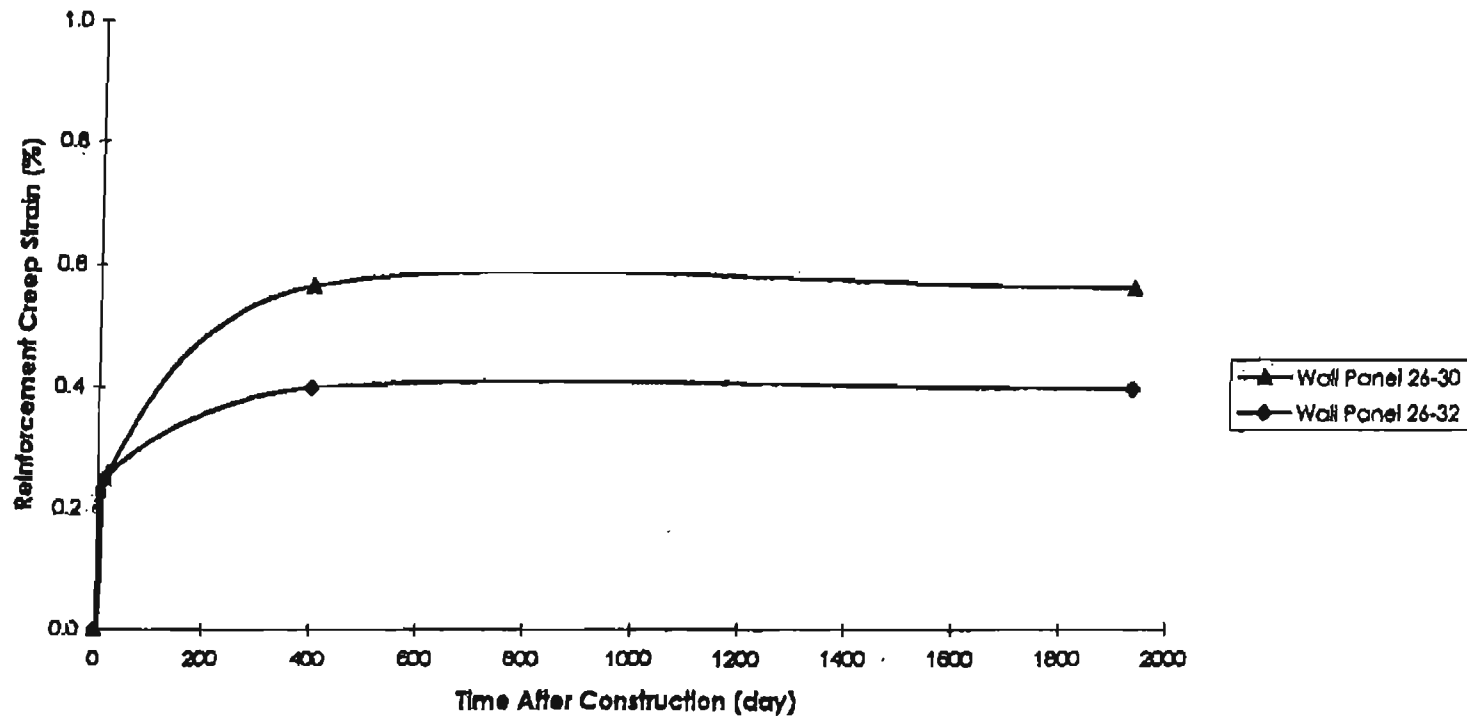


Figure 3.21 Reinforcement strain versus time curve for the Tanque Verde-Wrightstown-Pantano Roads wall (after Crouse and Wu, 2001)

### 3.5.3 NGI Wall

#### A. Project Description

In 1987, the Norwegian Geotechnical Institute (NGI) built a full-scale GRS test wall in Skedsmo, Norway. The wall was 15.7 ft high. Figure 3.22 shows a typical cross-section of the test wall. The purpose of the wall was to examine the characteristics of creep in the reinforcement. Skedsmo is located near the city of Oslo, Norway, in northern Europe. The climate at Oslo is moderate with temperatures ranging from 38° Fahrenheit in the winter to 64° Fahrenheit in the summer. Rainfall can be heavy at times with approximately 40 inches of rainfall annually.

The wall was instrumented in two sections, Sections 'J' and 'N', each with a different arrangement and spacing of the reinforcement (Section 'N' had twice as many layers of reinforcement as Section 'J'). Approximately four years of performance data have been published for the two instrumented sections (Fannin and Herman, 1992). Following construction, the wall was monitored for approximately four weeks under self-weight. Thereafter, the top of the wall was cyclically loaded by using water tanks that applied a maximum contact pressure of 6,000 lb/ft<sup>2</sup>. After approximately two months of the cyclic loading, the tanks were removed and a permanent 10 ft high surcharge was placed on top of the wall, applying a uniform and sustained pressure of 10,000 lb/ft<sup>2</sup>.

Detailed information concerning the design and instrumentation of the wall has been reported by Fannin and Hermann (1990 and 1992).

#### B. Measured Performance and Discussions

The performance of the Norwegian Geotechnical Institute project wall (Sections 'J' and 'N') was monitored for approximately four years after construction. Both the force and strain were measured in the reinforcement.

The mean total creep strain in the reinforcement for the two sections following application of the permanent surcharge loading is illustrated in Figure 3.23. The creep strain was determined from the incremental increase in the total strain beginning 10 days after the surcharge was placed. The maximum creep

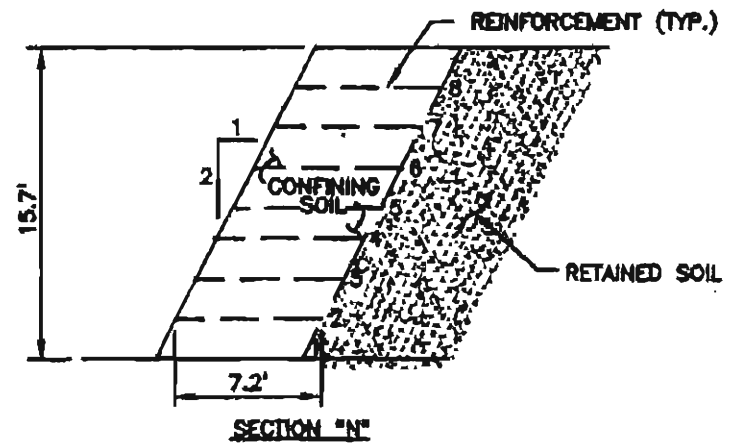
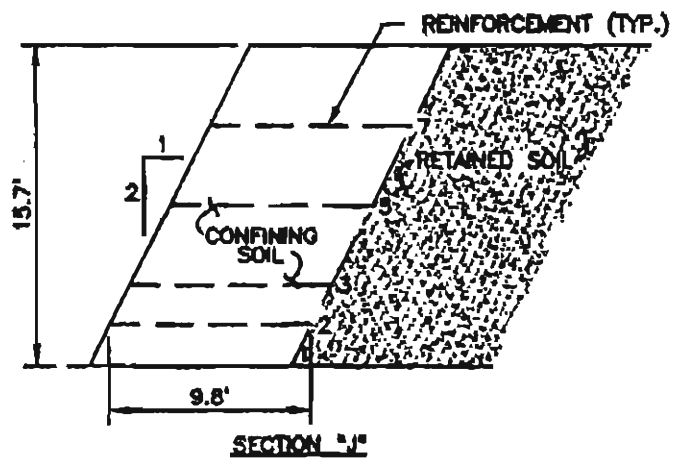


Figure 3.22 Typical cross-section of the NGI wall (after Fannin and Hermann, 1990)

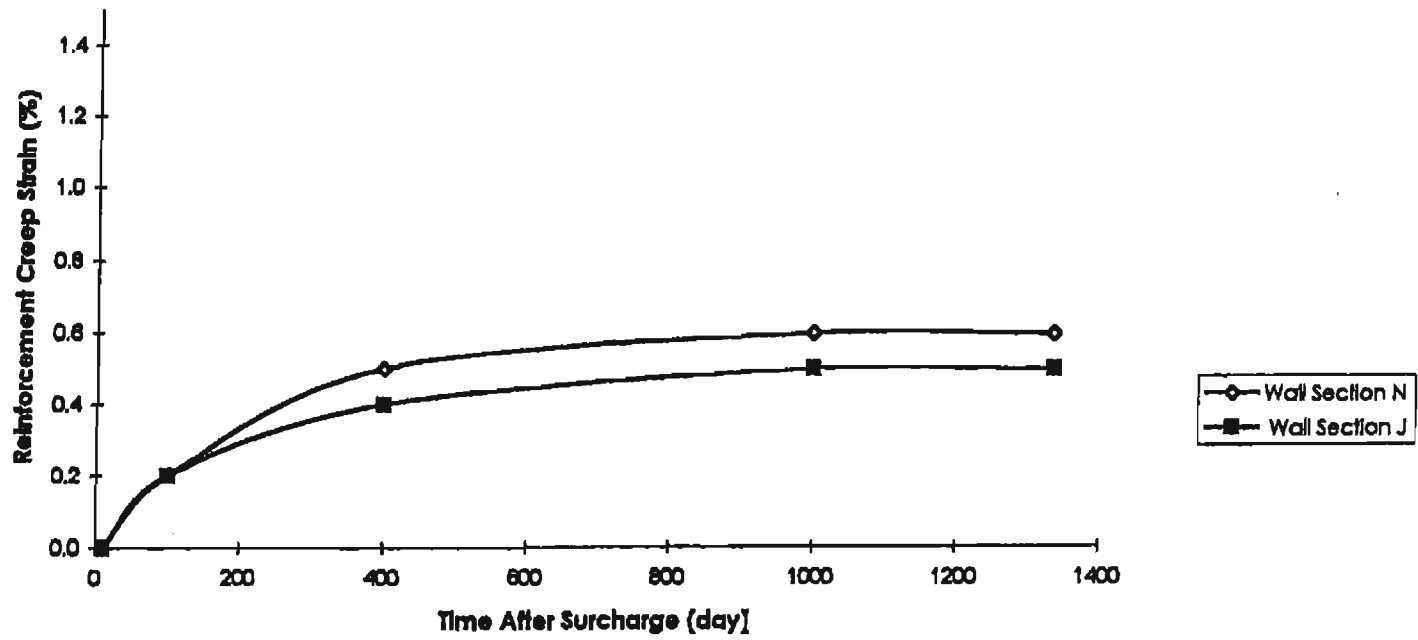


Figure 3.23 Reinforcement strain versus time curve for the NGI wall (after Crouse and Wu, 2001)

strains after one year were approximately 0.4% and 0.5% in Sections “J” and “N”, respectively. The increase in the maximum creep strain over the next three years was approximately 0.1% for both Sections.

#### 3.5.4 JR Wall

##### A. Project Description

Two test embankments were constructed at the Experiment Station of Japan Railway Technical Research Institute near Tokyo, Japan. The test embankments were part of a series of embankments constructed with sand and Kanto loam (a prevailing clay in Tokyo area) in the 1980's to develop an internal reinforcing system that could withstand its heavy precipitation events (Tatsuoka, et al., 1992). The first test embankment (JR Number 1) was backfilled with sand while the second embankment (JR Number 2) was backfilled with clay. JR Number 1 (see Figure 3.24) was selected for this report. The embankment was 16.4 ft high and reinforced with 17 layers of reinforcement at 1 ft vertical spacing.

JR Number 1 was constructed in 1988 to evaluate the stability of GRS embankments with rigid facing. Instruments were installed during construction and monitored for approximately two years until 1990, when it was loaded to failure. The facing consisted of rigid cast-in-place concrete panels installed in five wall sections. The facing of one wall section was of discrete panel squares for comparison with the rigid panels. The detailed project information can be found in Tatsuoka, et al. (1992).

##### B. Measured Performance and Discussions

The performance of the Japan Railway Test Embankment JR Number 1 was monitored for approximately two years after construction. The vertical and lateral displacement and tensile force in the reinforcement were measured in three wall sections (cross sections D-D, F-F, and H-H). The cross-sections of the three wall sections are shown in Figure 3.25.

Figure 3.26 illustrates the measured results. It is seen that the tensile force in the reinforcement increased during the first eight months reaching a nearly

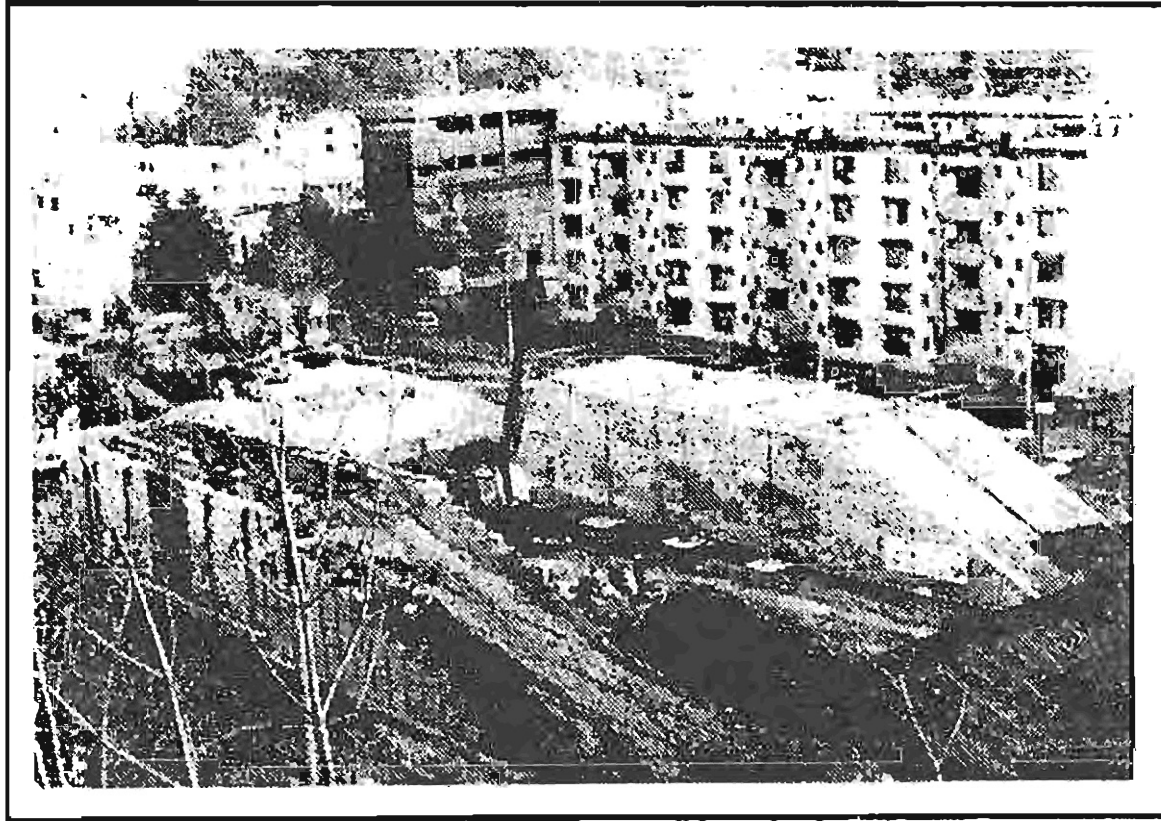
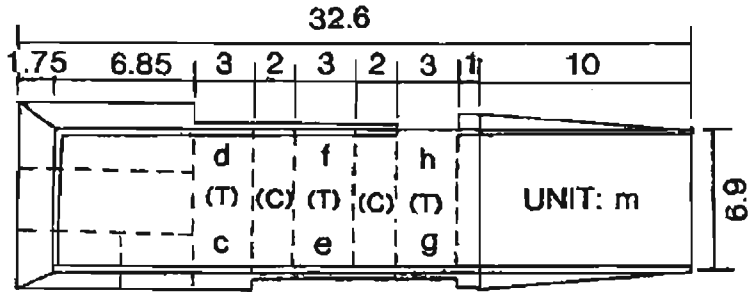
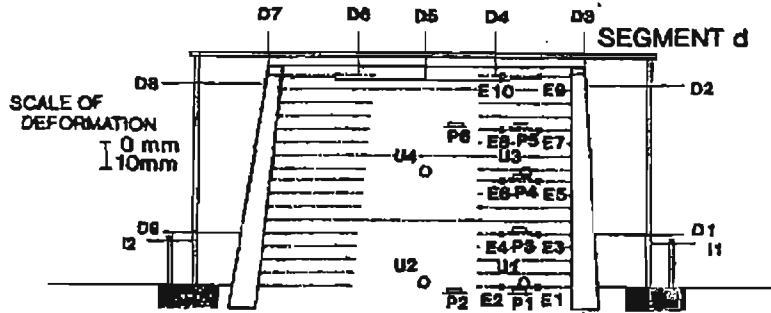


Figure 3.24 Japan Railway embankment: JR Number 1 (after Tatsuoka, et al., 1992)

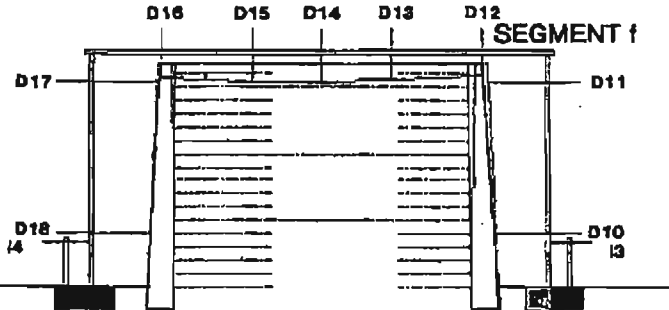


(a)

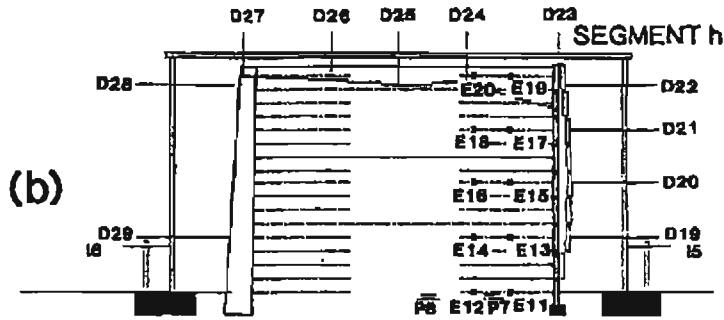
SECTION c-d



SECTION e-f



SECTION g-h



(b)

Figure 3.25 Cross-sections of the JR Number 1 embankment (after Tatsuoka, et al., 1992)

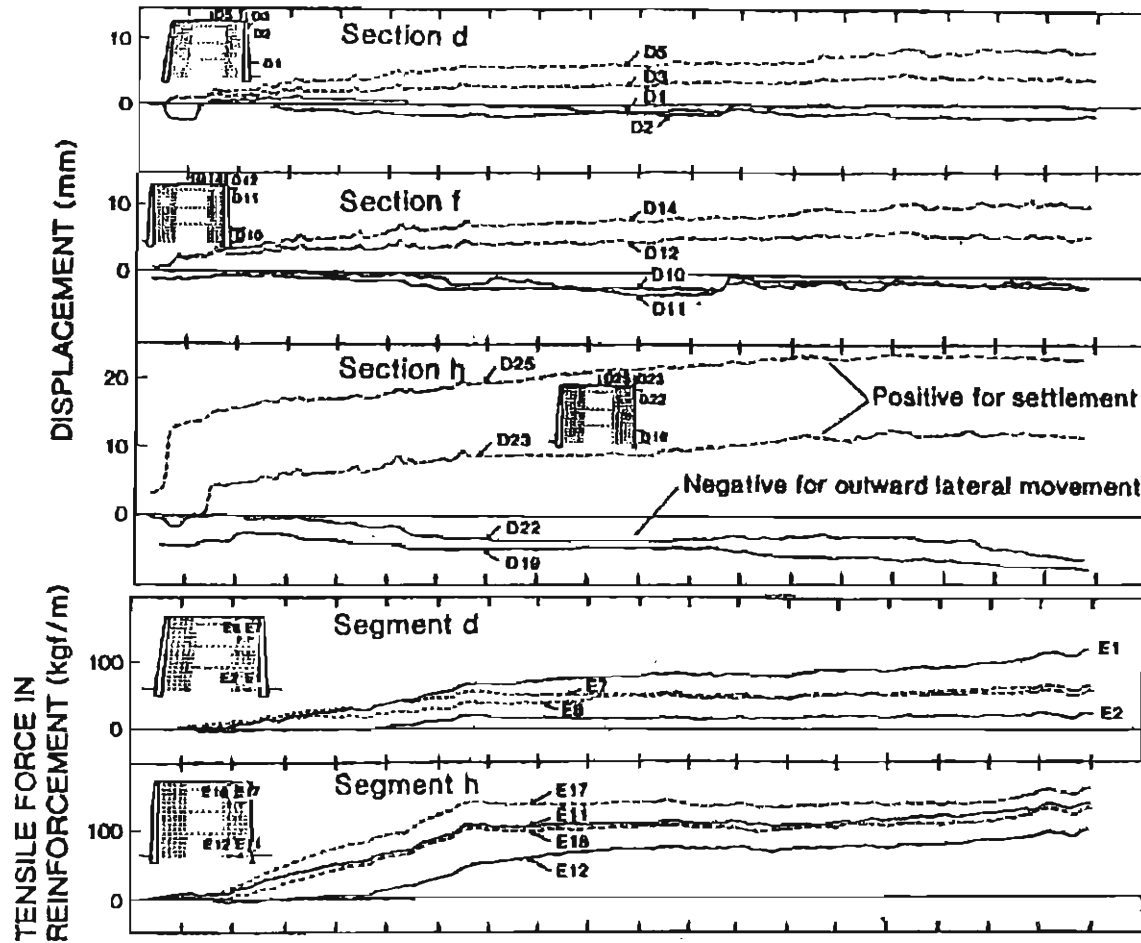


Figure 3.26 Measured results of the JR Number 1 embankment (after Tatsuoka, et al., 1992)

asymptotic state similar to the performance of the other projects. The maximum tensile force in the reinforcement was approximately 131 lb/ft. This is approximately 0.07 of the short-term strength (1,880 lb/ft).

### 3.5.5 Highbury Wall

#### A. Project Description

The Royal Military College of Canada has published several papers documenting the long-term performance of a GRS wall used in reconstructing and widening Highbury Avenue in London, Ontario, Canada. The wall was 23.3 ft high. Figure 3.27 shows a typical cross-section of the GRS wall. Props were employed to support the wall face during construction. The wall was instrumented during construction in late 1989. Approximately two years of performance data have been published through August of 1991 (Bathurst, 1992). The research objective for the project was to collect performance data from a well-instrumented in-service GRS wall to evaluate its long-term performance.

#### B. Measured Performance and Discussions

The Highbury Avenue Wall was monitored for approximately two years. Reinforcement strain was measured after the props holding the concrete panels were removed. Reinforcement strain was measured thereafter in December 1990; then in March 1990; July and August 1990; and a year later in August 1991. The creep strain was based on the incremental change in the strain since December 1990.

The maximum reinforcement creep strain was approximately 1.5%, which occurred about 7 months after prop release. The mean creep strain over time is plotted in Figure 3.28. It is seen that the mean creep strains decreased after reaching the maximum value.

### 3.5.6 Algonquin Wall

#### A. Project Description

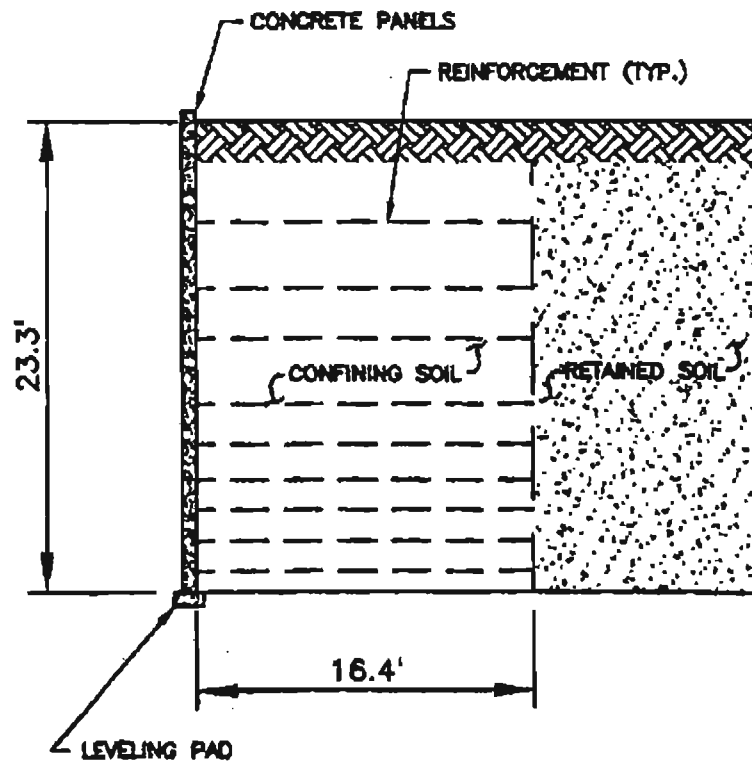


Figure 3.27 Typical cross-section of the Highbury Avenue wall (after Bathurst, 1992)

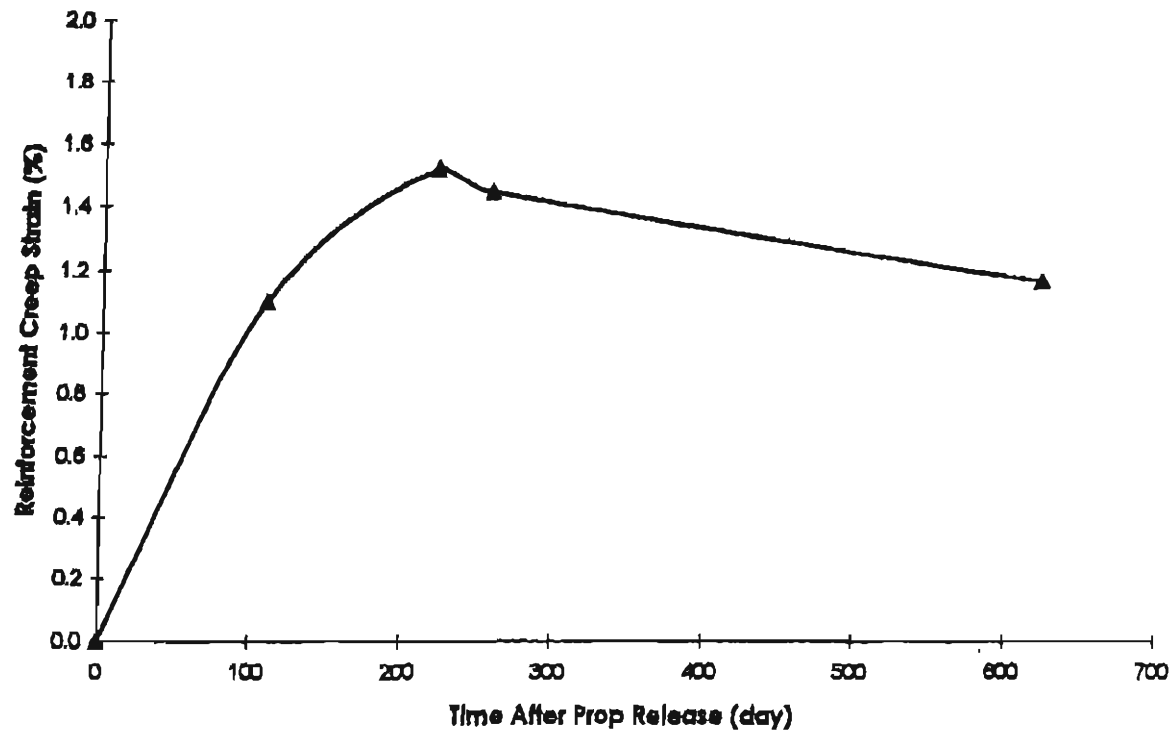


Figure 3.28 Reinforcement strain versus time curve for the Highbury Avenue wall (after Crouse and Wu, 2001)

From 1984 to 1989, the FHWA sponsored several soil reinforcement research projects at its stone quarry in Algonquin, Illinois. One project consisted of a wall referred to as "Wall-9". The wall was built to quantify the long-term behavior of continuous filament polyester geogrid reinforcement and dry-stacked, soil-filled facing units (Simac, et al., 1990).

Figure 3.29 shows a typical cross-section of the GRS wall. The test wall was 20 ft high and constructed with a very low factor of safety to evaluate the applicability of existing design methods. The internal stresses were monitored for three months, then an inclined surcharge approximately 7 ft high was placed and monitored for approximately 1.3 years.

#### **B. Measured Performance and Discussions**

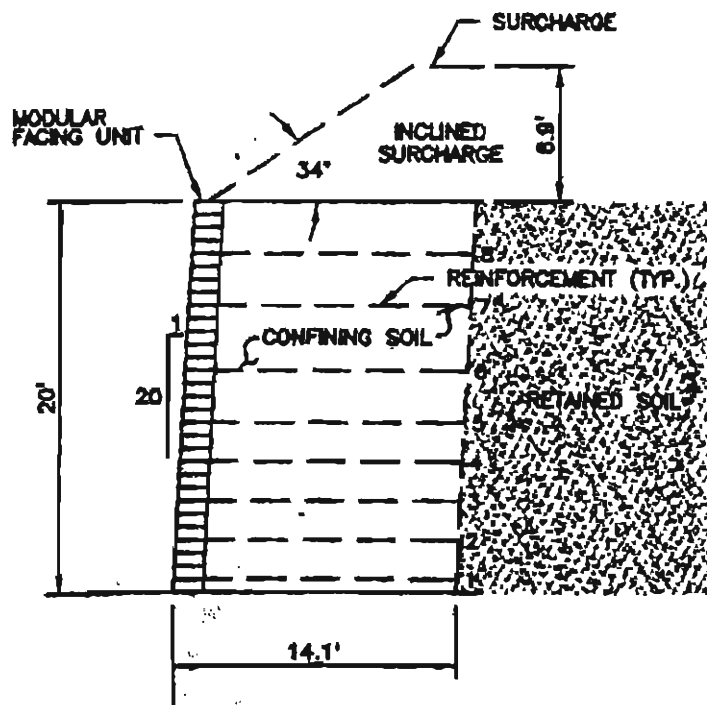
Wall-9 built for the FHWA project was monitored for approximately one year. Reinforcement strain and total wall movement were recorded more frequently than most other projects. Instrument readings were recorded almost on a daily basis during construction and during placement of the surcharge load. The surcharge was completed on November 10, 1989. Thereafter instrument readings were recorded nine times up through November 11, 1990.

The maximum creep strain computed after the surcharge load was placed is plotted in Figure 3.30. The creep strain was based on the incremental increase in the total strain. As shown in Figure 3.30, the creep strain appeared to be still increasing one year after the surcharge was applied. However, the creep strains were very small. The maximum creep strain was approximately 0.7% over the one-year monitoring period. The total lateral movement after the props were released was approximately 3.6 in. The measurement was based on the vertical inclinometer directly behind the face of the wall.

### **3.5.7 Seattle Wall**

#### **A. Project Description**

In March of 1989, the Washington State Department of Transportation designed and supervised the construction of a series of GRS walls to provide a



**Federal Highway Administration Project**  
**Wall No. 9**  
**Algonquin, Illinois, USA**

Figure 3.29 Typical cross-section of the FHWA wall (after Simac, et al., 1990)

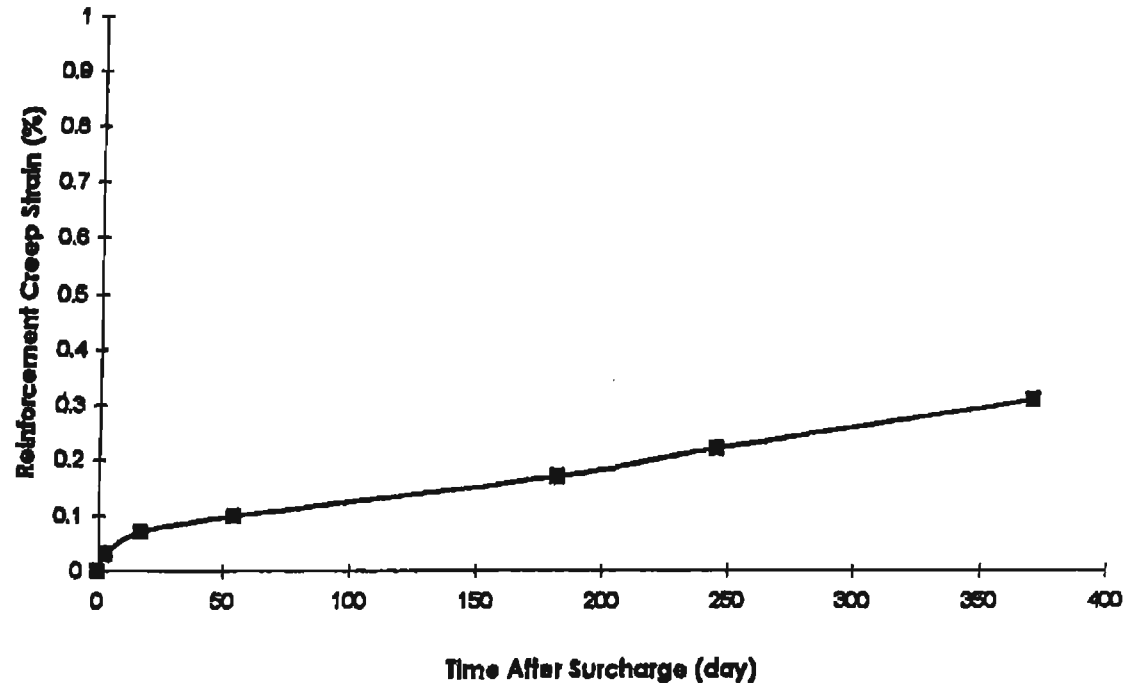


Figure 3.30 Reinforcement strain versus time curve for the FHWA wall (after Crouse and Wu, 2001)

preload fill in an area of limited right-of-way located in Seattle, Washington (see Figure 3.31). The tallest wall (the southeast wall) of this project had a height of 41.3 ft. This was the tallest GRS wall in North America at the time. Being a temporary wall, the wall was constructed with a wrapped-face. The backfill was a gravelly sand. Figure 3.32 shows a typical cross-section of the wall. After the wall was constructed, a 17.4-ft high temporary surcharge fill was placed to reduce post-construction settlement. Since this wall was significantly higher than any previously constructed wall, instrumentation was installed to monitor its performance. The wall was monitored for approximately one year, after which it was demolished. Specific design information can be found in Allen, et al. (1992).

#### **B. Measured Performance and Discussions**

The southeast wall for the Seattle Preload Fill project was monitored for approximately one year after construction. Similar to the FHWA wall, instrument readings were recorded on a frequent basis. The creep strains in the geotextile 11 months after fill placement were very small, with a maximum creep strain of about 0.15%. The maximum reinforcement creep strain in the reinforcement over time is illustrated in Figure 3.33. The creep strains were determined immediately after the surcharge was placed on the wall. The creep rate was approximately  $4.5 \times 10^{-6}$ /day one month after fill placement, and  $2.0 \times 10^{-6}$ /day 10 months after fill placement. The rates were approaching zero 11 months after fill placement.

### **3.5.8 Summary and Conclusions on Long-Term Performance of the In-Service GRS Walls**

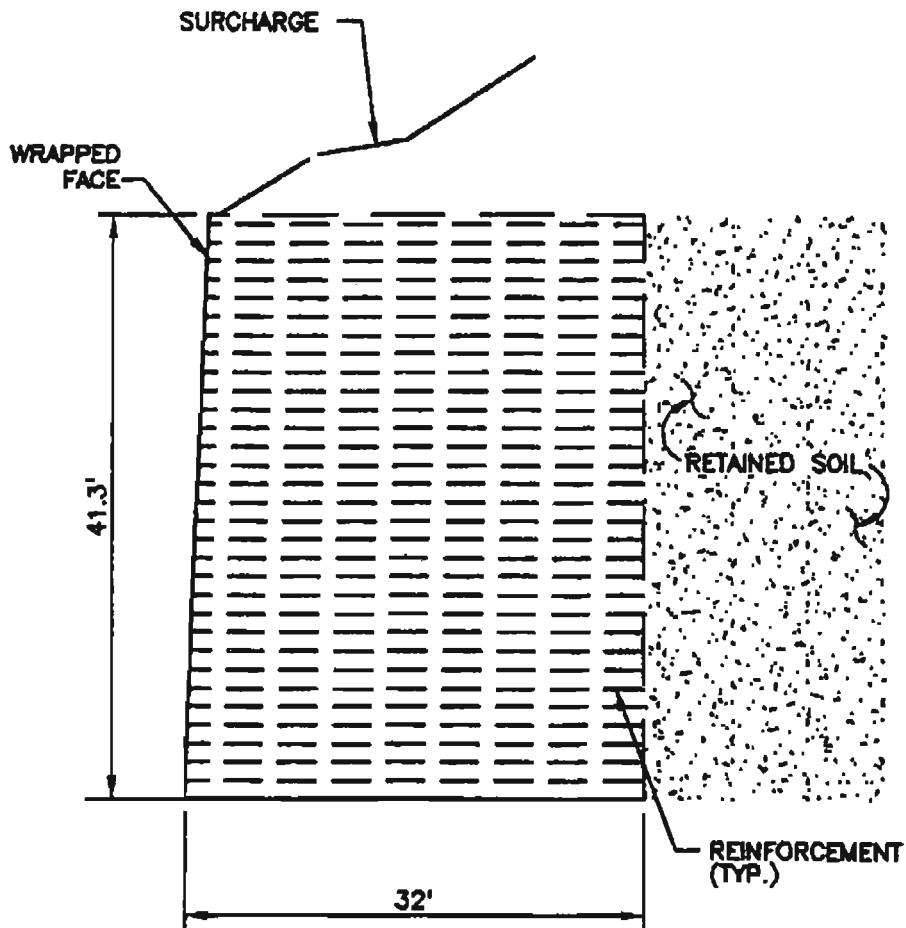
Table 3.2 shows a summary of the wall characteristics and measured performance of the GRS walls. From the measured results on long-term wall performance, two general conclusions can be made:

1. Creep deformation of the geosynthetics in GRS walls constructed with well-compacted granular backfill is very small, typically less than 1.0%.

The in-service GRS walls described above represent a variety of wall types using granular backfill. The maximum creep strains in the



Figure 3.31 The Seattle GRS wall



Seattle Preload Fill Project  
Southeast Wall  
Seattle, Washington, USA

Figure 3.32 Typical cross-section of the Seattle wall (after Allen, et al., 1992)

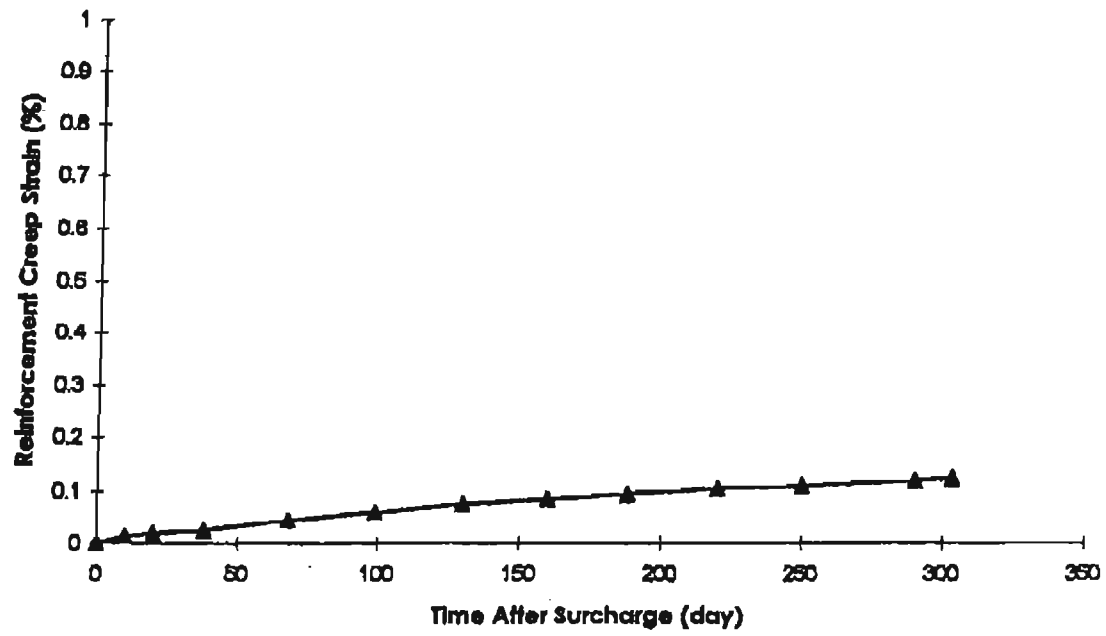


Figure 3.33 Reinforcement strain versus time curve for the Seattle wall (after Crouse and Wu, 2001)

Table 3.2 Characteristics and Measured Performance of the Selected In-Service Walls (Crouse and Wu, 1996)

Project	Wall Name	H (ft)	t (years)	m	$\epsilon_{cm\max}$ (%)	Wall Movement	
						$Y_{\max}$ (in.)	$X_{\max}$ (in.)
Interstate-70 through Glenwood Canyon (Glenwood Canyon wall)	Geotextile Earth Retaining Wall	16	0.6	NA	NA	3.5	5.15
Tanque Verde-Wrightstown-Pantano (Tucson wall)	Wall Panel 26-30	15.6	7	-0.92	< 1.0	NA	3.7
	Wall Panel 26-32	16.1	7	-0.13	< 1.0	NA	3.7
Norwegian Geotechnical Institute (NGI wall)	Wall Section J	15.7	4	-1.10	0.5	NA	NA
	Wall Section N	15.7	4	-1.08	0.6	NA	NA
Japan Railway Test Embankment (JR wall)	JR Embankment No. 1	16.4	2	NA	0.5	1.0	- 0.4
Highbury Avenue (Highbury wall)	Highbury Ave. Wall	23.3	2	-1.5	1.5	NA	1.7
Federal Highway Administration (Algonquin Wall)	Wall No. 9	20	1.3	-0.57	0.8	NA	- 2.0
Seattle Preload Fill (Seattle wall)	Southeast Wall	41.3	1	-0.41	1.0	1.6	6.3

Legend:

NA = Not available in the literature

H = wall Height

t = Monitoring duration

$\epsilon_{cm\max}$  = maximum creep strain in reinforcement

$Y_{\max}$  = Maximum vertical movement

$X_{\max}$  = Maximum horizontal movement

m = creep modulus (Equation 3.1)

reinforcements for all the walls were less than 1.0%, with the exception of Highbury wall (a propped panel wall), for which the maximum reinforcement creep strain was 1.5%.

2 The deformation of GRS walls constructed with well-compacted granular backfill will diminish with time and stress relaxation is likely to occur.

In all of the GRS walls described above, the creep rate was found to decrease with time at a decreasing rate. As the rate of deformation becomes very small, the tensile forces in the reinforcement are likely to decrease with time as well, i.e., experiencing "stress relaxation". It is conceivable that the forces in the geosynthetic reinforcement will eventually reduce to zero over time, provided that there is no change in the loading condition.

### **3.6 Rate of Creep Deformation: Field Performance and the CTI**

#### **Performance Tests**

Creep rate refers to the time-rate at which a GSR retaining wall deforms under a sustained load. A constant creep rate would indicate that the wall is deforming at a constant rate (so-called "secondary creep"). An increasing creep rate would indicate that the wall is deforming at an increasing rate (the so-called "tertiary creep"). In either case, the deformation could conceivably lead to excessive deformation or failure. Conversely, a decreasing creep rate would indicate that the wall was stabilizing with time (so-called "primary creep"). It is important to ensure that a GRS wall will experience only primary creep in a design and that the overall creep deformation is not excessive.

#### **3.6.1 Creep Rate of In-Service GRS Walls**

Figure 3.34 shows the relationship between creep rates of the seven selected projects (as described in Section 3.5) and time, both plotted on logarithmic scales. As shown in Figure 3.34, there is a decreasing trend in the creep rates for all seven GRS walls, indicating the walls were stabilizing over

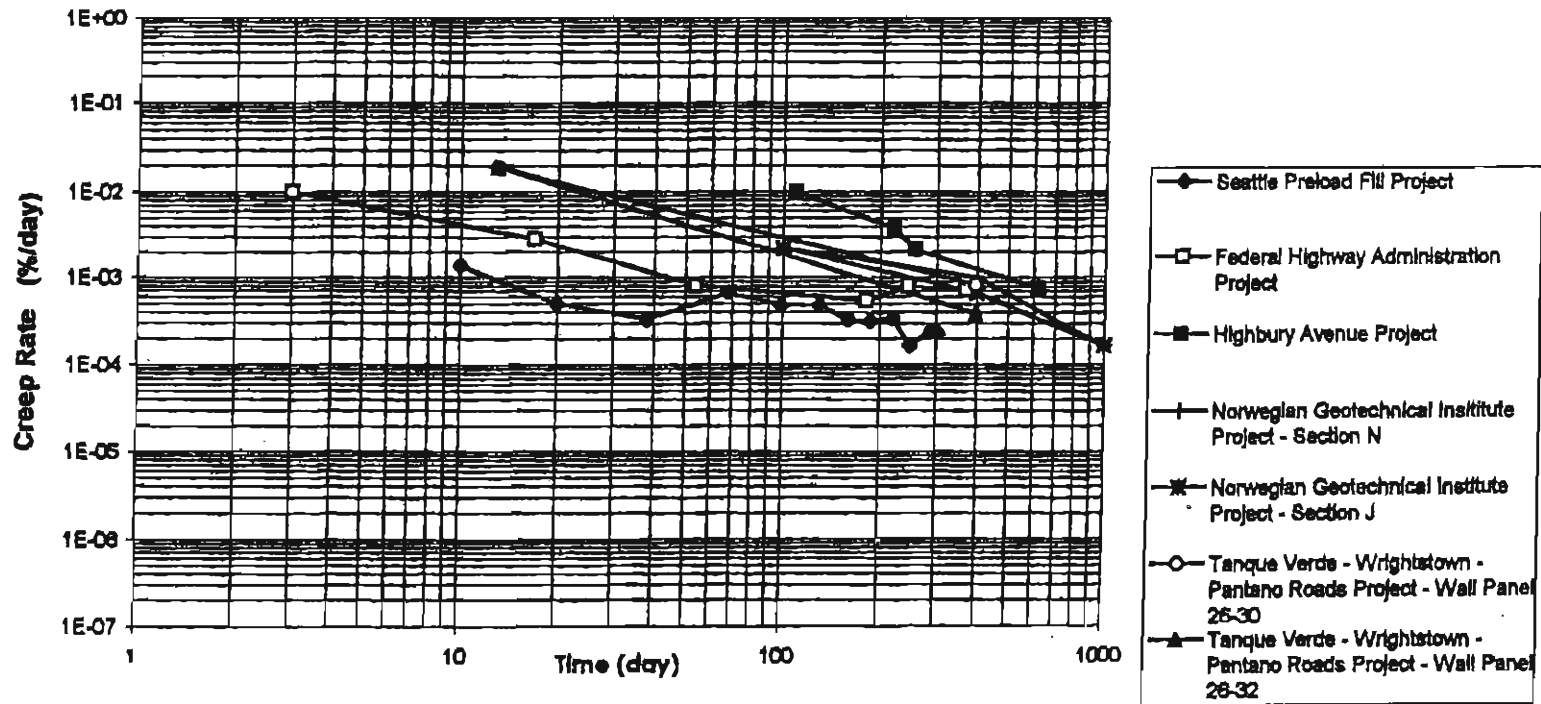


Figure 3.34 The relationship between creep rate and time for the in-service GRS walls (after Crouse and Wu, 2001)

time. The creep rate versus time relationship can be approximated as being linear. The slope of the linear relationship is referred to as “creep modulus,”  $m$ , as shown in Figure 3.35.

The  $m$  value provides a convenient means to quantify the long-term performance of a GRS wall. The  $m$  values of the seven selected projects are also listed in Table 3.2. The  $m$  values range from -0.41 to -1.50 (note: a negative value indicating the strain rate decreases with time, and a larger absolute value indicating a faster creep rate). This is not considered a wide range given the large variety of wall height, reinforcement type, reinforcement spacing, backfill, and facing type.

### 3.6.2 Creep Rate of the SGIP Tests

The test conditions of the 11 SGIP tests of soil-geosynthetic composites conducted by Ketchart and Wu (1996), as described in Section 3.3.2, can be summarized as follows:

- Test D-1: Test D-1 was performed using a heat-bonded nonwoven polypropylene low-strength geotextile having a short-term tensile strength of 420 lb/ft. and an average vertical pressure of 15 lb/in<sup>2</sup> at a temperature of 70°F. The test was performed to determine the creep behavior of the soil/geosynthetic composite using a low-strength reinforcement. Reinforcement strain was measured in addition to lateral and vertical displacement.
- Test H-1: Test H-1 was performed using a woven geotextile having a short-term tensile strength of 4800 lb/ft and an average pressure of 30 lb/in<sup>2</sup> at a temperature of 125°F. The test was performed to determine the creep behavior of the soil/geosynthetic composite using a large load at an elevated temperature.
- Test R-1: Test R-1 was performed using a woven geotextile having a short-term strength of 4800 lb/ft and an average vertical pressure of 15 lb/in<sup>2</sup> at a temperature of 70°F. The test was performed to determine temperature effects on the creep behavior of the soil/geosynthetic composite by comparing the results with test R-2.
- Test R-2: Test R-2 was performed using the same material and loading as R-1 except at an elevated temperature of 125°F. The test was performed to determine temperature effects on creep behavior of the

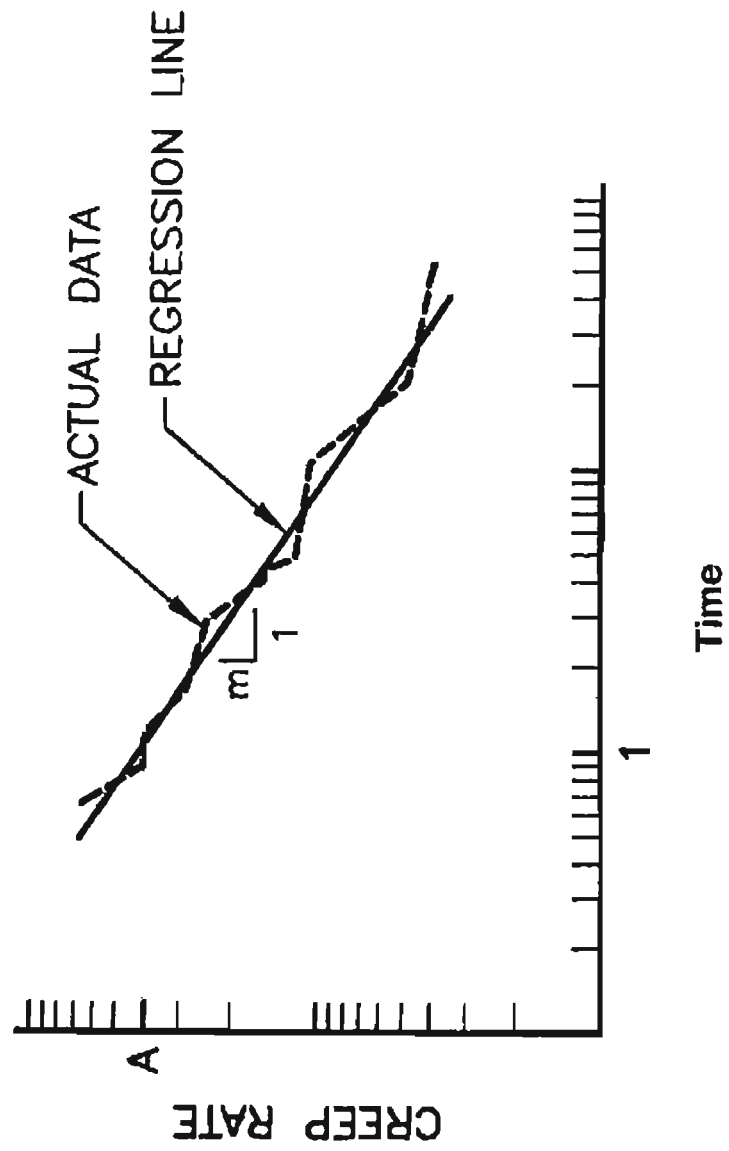


Figure 3.35 The creep modulus,  $m$

soil/geosynthetic composite by comparing the results with test R-1.

- Test R-3: Test R-3 is a duplicate test of R-2 to determine the repeatability of the test method.
- Test W-1: Test W-1 was performed using a woven geotextile having a short-term tensile strength of 1440 lb/ft and an average pressure of 15 lb/in<sup>2</sup> at an elevated temperature of 125°F. The test was performed to determine the temperature impacts to the creep behavior of the soil/geosynthetic composite using a low-strength reinforcement.

The granular backfill consisted of a road base comprising a silty sandy gravel. The soil was prepared 2% wet of the optimum moisture content and compacted to 95 percent of the relative density or approximately 125lb/ft<sup>3</sup>. The soil had an internal friction angle of 34°.

The reinforcement creep rates over the time period for each of the above tests are shown in Figure 3.36. The creep rate based on the measured maximum reinforcement strain for test D-1 is also plotted in the Figure. It is seen that there is a linear decreasing trend in the creep rates of all the tests. A linear regression on each of the data sets revealed that the confidence coefficient (i.e., the R<sup>2</sup> value) was generally on the order of 0.94, indicating a fairly good linear fit. Moreover, the slopes of the linear relationship, or the m values, are on the same order of magnitude compared with the m values of the in-service walls.

### 3.6.3 Creep Rate Equation

Assuming that there is a linear relationship between log-(creep rate) and log-(time), an equation for creep strain rate can be expressed as:

$$\frac{d\varepsilon_c}{dt} = A(t)^m \quad (\text{Equation 3.1})$$

in which,	$\varepsilon_c$	creep strain, (%)
	t	time, (days)
	A	reference creep rate, $d\varepsilon_c/dt$ at $t = 1$ day, (%/day)
	m	creep modulus, slope of $\log(d\varepsilon_c/dt)$ vs. $\log(t)$ line

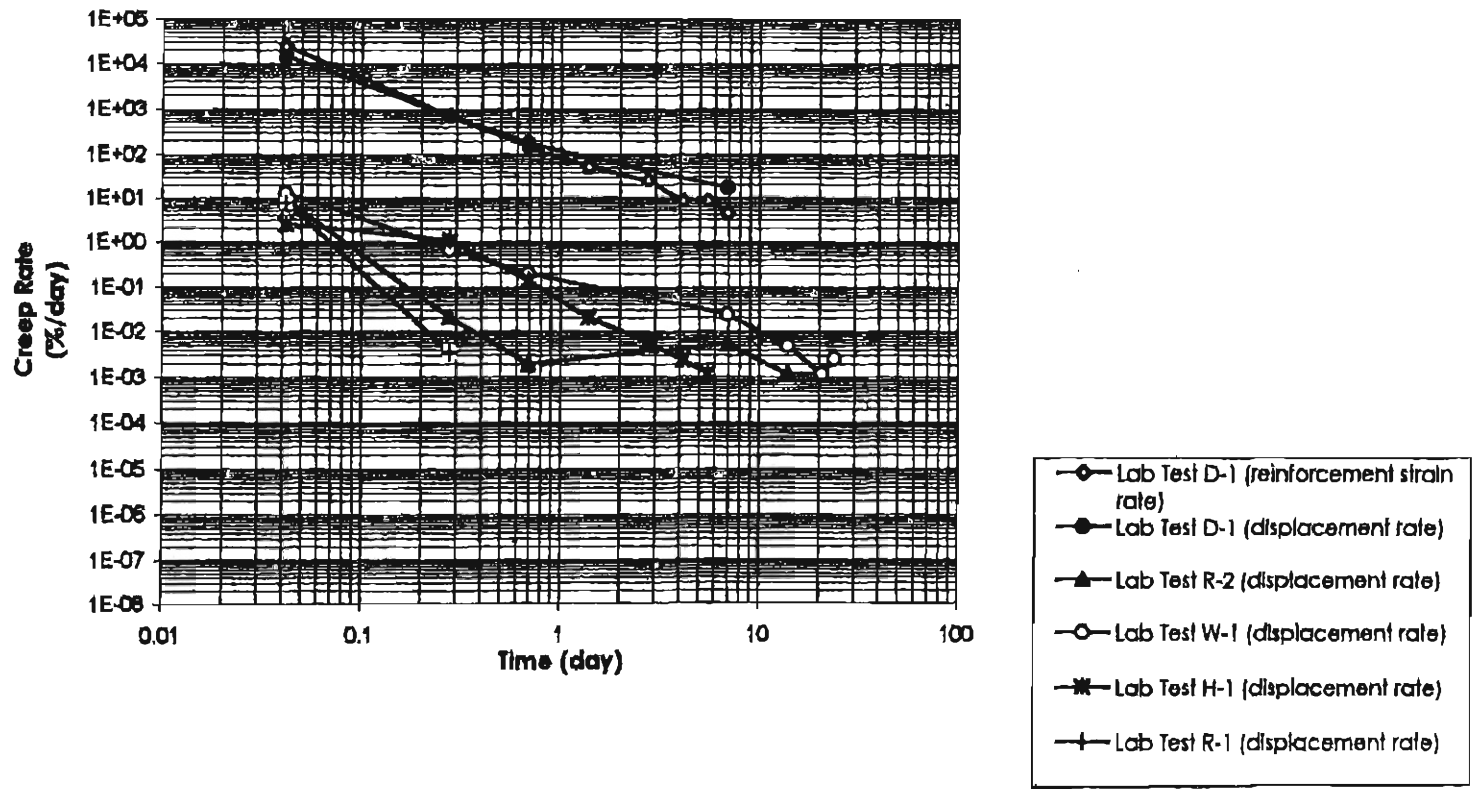


Figure 3.36 The relationship between creep rate and time for soil-geosynthetic composites (after Crouse and Wu, 2001)

The above equation is referred to as the “creep rate equation.” The creep strain can be estimated by integrating Equation 3.1 over the time period of interest.

### **3.7 Proposed Methods to Account for Long-Term Deformation in Design**

Creep deformation of a GRS wall is a result of soil-geosynthetic interaction. If the backfill has a tendency to creep faster than the geosynthetic reinforcement, the creep rate of the geosynthetic reinforcement will accelerate. On the other hand, if the backfill has a tendency to creep slower than the geosynthetic reinforcement, the creep rate of the geosynthetic reinforcement will become smaller. For a GRS wall with a well-compacted granular backfill, the time-dependent deformation will be very small and the rate of deformation will typically decrease rapidly with time (*after all, the geosynthetic cannot creep by itself!*). This means that creep will cease soon after construction. *The AASHTO guidelines have failed to address this very important soil-geosynthetic interactive creep behavior.* Moreover, the tensile forces induced in geosynthetic reinforcement are typically very small at working stresses due to stress redistribution. The very small tensile forces also contribute to very small creep deformation.

The author is convinced that the fundamental design concept of GRS walls in the AASHTO design guidelines (and in all prevailing design methods) is fundamentally unsound (see Section 1.3). Until a rational design method becomes available, it is proposed that the cumulative long-term reduction factor,  $k$ , be applied to the ultimate strength of a geosynthetic reinforcement to account for long-term deformation in design. The use of the partial safety factors to obtain the  $k$  value should be discouraged in view of the fact that they are somewhat arbitrary rather than based on any sound probabilistic analysis or sufficient empiricism.

#### **3.7.1 Cumulative Long-Term Reduction Factor, $k$**

Using the cumulative long-term reduction factor,  $k$ , the design strength of geosynthetic reinforcement,  $T_{\text{design}}$ , can be determined as:

$$T_{\text{design}} = T_{\text{short-term}} * k \quad (\text{Equation 3.2})$$

in which,  $T_{\text{short-term}}$  is the short-term tensile strength of the geosynthetic reinforcement (i.e., the minimum average roll value, MARV) that should be determined in accordance with the ASTM Test Method D4595 (the wide-width strip method). The cumulative long-term reduction factor,  $k$ , is to reflect all the factors affecting long-term design strength of a geosynthetic reinforcement, including creep, construction damage, environmental attack, degradation, uncertainties, etc. (note that long-term degradation occurred after construction is deemed a “non-issue”, see Sections 1.3 and 2.2.4, provided that the provisions of the fill described in Section 1.4 are satisfied).

Table 3.3 shows the proposed values of the cumulative long-term reduction factor. These values were based on the author's own experiences and judgment with the following in mind:

- (1) The long-term reduction factors suggested in the current AASHTO guidelines for design of GRS walls are too large, and result in overly conservative designs (see, for example, Section 1.3).
- (2) Creep susceptibility of geosynthetic reinforcement is strongly dependent on the time-dependent deformation behavior of the backfill. Creep deformation will be negligible when a well-compacted backfill is employed (see Sections 3.3, 3.4 and 3.5).
- (3) Reinforcement spacing has a pronounced effect on the soil-reinforcement interaction, hence a significant effect on the soil-reinforcement interactive creep behavior (see Section 1.2). With a well-compacted backfill, closely spaced reinforcement will result in

Table 3.3 Recommended Values for Cumulative Long-Term Reduction Factor, k

Backfill Properties and Placement Conditions	Reinforcement Spacing, s	Geosynthetic Polymer Type*	Cumulative Reduction Factor, k
Gradation: 100% passing 50 mm (2 in.) sieve 30% to 100% passing No. 4 sieve 10% to 60% passing No. 50 sieve 5% to 20 % passing No. 200 sieve  $PI \leq 4$ $LL \leq 35$ $\gamma_d = 95\% \gamma_{d(max)}$ , per AASHTO T-99 $\omega = \pm 2\% \omega_{opt}$	$s \leq 8$ in.	All types	0.45
	8 in. < $s \leq 16$ in.	All types	0.35
	$s > 16$ in.	PET	0.25 <sup>**</sup>
		PP and PE	0.22 <sup>**</sup>
Gradation: 100% passing 50 mm (2 in.) sieve 30% to 100% passing No. 4 sieve 10% to 60% passing No. 50 sieve 13% to 20 % passing No. 200 sieve  $5 \leq PI \leq 8$ $LL \leq 35$ $\gamma_d = 95\% \gamma_{d(max)}$ , per AASHTO T-99 $\omega = \pm 2\% \omega_{opt}$	$s \leq 8$ in.	All types	0.40
	8 in. < $s \leq 16$ in.	PET	0.33
		PP and PE	0.30
	$s > 16$ in.	PET	0.20 <sup>**</sup>
		PP and PE	0.15 <sup>**</sup>

Note: \* PET = polyester, PP = polypropylene, PE = polyethylene  
 \*\*for geosynthetic with unit weight < 8 oz/yd<sup>2</sup>, use 2/3 of the k value

smaller creep deformation.

- (4) Long-term deterioration of geosynthetic reinforcement is generally not a design issue (see Sections 1.3 and 2.2.4).
- (5) Polymer type and weight of geosynthetic reinforcement have a minor effect on the creep deformation, especially when reinforcement spacing is relatively large. Polypropylene and polyethylene generally exhibit larger creep deformation than polyester (see Section 3.1). Heavier/stronger geosynthetic will experience less creep deformation.

It may be interesting to mention that the U. S. Forest Service design method (Steward, et al., 1977 & 1983) has used k-values much larger than those in the current AASHTO guidelines. Note that the U. S. Forest Service method has been used in the design of thousands of GRS walls around the world without any reported long-term deformation issues (other than when a cohesive backfill was employed). Without regards to the backfill or reinforcement spacing, the U. S. Forest Service design method uses "equivalent" long-term reduction factors of 0.30 to 0.37 for polyester needled geotextile reinforcements, 0.23 to 0.29 for polypropylene needled geotextile reinforcements, 0.17 to 0.21 for polypropylene bonded geotextile reinforcements, and 0.10 to 0.13 for polypropylene woven geotextile reinforcements. These "equivalent" k-values were obtained by combining the recommended creep reduction factors in the design method with a safety factor of 1.2 to 1.5 required for determining reinforcement spacing. The difference in the assumed earth pressure between the U. S. Forest Service method (i.e.,  $K_o$ ) and the AASHTO guidelines (i.e.,  $K_a$ ) is also accounted for in obtaining the equivalent k-values.

### 3.7.2 A Rational Method for Predicting Creep Deformation

When a less-than-desirable fill is employed, it is recommended that a SGIP test (see Section 3.3.2) be conducted to confirm that a given

reinforcement with the backfill under the prescribed placement conditions will not experience excessive long-term deformation. The test should be conducted by using the soil and geosynthetic reinforcement to be used in actual construction of the wall. The soil density and moisture should be prepared in accordance with the anticipated placement conditions, as should the reinforcement spacing. The sustained load used in the test should correspond to the maximum anticipated vertical stress in the soil mass. The creep modulus,  $m$ , and the reference strain rate,  $A$ , should be obtained from the test results. The creep rate can be computed by the creep rate equation (i.e., Equation 3.1). The creep strain over the design life of the wall can be estimated by integrating the creep rate equation over the design life.

### 3.7.3 Measures for Alleviating Excessive Long-Term Deformation

If the creep deformation of a wall is judged to be excessive, the following preventive measures should be considered to reduce the long-term deformation:

1. replace the geosynthetic reinforcement
2. increase the fill placement density
3. replace the fill
4. preload the reinforced soil mass

It is to be noted that replacing the geosynthetic reinforcement generally does not have a significant impact on the creep deformation. It is the first preventive measure to consider because of its ease and cost. Preloading, on the other hand, can significantly reduce the creep deformation (Wu, et al., 2001). Ketchart and Wu (2001) have recently completed a study on the effects of preloading and prestressing on the performance of GRS structures. It was concluded that preloading and prestressing could significantly reduce creep deformation of a GRS structure. Tatsuoka and his associates at the University of Tokyo, Japan have observed similar behavior in a production bridge pier constructed in Kyushu, Japan (Tatsuoka, et al., 1997; Uchimura, et al., 1998).

Ketchart and Wu (2001) have developed a laboratory test protocol, based on the SGIP test (as described in Section 3.3.2), to assess the potential benefits (or lack of) due to preloading and/or prestressing. In the absence of laboratory tests, an analytical model has also been established to evaluate the effects of preloading and/or prestressing.

## Chapter 4

### TRUNCATED BASE WALLS AND CTI TAILS

Where excavation of an existing slope is needed to allow the placement of full design length of reinforcement, it is desirable to have truncated length of reinforcement near the base of the wall (referred to as a truncated-base wall), as shown in Figure 4.1. This feature is not allowed in the current AASHTO guidelines for design and construction of GRS walls. However, a number of truncated-base GRS walls have been successfully constructed with satisfactory performance characteristics. The performance of truncated base GRS walls has been studied by the finite element method of analysis by Chou and Wu (1993) and Thomas and Wu (2000).

The CTI tails are short reinforcement sheets, generally about 3 ft long, placed at the wall face to increase facing stability. The CTI tails are generally installed between alternating courses of facing blocks to increase facing stability without having to install full-length reinforcement at each course of facing blocks. Robert Barrett was the first to propose such a measure. Note that the upper 2/3 of the GRS wall shown in Figure 4.1 uses the CTI tails. A large number of GRS walls have been constructed with the CTI tails with satisfactory performance. An extensive study on the CTI tails has been conducted by Thomas and Wu (2000) using the finite element method of analysis.

#### 4.1 Studies on Truncated-Base Walls and the CTI Tails

##### 4.1.1 Finite Element Analysis by Chou and Wu (1993)

Using the control wall described in Section 2.2.9 as the base case, Chou and Wu (1993) analyzed the effect of truncated base. Figure 4.2 shows the configuration of the truncated wall (referred to as a wall with trapezoidal wall). Figure 4.3 shows a comparison of the lateral wall movement between the trapezoidal wall and the control wall. It is seen that there is not much difference

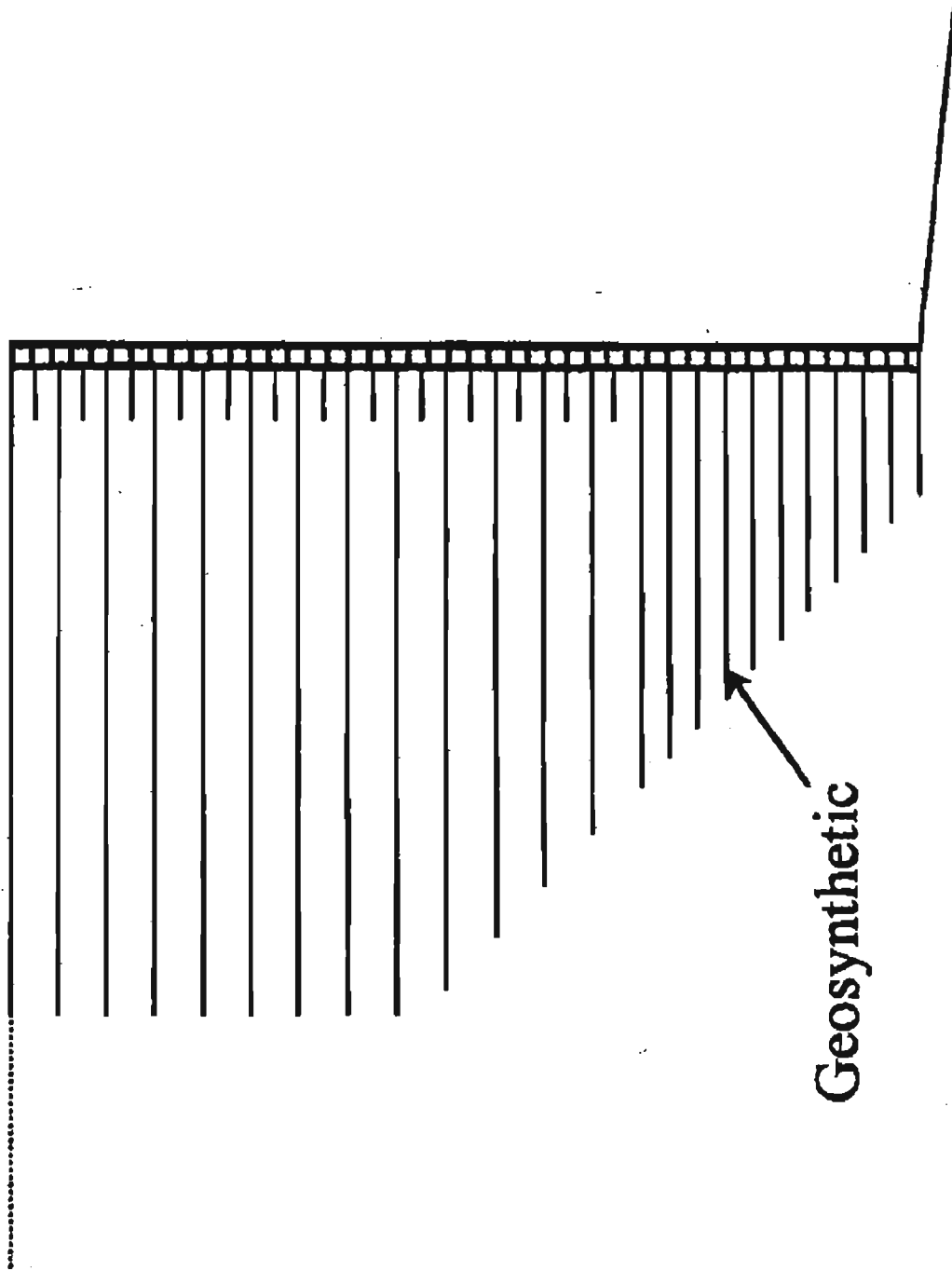


Figure 4.1 A truncated-base wall

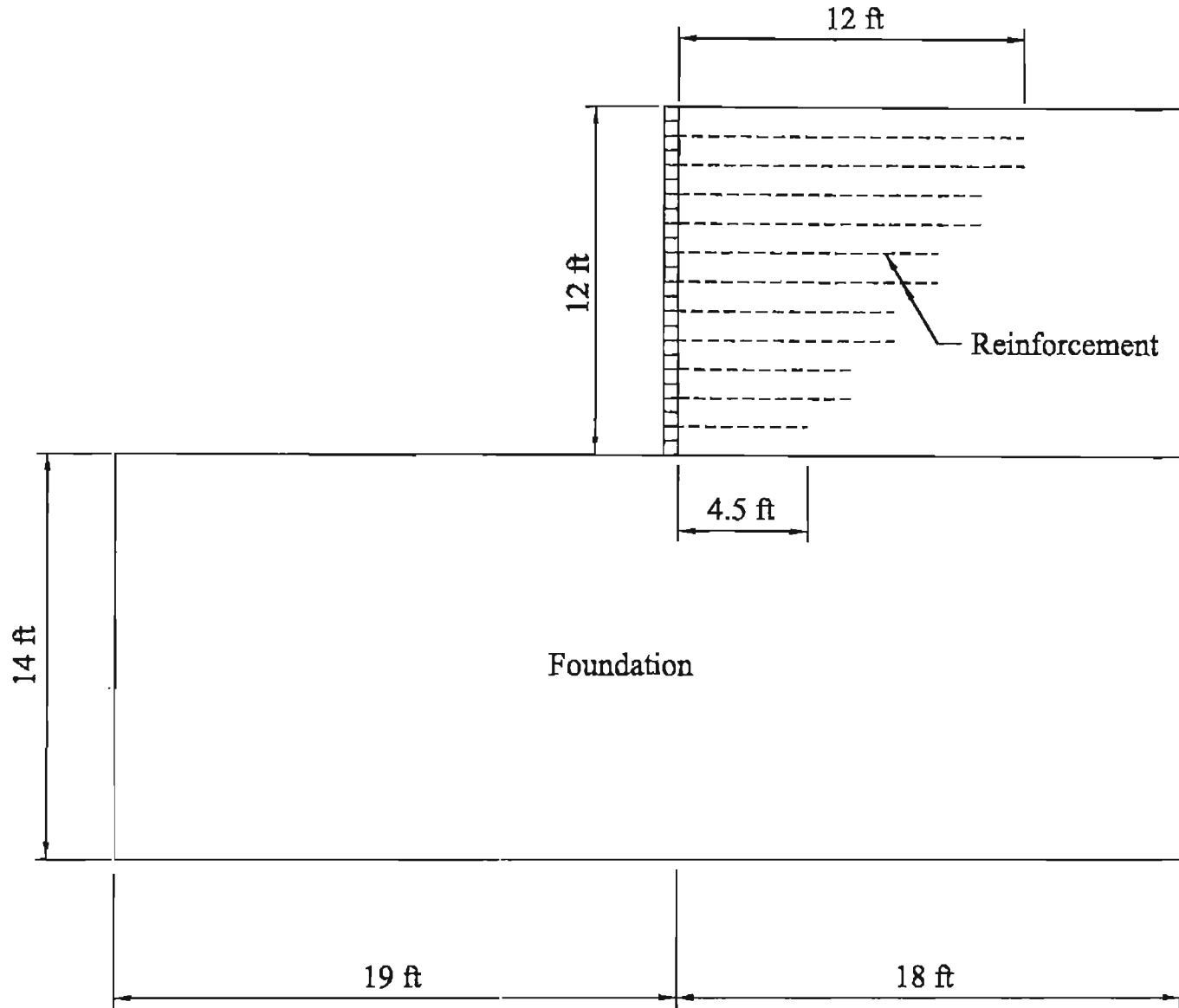


Figure 4.2 Configuration of a truncated-base wall (after Chou and Wu, 1993)

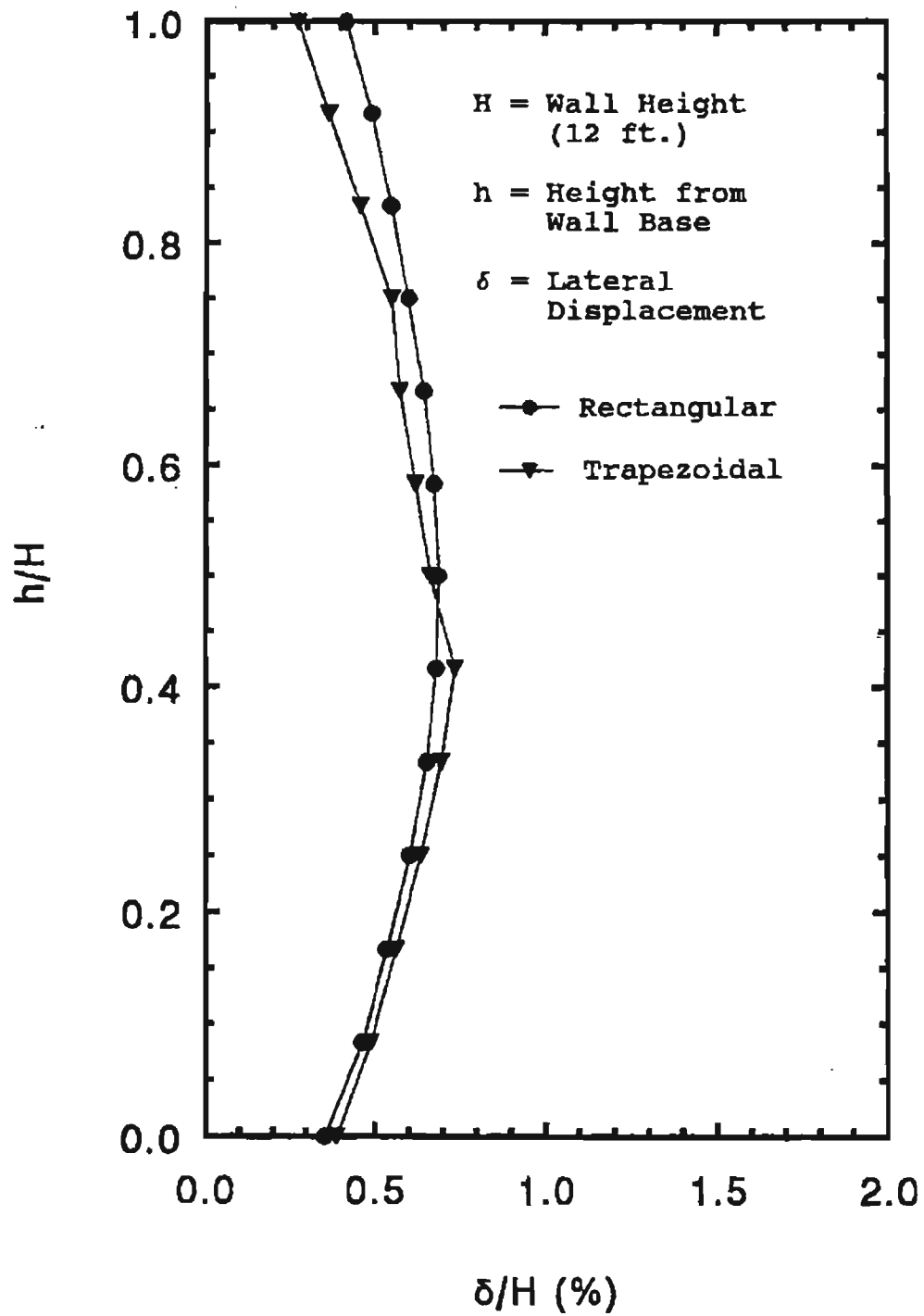


Figure 4.3 Lateral wall movements of truncated base wall and the control wall (after Chou and Wu, 1993)

between the two, with the trapezoidal wall having slightly larger movement in the lower portion of the wall and slightly smaller movement at upper portion of the wall. The tensile strains in the reinforcement at three different heights are shown in Figure 4.4. The corresponding strains of the control wall are also shown for comparison. The strains in the trapezoidal wall are generally smaller. It suggests that the truncated-base wall is a viable alternative when excavation into existing slope is needed for placement of full-length reinforcements.

#### 4.1.2 DeBeque Canyon Wall

In 1996, the Colorado Department of Transportation and Yenter Company constructed a 25 ft high, 800 ft long GRS wall in DeBeque Canyon along Interstate Highway-70 (see Figure 4.5). A road base material was used as backfill and two woven polypropylene geotextiles of different weights (400 lb/in. in the lower portion and 170 lb/in. in upper portion of the wall) were employed as reinforcement. The CTI tails were installed at alternating layers. The wall was situated over a "firm" foundation.

Except for a 30 ft long control section, the GRS wall was constructed with a truncated base. Lateral movement of the wall was measured at two sections, one at the control section (with full-length reinforcement) and the other at a selected section (with truncated reinforcement). In addition, tensile strains in the reinforcement were measured in some selected sections.

Figure 4.6 shows the cross-section of the control wall, where the reinforcements were extended to the full length at all depths. Also shown in the Figure are the measured lateral displacements along the wall height. The displacements shown in the Figure are those that occurred from November 1996 (end of construction) to May 1997. Figure 4.7 shows the configuration of the truncated-base wall and measured lateral displacements along the wall height over the same period of time. It is seen that the lateral displacements of both walls are on the order of 1/8 in. to 1/4 in., with the maximum value being about 5/16 in. It can be concluded from the measured results that the

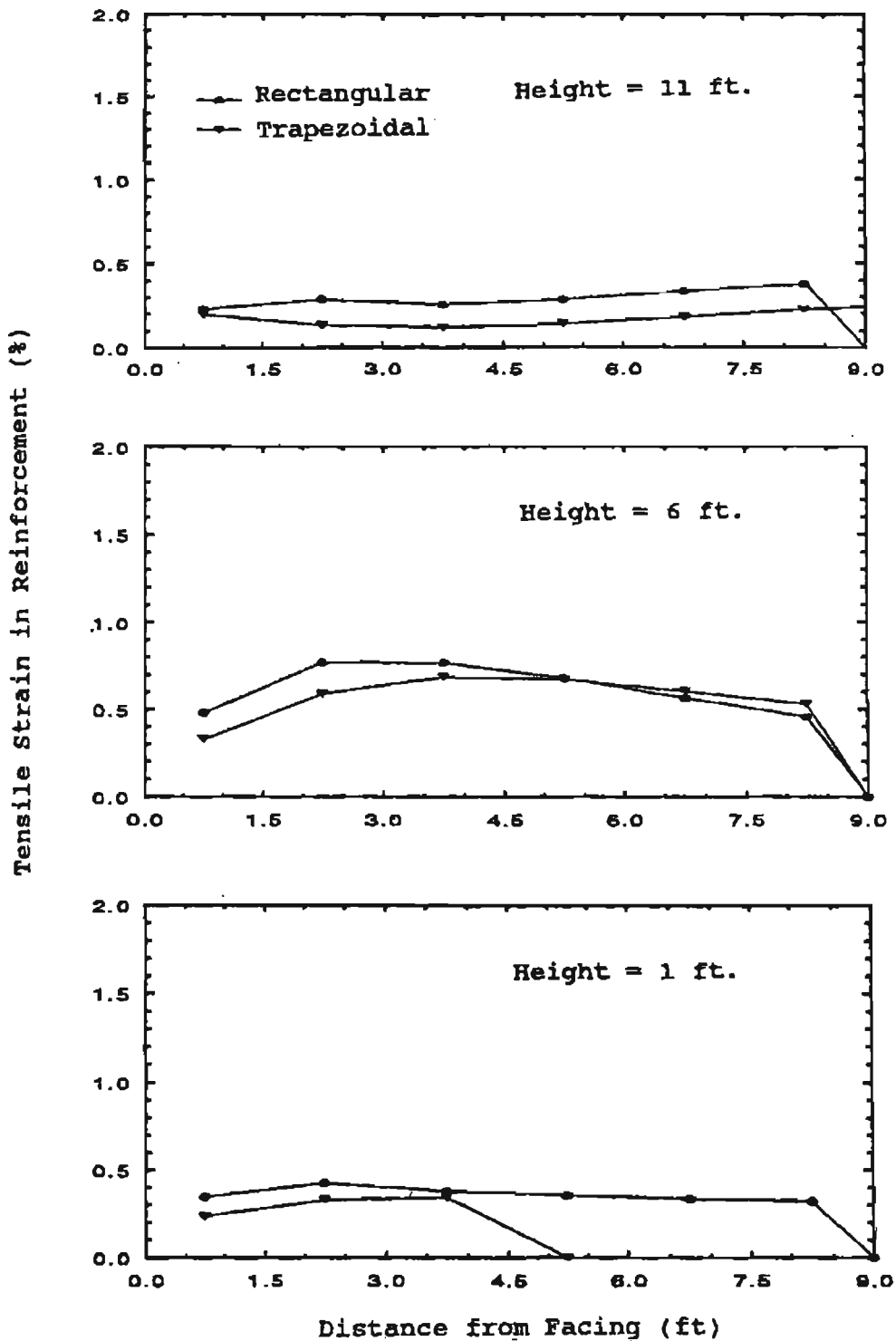


Figure 4.4 Tensile strains of truncated base wall and the control wall (after Chou and Wu, 1993)

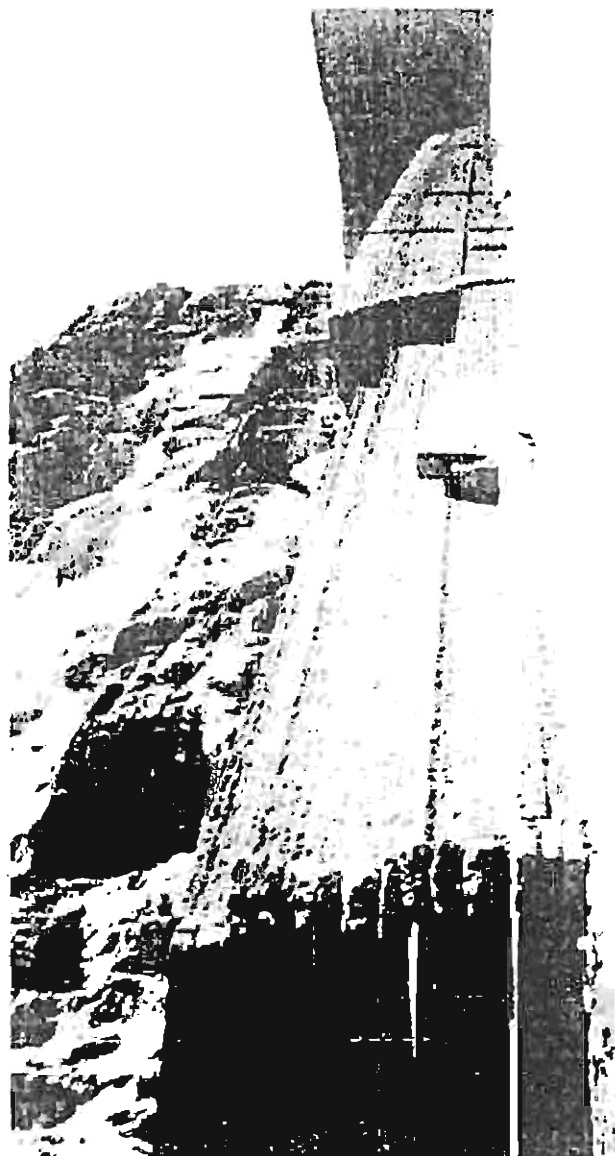


Figure 4.5 The DeBeque canyon wall (courtesy of R. K. Barrett)

TOTAL MOVEMENT  
OF BLOCKS  
OCT - MAY 1997 \*

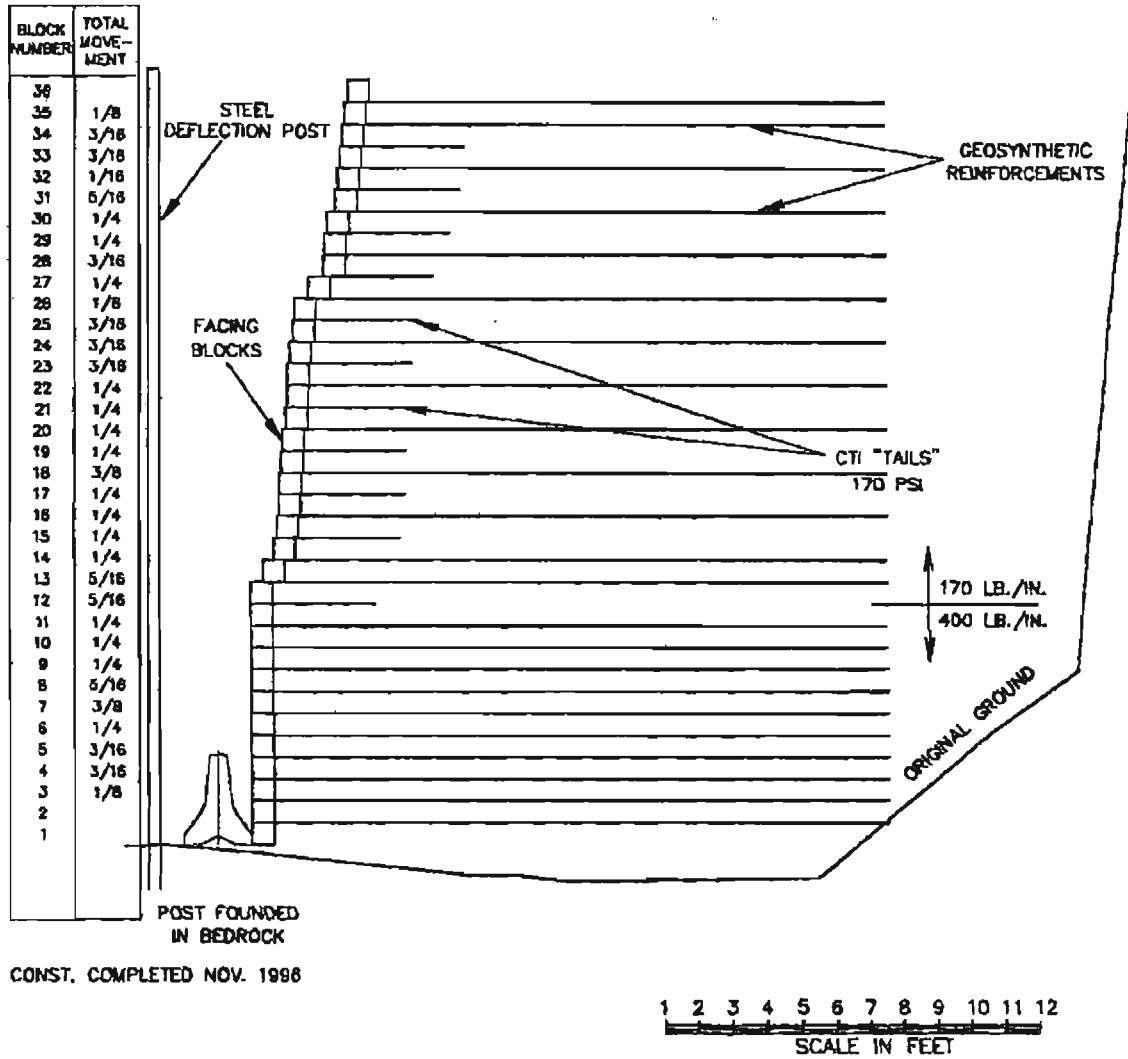


Figure 4.6 Cross-section of the control wall

TOTAL MOVEMENT  
OF BLOCKS  
OCT - MAY 1997 \*

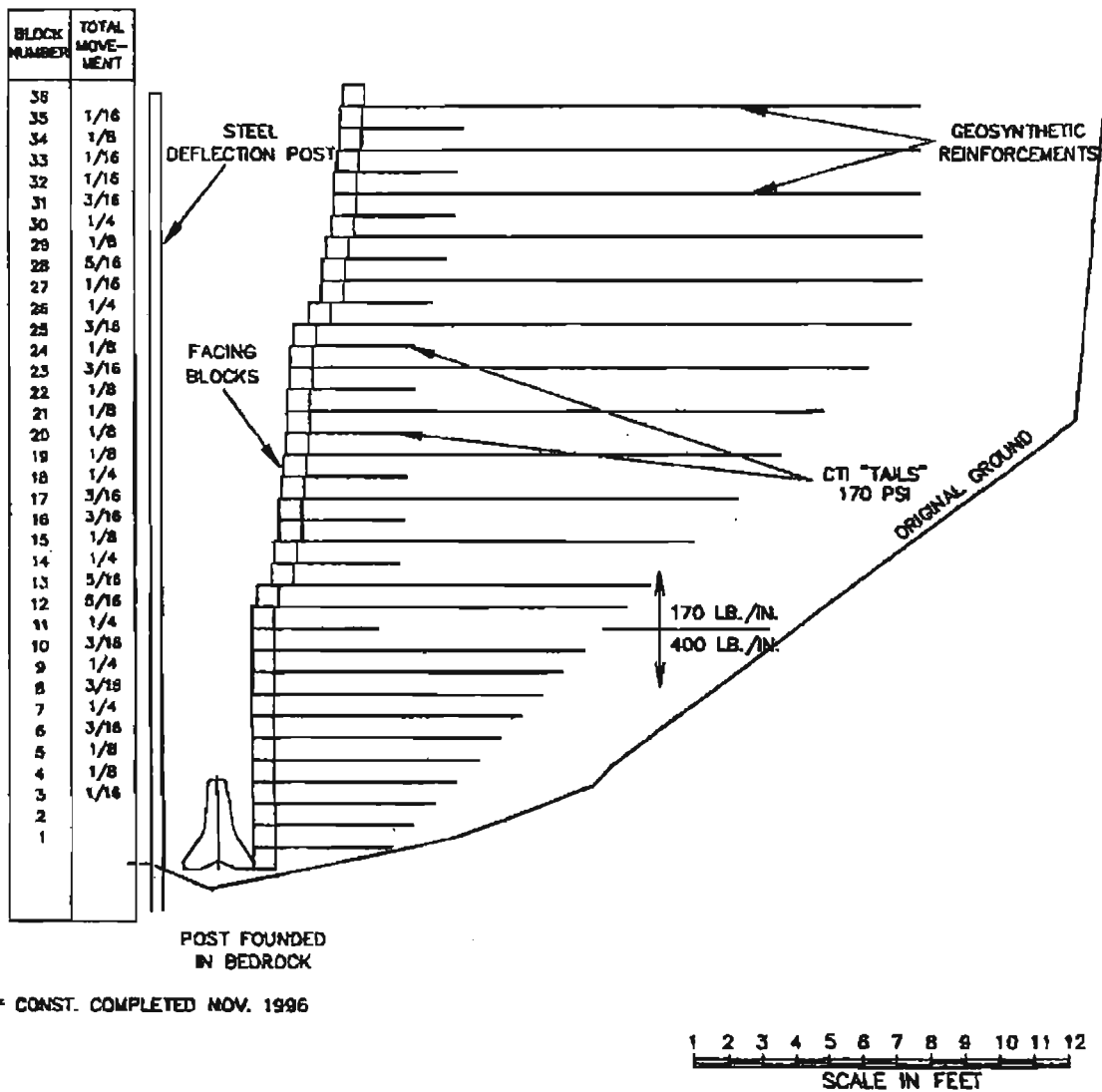


Figure 4.7 Cross-section of the truncated base wall.

truncated-base wall performed essentially the same as the full-length reinforcement wall.

#### 4.1.3 Finite Element Analysis by Thomas and Wu (2000)

Thomas and Wu (2000) conducted an extensive study on truncated-base walls and the CTI tails. The study was conducted by the finite element method of analysis using the computer code GREWS. GREWS was modified from DACSAR (described in Section 2.2.9) for design and analysis of GRS walls. The study investigated the effects of backfill soil, foundation soil, angle of truncation, use of the CTI tails, surcharge, and reinforcement properties on wall performance. Both the effects of a single factor and synergistic effects of multiple factors were investigated.

To verify the analytical model, an analysis was first performed on the DeBeque canyon wall (see Section 4.1.2). The finite element model was shown to be capable of simulating the wall performance. Figure 4.8 shows a comparison of the measured strains in the reinforcements at three different depths and the analytical results. The agreement is considered satisfactory, especially in the absence of the constitutive relationships of the soil.

The findings of the study can be summarized as follows:

- Truncated reinforcement at the base of a GRS wall is a viable and practical alternative for use when excavation for full embedment of the geosynthetic reinforcement is not practical.
- When designing GRS walls with a truncated base, external stability should be thoroughly checked. Truncated-base GRS walls have a stronger tendency to have a global sliding failure. The length of reinforcement at the lowest level should be at least 3 ft for any wall height.
- The type and compaction of the backfill material plays a significant role in the performance of a GRS wall with a truncated base. The use of cohesive backfill should be avoided when a truncated-base wall is

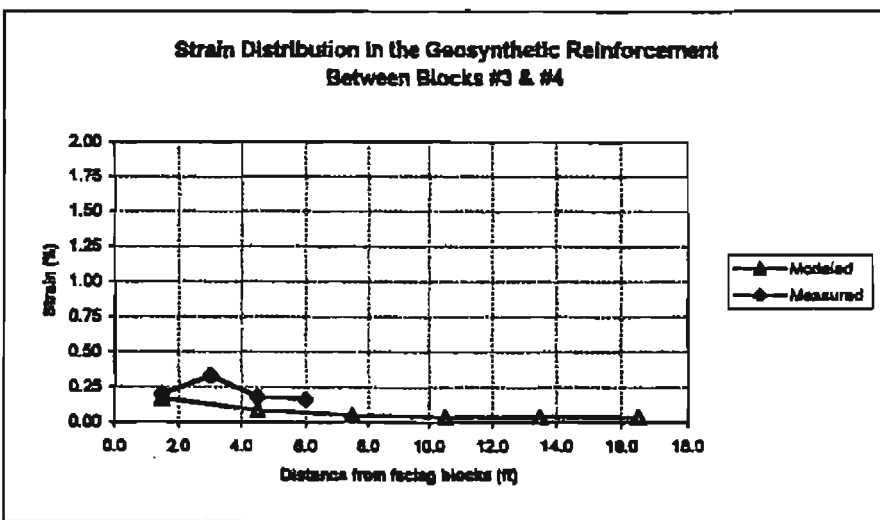
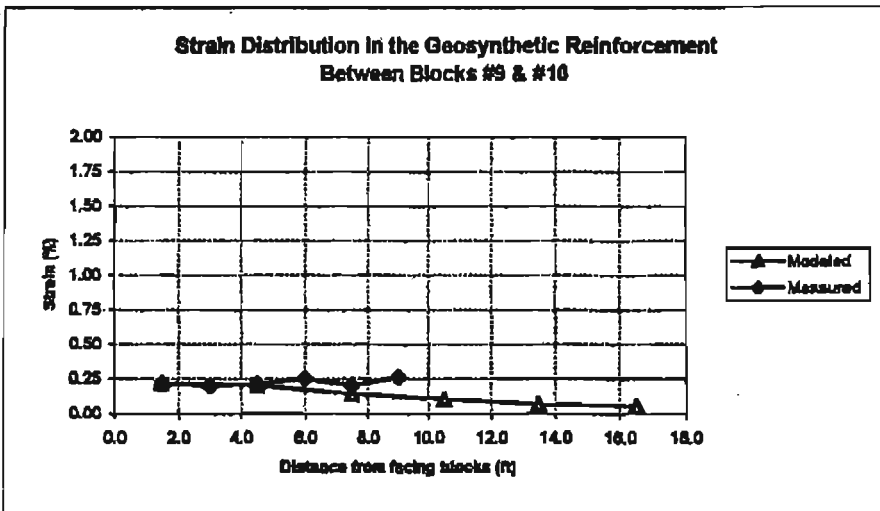
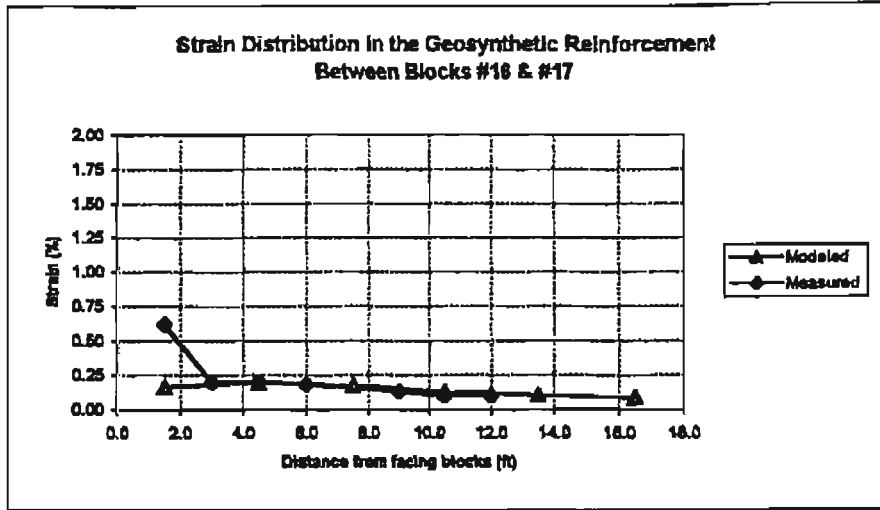


Figure 4.8 Comparison of measured and analytical reinforcement strains at three different depths (after Thomas and Wu, 2000)

- employed.
- An angle of truncation greater than 45 degrees may be used with densely compacted granular backfill. Angles of truncation greater than 45 degrees should be avoided in lower strength granular backfills.
  - The strength of the foundation soil has a significant effect on the performance of a truncated base GRS wall, more so than on a full-length GRS wall. Due to the additional concentrated loading of the truncated base, a GRS wall on a soft foundation will tend to rotate about the top of the wall due to excessive foundation settlement.
  - If significant surcharge loading is anticipated on a truncated-base GRS wall, good quality backfill with good compaction should be used. The additional loading due to the surcharge will tend to accelerate the global sliding failure.
  - For a truncated-base GRS wall with granular backfill, decreasing the reinforcement stiffness from 4000 lb/in. to 450 lb/in. does not significantly affect the deformation of the wall. For walls with cohesive backfill, however, the reduction in reinforcement stiffness will significantly affect the wall performance.
  - The use of the CTI tails, generally 3 ft in length, in the upper 1/3 to 1/2 of the wall section does not noticeably impact the performance of a GRS wall, even a truncated-base GRS wall.

#### **4.2 Proposed Guidelines for Truncated Base and Tails**

It is proposed that a truncated-base wall may be used when a well-compacted granular backfill is employed in the construction of a GRS wall on a competent foundation and when placement of full-length reinforcement is impractical. The reinforcement length at the lowest level should be at least 3 ft and the truncation angle can be as high as 45 degrees from the horizontal plane. When using a truncated base, the external stability of the GRS wall needs to be checked thoroughly.

The CTI tails of 3 ft in length measured from the back of the facing blocks can be employed to increase facing stability. This measure should only be used with well-compacted granular backfill.

## Chapter 5

### EMBEDMENT AND LEVELING PAD

Stemming from the design concept of externally stabilized retaining walls, the current AASHTO design guidelines for GRS walls require that the embedment (measured from the adjoining ground surface to the bottom of the footing) should be greater than the maximum frost penetration depth with a minimum value of 2 ft, and should be at least  $H/5$  to  $H/20$  ( $H$  = wall height), depending on the slope of the ground surface in front of the wall.

As described in Section 1.2, an externally stabilized retaining wall relies on the retaining structure to resist the lateral earth pressure due to soil weight and external loads. To increase stability of the retaining structure, the structure needs to be embedded at some depth. It is also necessary to embed the base of the retaining wall below the maximum depth of frost penetration to avoid excessive movement due to frost action. However, an internally stabilized GRS wall, when properly designed and constructed, is sufficiently stable by itself without any means of external support (see Chapter 2); it is not necessary to embed the base of a GRS wall.

Also, in the AASHTO guidelines, it is indicated that there needs to be a concrete leveling pad installed under the first course of facing blocks. This rigid pad often makes leveling of blocks difficult as can be testified by builders of GRS walls.

#### 5.1 Field Performance

A large number of in-service GRS walls have been constructed with zero or very small embedment, such as the Commerce City wall (Section 2.2.3), the DeBeque Canyon wall (Section 4.1.2) and hundreds of walls constructed over the years by Yenter Companies. These walls have demonstrated excellent performance characteristics without any deformation or stability problems.

## 5.2 Proposed Embedment and Leveling Pad

It is proposed that embedment of GRS walls is not necessary for the internal stability. GRS walls can be safely constructed with zero embedment or a small embedment (say  $\leq 8$  in., one typical block height).

If the foundation contains frost-susceptible soils, they should be excavated to at least the maximum frost penetration line and replaced with non-frost-susceptible soil. If the foundation is considered less than competent, the use of a reinforced soil foundation (e.g., Huang and Tatsuoka, 1990; Yetimoglu and Wu, 1994; Adams and Collin, 1997; Adams, et al., 1997) may be used to increase the bearing capacity and reduce the settlement. Barreire and Wu (2001) have recently completed a study to develop guidelines for design and construction of reinforced soil foundations. The guidelines include a procedure to evaluate potential benefits (or lack of) for employing a reinforced soil foundation.

It is also proposed that, in lieu of the concrete leveling pad under the first course of facing blocks, a leveling pad of compacted gravel or compacted road base material be used (unless the ground surface is level and the foundation soil is very competent). The use of a road base pad will ease the leveling process and facilitate construction of a straighter wall. The typical dimensions of the road base leveling pad should be about 6 in. thick and 18 in. wide for walls less than 30 ft high.

## **Chapter 6**

### **CONCLUDING REMARKS**

The author is convinced that the basic design concept of GRS walls in the AASHTO design guidelines (and in all prevailing design methods) is fundamentally unsound (see the discussions in Section 1.3). A rational design method needs to be able to characterize the soil-reinforcement interactive behavior.

Until a rational design method becomes available, revisions on four aspects of the AASHTO guidelines for design and construction of geosynthetic-reinforced soil walls are proposed. The proposed revisions are on: (1) lateral earth pressure on wall facing, (2) long-term deformation, (3) truncated base walls and CTI tails, and (4) embedment and leveling pad. The proposed revisions are based on research findings and field measured behavior of geosynthetics and GRS structures, as well as on the author's experiences.

Over the past 15 years, the Colorado Department of Transportation and Turner-Fairbank Highway Research Center (TFHRC) of FHWA have sponsored many GRS research projects on which the author served as the principal investigator. The findings of these research projects have led the way to the proposed revisions.

It is important to note that Yenter Companies of Arvada, Colorado has employed a major part of the proposed revisions in the design and construction of a large number of GRS walls, and has enjoyed great success. The author has benefited from the teaching of Yenter's projects. The author is further inspired by Bob Barrett's relentless efforts to unveil the truth about GRS structures.

## REFERENCES

AASHTO, *Standard Specifications for Highway Bridges, with 2000 Interim Revisions*. American Association of State Highway and Transportation Officials 16th Edition, Washington, D.C., USA, 760 p.

Adams, M.T. and Collin, J.G. (1997), "Large Model Spread Footing Load Tests on Geosynthetic Reinforced Soil Foundations," *Journal of Geotechnical Engineering*, ASCE, Vol., 123, No. 1, pp. 66-72.

Adams, M.T. (1997a), "Performance of Prestrained Geosynthetic Reinforced Soil Bridge Piers." *Mechanically Stabilized Backfill* (Wu, editor), A.A. Balkema Publisher, Rotterdam, Netherlands, pp. 35-53.

Adams, M.T. (1997b), "Geosynthetic-Reinforced Bridge Pier," *Public Roads*, Winter 1997.

Adams, M.T., Lutenegger, A.J., and Collin, J.G. (1997), "Design Implications of Reinforced Soil Foundations Using Soil Strain Signatures and Normalized Settlement Criteria," *Mechanically Stabilized Backfill* (Wu, editor), A.A. Balkema Publisher, Rotterdam, Netherlands, pp. 159-165.

Allen, T.M., Christopher, B.R., and Holtz, R.D. (1992), "Performance of a 12.6 m High Geotextile Wall in Seattle, Washington," *Geosynthetic-Reinforced Soil Retaining Walls* (Wu, editor), A.A. Balkema Publisher, Rotterdam Netherlands, pp. 81-100.

Ballegeer, J.P. and Wu, J.T.H. (1993), "Intrinsic Confined and Unconfined Load-Deformation Properties of Geotextiles," *Geosynthetic Soil Reinforcement Testing Procedures* (Cheng, editor), ASTM STP 1190, pp. 16-31.

Barreire, W. and Wu, J.T.H. (2001), "Guidelines for Design and Construction of Reinforced Soil Foundations," Research Report, Department of Civil Engineering, University of Colorado at Denver.

Barrett, R.K. (1996), "Bed Sheets as Earth Reinforcements?" videotape, 5:30 minutes, Colorado Transportation Institute.

Bathurst, R.J. (1992), "Case Study of a Monitored Propped Panel Wall", *Geosynthetic-Reinforced Soil Retaining Walls* (Wu, editor), A.A. Balkema Publishers, Rotterdam, Netherlands, pp. 159-166

Bell, J.R., Barrett, R.K. and Ruckman, A.C. (1983), "Geotextile Earth-Reinforced Retaining Wall Test: Glenwood Canyon, Colorado," *Transportation Research Record*, No. 916, National Academy Press, Washington, D.C., pp. 59-69.

Bell, J.R. and Barrett, R.K. (1995), "Survivability and Durability of Geotextiles Buried in Glenwood Canyon Wall," *Transportation Research Record*, No. 1474, National Academy Press, Washington, D.C., pp. 55-63.

Berg, R.R., Bonaparte, R., Anderson, R.P, and Chouery, V.E. (1986), "Design, Construction and Performance of Two Geogrid Reinforced Soil Retaining Walls," Proceedings, Third International Conference on Geotextiles, Vienna, Austria, pp.401-406.

Bonaparte, R., Holtz, R.D. and Giroud, J.P. (1987), "Soil Reinforcement Design Using Geotextiles and Geogrids," *Geotextile Testing and the Design Engineer*, ASTM STP 952, J.E. Fluet, Jr., Ed., American Society for Testing and Materials, Philadelphia, pp. 69-116.

Bright, D.G., Collins, C.G., and Berg, R.R. (1994), "Durability of Geosynthetic Soil Reinforcement Elements in Tanque Verde Retaining Wall Structures," *Transportation Research Record*, No. 1439, National Academy Press, Washington, D.C., pp. 46-54.

Boyle, S.R. (1995), "Unit Cell Tests on Reinforced Cohesionless Soils," Proceedings, Geosynthetics' 95 Conference, pp. 1221-1234.

Broms, B.B. (1977), "Triaxial Tests with Fabric-Reinforced Soil," C.R. Coll. Inst. Soils Text (Paris), Vol. 3, pp. 129-133.

Broms, B.B. (1978), "Design of Fabric Reinforced Retaining Structures," Proceedings, Symposium on Earth Reinforcement, ASCE, Pittsburgh, p. 282.

Chou, N.N.S. and Wu, J.T.H. (1993), "Investigating Performance of Geosynthetic-Reinforced Soil Walls," Report No. CDOT-DTD-93-21, Colorado Department of Transportation, 197 p.

Christopher, B. R., Bonczkiewicz, C., and Holtz, R.D. (1994), "Design, Construction and Monitoring of Full-Scale Test Soil Walls and Slopes," *Recent Case Histories of Permanent Geosynthetic Reinforced Soil Retaining Walls* (Tatsuoka and Leshchinsky, editors), A.A. Balkema Publisher, Rotterdam, Netherlands, pp. 45-60.

Claybourn, A.F. and Wu, J.T.H. (1991), "Case History Comparison of Geosynthetic-Reinforced Soil Walls," Proceedings, Geosynthetics '91 Conference, Atlanta, pp. 549-559.

Claybourn, A.F. and Wu, J.T.H. (1992), "Failure Loads of the Denver Walls by Current Design Methods," *Geosynthetic-Reinforced Soil Retaining Walls* (Wu,

editor), A.A. Balkema Publisher, Rotterdam, Netherlands, pp. 61-77.

Claybourn A.F. and Wu, J.T.H. (1993), "Geosynthetic-Reinforced Soil Wall Design," Geotextiles and Geomembranes, Vol. 12, pp. 707-724.

Collin, J.G. (1986), "Earth Wall Design," Ph.D. Thesis, Department of Civil Engineering, University of California, Berkeley.

Collin, J.G., Bright, D.G., and Berg, R.R. (1994), "Performance Summary of the Tanque Verde Project - Geogrid Reinforced Soil Retaining Walls," Proceedings, Earth Retaining Session, ASCE Convention, Atlanta, GA.

Crouse, P.E. and Wu, J.T.H. (1996), "Long-Term Performance of GRS Retaining Walls," Research Report, Department of Civil Engineering, University of Colorado at Denver, 113 p.

Derakhashandeh, M. and Barrett, R.K. (1986), "Evaluation of Fabric Reinforced Earth Wall," Colorado Department of Highway and Federal Highway Administration Report, CDOH-DTP-R-86-16.

Fannin, R.J. and Hermann, S. (1990), "Performance Data for a Sloped Reinforced Soil Retaining Walls," Canadian Geotechnical Journal, Vol. 27, No. 5, pp. 676-686.

Fannin, R.J. and Hermann, S. (1992), "Geosynthetic Strength - Ultimate and Serviceability Limit State Design," Proceedings of the ASCE Specialty Conference on Stability and Performance of Slopes & Embankments II, University of California, Berkeley, Ca., pp. 1411-1426.

FHWA (1989), "Tensar Geogrid-Reinforced Soil Wall," Federal Highway Administration Report FHWA-EP- 90-001-005, Washington, D.C.

Fishman, K.L., Desai, C.S., and Sogge, R.L. (1993), "Field Behavior of Instrumented Geogrid Soil Reinforced Wall," Journal of Geotechnical Engineering, Vol. 119, No. 3, August 1993, pp 1293-1307.

Geoservices, Inc. (1989), "Geotextile Engineering Workshop--Design Examples," Federal Highway Administration Publication No. FHWA-HI-89-CO2.

Helwany, S.M.B. (1994), "Loading Tests of a New Mechanically Stabilized Backfill Wall System," Report to Colorado Department of Transportation.

Helwany, S.M.B. and Wu, J.T.H. (1995), "A Numerical Model for Analyzing Long-Term Performance of Geosynthetic-Reinforced Soil Structures," Geosynthetics International, Vol. 2, No. 2, pp. 429-453.

Den Hoedt, G. (1986), "Creep and Relaxation of Geotextile Fabrics," Geotextiles and Geomembranes, Vol. 4, No. 2, pp. 83-92.

Huang, C.C. and Tatsuoka, F. (1990), "Bearing Capacity of Reinforced Horizontal Sand Ground," Geotextiles and Geomembranes, Vol. 9, pp. 51-82.

John, N.W.M. (1985), "Collapse Test on a Reinforced Soil Wall," *Failure in Earthworks*, Thomas Telford Ltd., London.

Juran, I. and Christopher, B.R. (1989), "Laboratory Model Study on Geosynthetic Reinforced Soil Retaining Walls," Journal of Geotechnical Engineering, ASCE, Vol. 115, No. 7.

Ketchart, K. and Wu, J.T.H. (1996), "Long-Term Performance Tests of Soil-Geosynthetic Composites," Report No. CDOT-CTI-96-1, Colorado Department of Transportation, 156 p.

Ketchart, K. and Wu, J.T.H. (1997), "Loading Test of a GRS Wall Reinforced with a AMOCO Geotextile," Research Report, Department of Civil Engineering, University of Colorado at Denver.

Ketchart, K. and Wu, J.T.H. (2001), "Performance Test for Geosynthetic-Reinforced Soil including Effects of Preloading," Federal Highway Administration Report, FHWA-RD-01-018, 270 p.

Koerner, R.M. (1998), *Designing with Geosynthetics*, Fourth Edition, Prentice Hall Publisher, 761p.

Kokkalis, A. and Papacharisis, N. (1989), "A Simple Laboratory Method to Estimate In-Soil Behavior of Geotextiles," Geotextiles and Geomembranes, Vol. 8, pp. 147-157.

Kutara, K., Aoyama, N., Yasunaga, H., and Kato, T. (1988), "Long-Term Pullout Tests on Polymer Grids in Sand," Proceedings, Symposium on Theory and Practice of Earth Reinforcement, A.A. Balkema Publisher, Rotterdam, Netherlands, pp. 117-122.

Leshchinsky, D. and Field, D.A. (1987), "In-Soil Load-Elongation Tensile Strength and Interface Friction of Nonwoven Geotextiles," Proceedings, Geosynthetics '87 Conference, New Orleans, pp. 238-249.

Leshchinsky, D. and Perry, E.B. (1987), "A Design Procedure for Geotextile-Reinforced Walls," Proceedings, Geosynthetics '87 Conference, New Orleans, Vol. 1, pp. 95-107

Ling, H.I., Wu, J.T.H., and Tatsuoka, F. (1992), "Short-Term Strength and Deformation Characteristics of Geotextiles under Typical Operational Conditions," Geotextiles and Geomembranes, pp. 185-219.

Ma, C.C.W. and Wu, J.T.H. (2000), "Field Performance of a New Reinforced Soil Retaining Wall with Full-Height Facing and Yielding Connection," Research Report, Department of Civil Engineering, University of Colorado at Denver.

McGown, A., Andrawes, K.Z., and Kabir, M.H. (1982), "Load-Extension Testing of Geotextiles Confined in Soil," Proceedings, Second International Conference on Geotextiles, Las Vegas, Vol. 3, pp. 793-798.

Mitchell, J.K. and Villet, W.C.B (1987), *Performance of Earth Slopes and Embankments*, NCHRP Report No. 290, Transportation Research Board, Washington, D. C.

Ohta, H. and Iizuka, A. (1986), "DAC SAR, Deformation Analysis Considering Stress Anisotropy and Reorientation," Report, Soil Mechanics and Foundation Engineering Laboratory, Department of Civil Engineering, Kanazawa University, Japan.

Schmertmann, G.R., Chouery-Curtis, V.E., Johnson, R.D. and Bonaparte, R., (1987), "Design Charts for Geogrid-Reinforced Soil Slopes," Proceedings, Geosynthetics '87 Conference, New Orleans, Vol. 1, pp. 108-120.

Sekiguchi, H., and Ohta, H. (1977), "Induced Anisotropy and Time Dependency in Clays." Proceedings, Ninth ICSMFE, Specialty Session 9, Tokyo, pp. 228-237.

Siel, B.D., Wu, J.T.H., and Chou, N.N.S. (1987), "In-Soil Stress-Strain Behavior of Geotextiles," Proceedings, Geosynthetics '87 Conference, New Orleans, pp. 260-265.

Simac, M.R., Christopher, B.R., and Bonczkiewicz, C. (1990), "Instrumented Field Performance of a 6 m Geogrid Soil Wall," *Geotextiles, Geomembranes and Related Products* (Den Hoedt, editor), A.A. Balkema Publisher, Rotterdam, Netherlands, pp. 53-59.

Steward, J.E., Williamson, R. and Mohney, J. (1977, Revised 1983), "Guidelines for Use of Fabrics in Construction and Maintenance of Low-Volume Roads," Chapter 5: Earth Reinforcement, USDA, Forest Service, Portland, Oregon.

Tatsuoka, F., Murata, O., Tateyama, M. (1992), "Permanent Geosynthetic-Reinforced Soil Retaining Walls Used for Railway Embankments,"

*Geosynthetic-Reinforced Soil Retaining Walls* (Wu, editor), A.A. Balkema Publisher, Rotterdam, Netherlands, pp. 101-130.

Tatsuoka, F., Uchimura, T., and Tateyama, M. (1997), "Preloaded and Prestressed Reinforced Soil," Soils and Foundations, Vol. 37, No. 3, pp. 79-94.

Uchimura, T., Tatsuoka, F., Tateyama, M., and Koga, T. (1998), "Preloaded-Prestressed Geogrid-Reinforced Soil Bridge Pier," Proceedings, Sixth International Conference on Geosynthetics, Atlanta, GA, pp. 565-572.

Whittle, A.J., Larson, D.G., and Abramento, M. (1991), "Annual Technical Report on Geosynthetic Reinforcement of Soil Masses," Research Report, Department of Civil Engineering, Massachusetts Institute of Technology.

Whittle, A.J., Germaine, J.T., Larson, D.G., and Abramento, M. (1992), "Measurement and Interpretation of Reinforcement Stresses in the APSR Cell," Proceedings, Symposium on Theory and Practice of Earth Reinforcement, A.A. Balkema Publisher, Rotterdam, Netherlands, pp. 179-184.

Wu, J.T.H. (1991), "Measuring Inherent Load-Extension Properties of Geotextiles for Design of Reinforced Structures," Geotechnical Testing Journal, Vol. 14, No. 2, pp. 157-165.

Wu, J.T.H. (1992a), "Predicting Performance of the Denver Test Walls: General Report," *Geosynthetic-Reinforced Soil Retaining Walls* (Wu, editor), A.A. Balkema Publisher, pp. 3-20.

Wu, J.T.H. (1992b), "Construction and Instrumentation of the Denver Test Walls," *Geosynthetic-Reinforced Soil Retaining Walls* (Wu, editor), A.A. Balkema Publisher, pp. 21-30.

Wu, J.T.H. (1994a), *Floor Discussion on Long-Term Creep Behavior, Recent Case Histories of Permanent GRS Retaining Walls* (Tatsuoka and Leshchinsky, editors), A.A. Balkema Publisher, Rotterdam, Netherlands, pp. 343-344.

Wu, J.T.H. (1994b), *Design and Construction of Low-Cost Retaining Walls: The Next Generation in Technology*, Colorado Transportation Institute, CTI-UCD-1-94, 152 p.

Wu, J.T.H., Helwany, S.M.B., and Barrett, R.K. (1993), "Loading Test of MSB Wall – A New Geosynthetic-Reinforced Retaining Wall System," Soil Reinforcement: Full Scale Experiments of the 80's, Paris, pp. 583-603.

Wu, J.T.H. and Helwany, S.M.B. (1996), "A Performance Test for Assessment of Long-Term Creep Behavior of Soil-Geosynthetic Composites," Geosynthetics

International, Vol. 3, No. 1, pp. 107-124.

Wu, J.T.H., Ketchart, K., and Adams, M.T. (2001), "GRS Bridge Piers and Abutments," Federal Highway Administration Report HFWA-RD-00-038, 136 p.

Wu J.T.H. and Tatsuoka F (1992), "Laboratory Model Study on Geosynthetic Reinforced Soil Retaining Walls," Discussion, Journal of Geotechnical Engineering, ASCE, Vol. 118, No. 3, pp. 496-498.

Yetimoglu, T. and Wu, J.T.H. (1994), "Bearing Capacity of Rectangular Footings on Geogrid-Reinforced Sand," Journal of Geotechnical Engineering, ASCE, Vol. 120, No. 12, pp. 2083-2099.

Yogarajah, I. and Saad, M.A. (1996), "Development of Horizontal Earth Pressures and Behavior of Single and Multi Segmented Walls," Proceedings, International Symposium on Earth Reinforcement, Fukuoka, Japan, A.A. Balkema Publisher, Rotterdam, Netherlands, pp. 553-558.